PRECIPITATION IN THE ALASKA CENTRAL ARCTIC

By

Joel W. Homan

RECOMMENDED:

Dr. Horacio Toniolo

Dr. Matthew Sturm

Dr. Larry Hinzman

Dr. Douglas Kane
Advisory Committee Chair

Dr. Leroy Hulsey, Chair
Department of Civil & Environmental Engineering

APPROVED:

Dr. Douglas Goering
Dean, College of Engineering and Mines

Dr. John Eichelberger
Dean of the Graduate School

7 December 2015
Date

PRECIPITATION IN THE ALASKA CENTRAL ARCTIC

A

DISSERTATION

Presented to the faculty

of the University of Alaska Fairbanks

in Partial Fulfillment of the Requirements

for the degree of

DOCTOR OF PHILOSOPHY

By

Joel W. Homan, M.S., B.S.

Fairbanks, Alaska

December 2015

Abstract

Environmental change currently stimulates much of the interest in high-latitude hydrologic studies, as northern areas are expected to be strongly impacted by warming. This thesis consists of a comprehensive assessment of solid and liquid precipitation throughout the Alaska Central Arctic. The founding hypothesis are: (1) the spatial distribution of snow and warm season precipitation are linearly related to elevation, (2) annual precipitation inputs are dominated by warm season precipitation when potential moisture sources are ice free, and (3) moisture responsible for snow-producing storms is primarily advected through atmospheric circulation.

To verify the validity of the hypothesis, the temporal variability and spatial distribution of snow and warm season precipitation were extensively measured. Snowpack patterns were established using over 1000 snow surveys from end-of-winter field campaigns. The snowpack distribution patterns were similar from year to year and relatively independent of elevation, with roughly an average of 100 mm of snow water equivalent (SWE) from the Arctic Coast to the Brooks Range divide. For the same 1500 m change in elevation, warm season precipitation has a large orographic change, which increases more than 240 mm. Warm season precipitation was evaluated using 31 meteorological stations and although a strong spatial distribution was found, no discernible long-term trends were identified in the somewhat limited 29 year data set.

The accumulation of end-of-winter SWE and warm season precipitation measurements were combined to evaluate the distribution of annual precipitation. Annual precipitation varies temporally and spatially over the Alaska Central Arctic. At high elevations, 70% of the annual precipitation is liquid, while at low elevations, liquid precipitation only represents 40% of the annual budget and end-of winter SWE becomes the dominate precipitation contributor.

Moisture responsible for snow-producing storms was found to originate from different sources depending on the time of year and ice cover conditions. North originating moisture is three times more likely to occur during the fall when sea ice is thin, or nonexistent. Mid-winter moisture was found to advect into the Arctic from the south. The timing and travel pathways of snowfall events were determined using an atmospheric model (HYSPLIT) and supplemental surface analysis charts.

Table of Contents

List of Figures

Page

List of Tables

Page

Acknowledgments

The success of this project was due in a large part to the effort of my major advisor, who actively participated in every aspect of the research from formulation of the concept through publication of results. Dr. Douglas Kane was the driving force behind many of our endeavors. Dr. Matthew Sturm, Dr. Horacio Toniolo, and Dr. Larry Hinzman served on my committee and significantly impacted the focus of my degree program and the quality of this manuscript. Dr. Matthew Sturm deserves special recognition for his help on using the HYSPLIT model. Although not on my committee, my success would not be possible without the hard work from Robert Gieck, who has spent countless hours in the field, installing equipment, collecting, reducing and analyzing data, putting in endless effort and care.

I am extremely grateful to the numerous graduate students and friends who contributed immensely to the task of data collection. I could not begin to name all who helped, but Erica Betts, Levi Overbeck, Celina Van Breukelen, John Mumm, and Erin Trochim are ones I worked with closely.

My life long family support was crucial in getting me to this point. I would never have dreamed of prosing a Ph.D. without the encouragement, confidence, and many sacrifices from Ashlee.

Funding for this project was a collective effort, including Alaska Department of Transportation and Public Facilities (ADOT&PF), National Science Foundation (NSF Snow-Net, AON, and TAON), Inland Northwest Research Alliance (INRA), Alaska Department of Natural Resources (ADNR), and U.S. Fish and Wildlife Service (USFWS).

Introduction

The Arctic has gained a certain amount of prominence in recent years due to environmental changes, and oil production and expanded oil exploration. The availability of environmental data for the Arctic Alaska can, however, best be described as sparse. This area was the focus of considerable oil/gas exploration immediately following World War II. Unfortunately, very little environmental data were collected in parallel with the exploration. Soon after the oil discovery at Prudhoe Bay, Alaska in November 1968, the U.S. Geological Survey (USGS) started collecting discharge data at three sites in the neighborhood of Prudhoe Bay and one small watershed near Barrow, Alaska. Unfortunately, additional complementary data, such as precipitation (both solid and liquid), were almost completely lacking, which deterred precipitation/runoff studies. In the mid-1980s, some small hydrologic research studies were initiated north of the Brooks Range, and this effort expanded during the next three decades (Kane et al., 2014).

Currently, concerns about environmental change have motivated much of the interest in high-latitude hydrologic studies, as northern areas are expected to be more strongly impacted by climate warming (ACIA, 2005). How will this warming impact the annual precipitation pattern in the Arctic? Possible scenarios include less snowfall and greater warm season precipitation due to longer summers and shorter winters (IPCC, 1996, 2001), a larger ice-free area of the Arctic Ocean with a longer ice-free duration (Maslanik et al., 1999; Vinnikov et al., 1999; Cavalieri et al., 2003), and more extreme summer precipitation events (Kane et al., 2008). Precipitation trends are presently not conclusive, therefore, potential impacts cannot be confidently predicted

The Intergovernmental Panel on Climate Change (IPCC, 1996, 2001) has consistently reported twentieth-century precipitation increases in northern high latitudes (55° – 85°N). For the period since 1960, the gauge-adjusted and basin-averaged data of Serreze et al. (2002) show no discernible trends in mean annual precipitation over the Ob, Yenisey, Lena, and Mackenzie Basins. However, summer precipitation over the Yenisey Basin decreased by 5 to 10% over the four decades since 1960 (Serreze et al., 2002). The uncertainties concerning precipitation emphasize the sparse short-term network of *in situ* measurements and the compounding effects of elevation in topographically complex regions of the Arctic, where the distribution of observing stations is biased toward low elevations and coastal regions.

What is known about precipitation across the Alaska Arctic is that snow plays a dominant role in the hydrologic cycle. Snow may accumulate on the ground for nine months with little to no melt and then ablate in a relatively short time, typically 10 to 14 days just before the summer solstice (Kane et al., 2008). The total water content of the snowpack at the end of winter comprises 30 to 40% of the annual precipitation (Kane et al., 2008). Warm season precipitation varies considerably from the coast to the headwaters in the Brooks Range (Kane et al., 2000). This rainfall study by Kane et al. (2000) was of data with a short duration, thus, prohibiting any meaningful statistical analyses. Past observational studies of precipitation in the Arctic are limited in duration and scale. The sparsity of meteorological stations and the discontinuity in observations is primarily responsible for our inadequate knowledge base.

The objective of this research was to make a comprehensive assessment of snow (solid) and warm season (liquid) precipitation. In order to obtain good spatial and temporal precipitation patterns, a network of widespread meteorological stations and/or field measurements are required for an informative duration. Consequently, this research used precipitation data from a collection of different organizations and research projects. Initially, meteorological stations were logistically established across the Alaska Central Arctic based on the ease of access from the Dalton Highway. At the summit of Atigun Pass, the U.S. Department of Agriculture (USDA), National Resources Conservation Service (NRCS) installed a station in 1983. In 1985, through a series of funded research projects, researchers at the University of Alaska Fairbanks (UAF), Water and Environmental Research Center (WERC), began installing meteorological stations in the Alaska Central Arctic. The number of UAF stations installed ranged from 1 in 1985 to 3 in 1986, 12 in 1996, 24 in 2006, 23 in 2010, and 7 in 2014. Meteorological data from the U.S. Bureau of Land Management (BLM) station (2008–2012) located in Umiat were also used in this investigation of the spatial and temporal variability in the magnitude of warm season precipitation. In total, this research used results from 31 meteorological stations that comprehensively spanned from 2 to 29 years.

Difficulties in measuring falling solid precipitation, as well as quantifying snow redistribution and winter-long sublimation, make ground-based snow surveys at winter's end the most reliable and economical approach for quantifying the snow water equivalent (SWE) that will contribute to snowmelt runoff. A snow survey dataset collected from numerous research

projects, and consisting of over 1000 snow surveys between the years of 2000 and 2013 was used during this investigation of solid precipitation.

Using the snow and warm season precipitation datasets from the collection of snow surveys and meteorological stations, respectively, a comprehensive assessment of annual precipitation could be made. The datasets were used to evaluate the hypothesizes that (1) the spatial distribution of snow and warm season precipitation are linearly related to elevation, with southward increases in precipitation from the Arctic Coast to the Brooks Range divide and (2) annual precipitation inputs are dominated by warm season precipitation when potential sources (mainly lakes and surrounding seas) of moisture are ice free.

To further enhance our understanding of snowfall and its distribution, the source of moisture responsible for snow-producing storms in the energy-limited and arid Alaska Arctic was evaluated. It was hypothesized (3) that snowfall in the Alaska Arctic was primarily the result of atmospheric circulation advecting moisture northward from the Pacifica Ocean. To complete this investigation, an additional network of 8 meteorological stations in northern Alaska, 5 stations located north of the Brooks Range and 3 to the south, were used. Automated snowfall data from the 8 meteorological stations were used to indicate the timing of snowfall events. Between the years of 2000 and 2014, 650 snowfall events were delineated. Using an atmospheric model (HYSPLIT: HYbrid Single Particle Lagrangian Integrated Trajectory) (Draxler and Hess, 1997) and weather surface analyses charts, the source of moisture for the 650 snowfall events was determined.

This dissertation represents a collection of papers on research completed in the Alaska Arctic. The intrinsic theme of each chapter is the distribution of precipitation, however, each paper will discuss different aspects of precipitation. Each paper was written to be published independently of the other, consequently there is some repetition between papers. Although each paper had one or more co-authors, I am solely responsible for the content of this thesis. The data collection and analysis for this project was truly a massive endeavor and reflects the efforts of several individuals. My contribution to this research included the collection of snow survey data post 2008, downloading and processing of meteorological data, running and analysis of an atmospheric model, and collection and interpretation of weather surface analysis charts. I wrote the first draft of all papers, and edited subsequent drafts to their final form.

Chapter 1, entitled "Arctic snow distribution patterns at the watershed scale," has been published in Hydrology Research and my co-author was Douglas L. Kane. Chapter 2, entitled "Warm season precipitation patterns in the Alaska Central Arctic," has been submitted to Arctic, Antarctic, and Alpine Research and was co-authored with Douglas L. Kane and Svetlana L. Stuefer. Chapter 3, entitled "Annual precipitation patterns in the Alaska Central Arctic," was written by myself and prepared for this thesis. Chapter 4, entitled "Winter Moisture Sources and Pathways in the Alaska Arctic," was submitted to the Journal of Hydrometeorology and was co-authored by Douglas L. Kane.

Chapter 1 Arctic Snow Distribution Patterns at the Watershed Scale[1]

1.1 Abstract

Watershed-scale hydrologic models require good estimates of spatially distributed snow water equivalent (SWE) at winter's end. Snow on the ground in arctic environments is susceptible to significant wind redistribution, which results in heterogeneous snowpacks. The scarcity and quality of data collected by snow gauges provides a poor indicator of actual snowpack distribution. Snow distribution patterns are similar from year to year because they are largely controlled by the interaction of topography, vegetation, and consistent weather patterns. Consequently, shallow and deep areas of snow tend to be spatially predetermined, resulting in depth (or SWE) differences that may vary as a whole, but not relative to each other. Our aim was to identify snowpack distribution patterns and establish their stability in time and space at a watershed scale. Snow patterns were established by: (1) using numerous field surveys from end-of-winter field campaigns, and (2) differentiating snowpacks that characterize small-scale anomalies (local scale) from snowpacks that represent a large-scale area (regional scale). We concluded that basic snow survey site descriptions could be used to separate survey locations into regional and local-scale representative sites. Removing local-scale influences provides a more accurate representation of the regional snowpack, which will aid in forecasting snowmelt runoff events.

---

[1] Homan, J. W. and Kane, D. L., 2015: Arctic snow distribution patterns at the watershed scale. *Hydrology Research*, 46(4): 507-520.

1.2 Introduction

Snow hydrology is an important component of the arctic hydrologic cycle. In Alaska, the north-flowing rivers of the Arctic drain three physiographic areas: Mountains, Foothills, and Coastal plain. The total water content of the snowpack at the end of winter within the Arctic comprises 30% to 40% of the annual precipitation (Kane et al. 1991, 2008b), and on average, about two-thirds of the snow water equivalent (SWE) leaves catchments as runoff (Kane et al. 2000, 2004, 2008a). On the other hand, the average runoff ratio for rainfall events is roughly one-third for most summer precipitation events (Kane et al., 2012). The higher runoff ratio in spring is mostly due to generally frozen subsurface conditions of the active layer. The low runoff ratio of the summer months is partially due to roughly 140 mm of evapotranspiration (ET) over the basin (Kane et al., 2004) and surface storage availability on the low-gradient Alaska Coastal Plain, where wetlands and lakes cover 82.9% of the landscape (Hall et al., 1994). There is also a disparity in the watershed areas that can contribute to runoff and subsequent runoff ratio. During snowmelt, the entire basin potentially contributes meltwater, while summer rainfall events generally only occur over a portion of the watershed (Kane et al., 2008b).

Heterogeneous snowpacks resulting from snow redistribution is also a major factor in increasing the snowmelt runoff. Much of the redistributed snow accumulates in valley bottoms, in hillside depressions such as shrubby water tracks, and on leeward sides of ridges. Snow drift formation in hillside depressions and valley bottoms generally results in proportionally higher water content close to or within drainage channels, which potentially increases runoff. The combination of above-average water content close to the drainage channels, reduced time of transport of hillslope meltwater due to water tracks, and a completely frozen active layer that limits subsurface meltwater storage produces a generally higher runoff ratio during snowmelt than is observed for rainfall runoff events (McNamara et al., 1998). Some extreme summer storms, however, have produced flows greater than the largest measured snowmelt flood, but only in small high-gradient headwater basins. For large arctic river basins here and elsewhere, the spring snowmelt floods dominate and can be expected every year (Kane et al., 2008b).

In the Alaska Arctic, where snow accumulation may last for nine months and then ablate in a relatively short time, typically 10 to 14 days just before the solstice, the end-of-winter SWE plays a significant hydrologic role in watersheds (Kane & Hinzman, 1988). The task of accurately quantifying solid precipitation in the Arctic is made difficult because it is a remote,

sparsely inhabited, and severely cold environment. Snowfall itself is a stochastic process, and variability is inevitable. Other than the inherent variability in snowfall, an additional problem is that often the quality of precipitation measurements from meteorological stations is poor. For instance, in the Alaska Arctic, snowfall precipitation has been shown to be underestimated by a factor of two or three when windy conditions prevail (Benson, 1982). Redistribution of snow by wind can create complex snow distributions resulting in heterogeneous or even patchy snowpacks (Elder et al., 1991; Seyfried & Wilcox, 1995; Prasad et al., 2001; Winstral et al., 2002; Anderton et al., 2004; DeBeer & Pomeroy, 2009).

The redistribution of snow may be complex, but generally forms consistent patterns. Since snow crystals behave similarly to other sediments, it tends to accumulate in areas where flow diverges or decelerates, while it erodes in areas of convergent or accelerated flow (Elder et al., 1991). Because of this, snow distribution patterns are similar from one year to the next because they are largely controlled by the interaction of topography, vegetation and consistent synoptic weather patterns (Sturm & Wagner, 2010). The number of wind events, wind magnitude and direction, vegetation density and canopy height, and topography (aspect, slope and elevation) are all factors that are important to the end-of-winter snowpack distribution (Elder et al., 1991; Pomeroy & Gray, 1995; Konig & Sturm, 1998; Winstral et al., 2002; Sturm & Wagner, 2010). Difficulties in measuring falling solid precipitation, as well as quantifying snow redistribution and winter-long sublimation, make ground-based snow surveys at winter's end the most reliable and economical approach for quantifying the SWE that will contribute to runoff.

The primary goal of this study is to provide better definition of the distribution of solid precipitation data for input into hydrologic models. Specifically, the intention is to improve the understanding of watershed-scale spatial variability of solid precipitation at winter's end in the central region of the Alaska Arctic including the Dalton Highway corridor (the only major transportation route). Snow survey data used for this investigation were collected from 2000 to 2013 by faculty, staff, and students at the Water and Environmental Research Center (WERC) at the University of Alaska Fairbanks (UAF). From the data collection, snowpack distribution patterns can be examined over the entire region.

Warm season precipitation patterns within a section of the study area (Kuparuk River watershed) were evaluated in 1993 and 1994 by Kane et al. (2000). Their findings indicate a

direct correlation between rainfall and elevation, with increasing precipitation from lower to higher elevations. While summer precipitation patterns were evident with elevation, the distribution of winter SWE was less conclusive. Most of these uncertainties arise from a sparse observational network and the short period of observation at the time of the study by Kane *et al.* (2000). This paper presents new findings using a long-term, widely distributed (2000–2013) snow dataset.

1.3 Study Domain

The study domain covers a 200 by 240 km region of Alaska's Central Arctic Slope that is bound by the Brooks Range on the south and the Arctic Ocean on the north, and includes the Chandler, Anaktuvuk, Itkillik, Kuparuk, Putuligayuk (Put), Sagavanirktok (Sag), Kadleroshilik (Kad), and Shaviovik River basins (Fig. 1.1). All of the watersheds drain north and eventually empty into the Arctic Ocean or another stream that eventually discharges to the ocean. The Putuligayuk lies entirely within the Coastal plain region; the Kuparuk and Kadleroshilik Rivers emanate from the Foothills and cross the Coastal plain; the Sagavanirktok, Shaviovik, Kavik, Itkillik, Anaktuvuk, and Chandler Rivers originate in the Brooks Range and cross both the Foothills and Coastal plain. The southern and northern boundaries of the domain are at between 68°N and 70°N latitude, while the western and eastern boundaries are between 153°W and 146°W longitude. Elevation within the study area ranges from sea level to 2675 m. The topography is characterized by a flat northern portion (generally referred to as *Coastal plain*) and by gently rolling hills and valleys (*Foothills*) and mountain ridges (*Mountains*) of the Brooks Range to the south.

The entire study area is underlain by continuous permafrost (250 to 300 m in the Brooks Range and up to 600 m along the coast; Osterkamp, 1984) and, on average, is snow-covered 8 to 9 months of the year. The region is mostly treeless with some patches of trees in the riparian areas in the Foothills. Vegetation consists of alpine plant communities in the mountainous region, tussock tundra in the Foothills, and sedge tundra on the Coastal Plain (Walker et al., 1989; CAVM Team, 2003). Willow and birch shrubs are common in riparian areas, and shrub height is variable, from approximately 0.3 to over 1 m. In response to climate warming in the Arctic, there is an increase in the abundance and extent of shrubs in tundra areas (Sturm et al., 2001, 2005; Tape et al., 2006).

1.4 Survey Locations

From 2000 to 2013, over 1000 snow surveys were conducted at roughly 200 locations. The snow survey dataset is a collection of results from numerous research projects, so the exact number of sites surveyed and their locations changed yearly. The distribution of snow survey sites is shown on a map of Alaska's Central North Slope (Fig. 1.1). The symbol classifications best describe the timing and duration of surveys, but they do not mean that the sites were visited every year within each classification. Ideally, sites would have been surveyed every year throughout the duration of the projects. Weather conditions, however, play a large role in the feasibility of reaching most of the remote survey sites, which are accessible only by snow machine and/or helicopter. High wind, fog, whiteout, and flat light conditions prevented some of the sites from being surveyed every year, although the goal was to monitor them if safely possible.

The snow survey sites were chosen to represent a wide range of snowpack conditions. Initially, from 2000 to 2005, the National Science Foundation (NSF) funded snow surveys that were primarily within the Kuparuk and Putuligayuk (Put) River watersheds (Fig. 1.1). In 2006, under an Alaska Department of Natural Resources (ADNR) project, snow surveys were extended eastward to the Sagavanirktok, Kadleroshilik, and Shaviovik River watersheds (Fig. 1.1). Also in 2006, additional sites were added in the Kuparuk River watershed on a project funded by the Alaska Department of Transportation and Public Facilities (ADOT&PF) (Fig. 1.1). Finally in 2009, data collection progressed further westward to the Anaktuvuk, Itkillik, and Chandler River watersheds under the ADOT&PF project (Kane et al., 2012) (Fig. 1.1).

Surveying along a uniform grid would have been inadequate at a watershed scale because the Arctic snowpack is very heterogeneous (Kane et al., 1991; Homan et al., 2010; Sturm & Wagner, 2010), with relatively shallow snow on hilltops, along ridges, and on steep slopes, while deeper snow accumulates in valley bottoms and water tracks, and on leeward slopes. Elevation, terrain, vegetation cover, and spatial distribution were all considered during the survey site-selection process. Snowmelt studies have shown that areas with deeper snow take several days or weeks longer to completely melt compared with areas of shallower snow (Hinzman et al., 1991). In the end, the snow survey sites were positioned to represent both 'regional' and 'local' snow conditions in order to capture a greater spatial variability of the snowpack. The regional-scale sites are more uniform and characteristic of larger-scale snow conditions (1 to 10 km^2), while

local-scale sites are smaller, tend to be linear and represent more limited features such as wind-scoured ridges (10 to 1000 m) or snowdrift (1 to 10 m) deposits within depressions such as streams and water tracks.

1.5 Snow Survey Methods

The snow surveys include snow density sampling and snow depth measurements collected over an area of 25 m by 25 m; this technique is often referred to as double sampling (Rovansek et al., 1993). The snow depth of the snowpack in Alaska is more variable than the density (Benson & Sturm, 1993; Sturm et al., 2010). Usually, double sampling yields an areal SWE estimate with a lower variance than is possible using collected snow cores only. In addition, considerably more snow depth measurements can be made in a unit of time compared with SWE measurements. Rovansek *et al.* (1993) showed that double sampling provides improved SWE estimates; they recommended sampling 12 to 15 snow depths for each snow core. This optimal ratio of snow depths to water equivalent, however, appears to vary greatly (from 1 to 23), depending on site, weather, and snow conditions. The UAF-WERC uses an optimal ratio of 10; that is, 50 depths accompany 5 snow cores at each survey site.

Snow cores are sampled using a fiberglass tube ('Adirondack') with an inside area of 35.7 cm^2 (diameter = 6.7 cm) and length of 152.4 cm (5ft), equipped with metal teeth on the lower end to cut through dense layers of snow. The advantage of the Adirondack for shallow snowpack is that its diameter is larger than many other types of snow tubes (like the Mt. Rose); thus, it provides a larger sample of the shallow Arctic snowpack. To obtain a complete snow core, the Adirondack tube is pushed vertically through the snow while turning, until soil is encountered. At this point, snow depth is recorded. The tube is then driven further into the organic layer and tipped sideways, retaining a vegetation plug. This extra step is important, because the base of the Arctic snowpack generally consists of poorly consolidated depth hoar and the organic plug acts as a stopper, ensuring that the complete snow column was sampled. The tube is then removed from the snowpack and the vegetation plug is discarded. The snow itself is either collected for weighing later in the laboratory or weighed immediately in the field.

The WERC uses constant 50 m lengths for the snow depth course, with a 1 m sampling interval along an L-shaped transect (Kane et al., 2012). Twenty-five depth measurements are made on each leg of the L; this strategy is used to account for the presence of snowdrifts in the

area of measurement. The directions of measurement are chosen randomly. Snow depth measurements are made using a T-shaped graduated rod (T-probe). The probe is simply pushed through the snow to the snow–ground interface. The SWE is defined as follows:

$$\text{SWE} = SD * (\rho_s / \rho_w) \quad (1)$$

where SD is an average of 50 snow depths, ρ_s is average snow density from the five snow core samples, and ρ_w is water density (Kane et al., 2012; Stuefer et al., 2013). Snow depths are reported in centimeters (cm), while SWE is reported in millimeters (mm).

1.6 Results

Winter in the Alaskan Arctic starts with snowfall and ends with snowmelt and subsequent runoff. In the Arctic, snow can fall any day of the year, but snow accumulation typically begins in September or early October and continues throughout the entire winter, with no significant midwinter melt. It is hypothesized, however, that both midwinter melt and rainfall are more likely as the climate warms. Snow accumulation occurs during a few large events, many small events, or somewhere in between, but more commonly from a variety of event sizes. It is incorrect to assume that snowfall at a given location is equivalent to snow accumulation recorded during field measurements or by a precipitation gauge, or that a location's measured accumulation can be easily extrapolated to another location. Snow on the ground in treeless arctic environments is susceptible to significant wind redistribution, which is normally accompanied by in-transit sublimation. As a result of both transport and sublimation, the end-of-winter snowpack is very heterogeneous, and depending on the survey location, the end-of-winter snowpack can be as thin as a dusting or can exceed a meter in depth.

1.6.1 Snowpack distribution

Though the snowpack itself may be heterogeneous, the redistribution of snow has been found to have some consistencies: snow is depleted from hilltops, ridges, and windward slopes, while it accumulates in valley bottoms, on leeward slopes, in any depressions such as water tracks and between hummocks, and within or around vegetation. To identify snowpack distribution patterns, SWE measurements from the long-term (2000–2013) snow dataset were used (Table 1.1). The 14-year dataset has a mean density of 246 kg/m^3 (Fig. 1.2a, Table 1.2) and exhibits a nearly symmetric distribution, while depth (mean = 42 cm) (Fig. 1.2b, Table 1.2) and

SWE (mean = 103 mm) (Fig. 1.2c, Table 1.2) have asymmetric distributions. The similarity between the SWE and depth frequency curves is indicative of the fact that SWE is more closely linked to depth than it is to density. This relationship is further verified by plotting SWE vs. depth (Fig. 1.3a), which has regression lines with R^2 values in the 0.80s. The correlation values are high, and the slopes of the regressions are equal to the mean densities, which they should be, given the equation of SWE (Equation 1). In comparison, a plot of density versus SWE (Fig. 1.3b) shows considerably more scatter and little to no correlation.

Due to the physical processes that lead to the densification of snow, it is known that there is a density to depth relationship, where greater snow depths have on average higher densities (Kojima, 1966). This is not the case with the current dataset, which illustrates almost no change in density with depth (Fig. 1.3c). The discrepancy is most likely a result of relatively shallow arctic snowpacks that do not reach sufficient compaction depths.

Within the dataset are distinctly different patterns for two different regions. One pattern exists at lower elevations (Lowlands < 225 m) and another at higher elevations (Uplands > 225 m) (Fig. 1.3-1.5, Table 1.2). The Uplands snow has on average a lower density (Fig. 1.3b and c, Fig. 1.4a) which is attributed to inland increases in thickness of the depth-hoar layer where greater temperature extremes (in particular, lower minimum temperatures) permit larger gradients to develop within the snow-pack (Hall et al., 1986). The density for depth hoar layers varies from 150 to 250 kg m^{-3}, while the density for wind packed layers (wind slab) fluctuates from 400 to 500 kg m^{-3} (Benson & Sturm, 1993). Overall, the Lowlands and Uplands snow densities were found to have poorly fit regressions with elevation (low R^2 values), which illustrates high variability (Fig. 1.5). It was statistically proven that snow density-to-elevation relationships did not exist with significant probability (p-values less than 0.01, 99% chance the statistical relationships are not 'real'). The separation of this region into these categories is, however, supported by Sturm and Stuefer (2013). Their findings showed that both wind speed and the number of wind events are greater along the coast and decrease from the Lowlands towards the Uplands, which could also facilitate higher Lowland densities by developing a greater extent of wind slab.

Other than higher densities, the Lowlands also have shallower and less variable snow depths and SWEs (Fig. 1.4b and c, Table 1.2). Initially, both snow depth and SWE slightly

increase with increasing elevations, indicating a weak orographic effect near the ocean (Fig. 1.5b and c). However, at elevations greater than 225 m, an orographic effect is no longer apparent, which is believed to be a result of decreasing moisture content with distance from the ocean (Liston & Sturm, 2002; Kane et al., 2012). The variability of snow depths and SWEs are high for both the Lowlands and Uplands and on a whole, elevation relationships were statistically proven to not exist with significant probability (p-values < 0.01).

Overall, at a watershed scale, the survey data demonstrate a slight decrease in SWE with increasing elevation (Fig. 1.6). More specifically, there is a decrease of only 9.4 mm of SWE for every 1000 m of elevation gain. This is a significant difference compared with summer precipitation, which increases more than 200 mm for the same 1000 m elevation gain (Kane et al., 2000). Essentially, the present dataset illustrates that the average SWE at winter's end is relatively independent of elevation on Alaska's Central North Slope, with roughly an overall average of 10 cm of water from the Coastal Plain to the Mountains.

All of the measured SWE values represent a certain percentage of Alaska's Central North Slope. Some SWE values might characterize small-scale anomalies (local scale), while others might signify a large-scale area (regional scale). Since our interest was in identifying snowpack distribution patterns at a watershed scale, snow survey sites that represent local-scale snowpacks needed to be identified and removed. After analyzing the long-term dataset, it was concluded that basic snow survey site descriptions could be used to separate the survey locations into regional and local-scale representative sites. The decisions were made using on-site terrain, vegetation and snow pattern characteristics (i.e. windswept ridge, valley bottom depression, thick willows ~1 m tall, broad open and flat). Descriptions strongly analogous with snow drifting or scouring were classified as local-scale, while the remaining snow survey sites were left to represent the regional snowpack. Local-scale classifications were further divided into high and low water content subdivisions (i.e. wind-swept = Low SWE, drifted landscapes = High SWE). Fifty-five additional survey sites and surveys were not included as a result of only being surveyed one year and lacking detailed site descriptions.

Of the classified snow survey sites, 25% represented local-scale snowpacks (Fig. 1.6, Table 1.3). Most of the snow survey sites consistently represented their pre-described classification (time after time having high or low SWE), but some locations occasionally have

water contents outside their domain. The SWE measurements from local-scale features were removed to provide a more accurate representation of the regional snowpack.The removal of local-scale outliers had very little effect on the overall average SWE (changed from 103 to 105 mm) and trend line slopes (not shown in Figure). The slight change in slopes is a result of a greater percentage of drifting (high SWE) outliers in the Lowlands and wind-swept (low SWE) outliers in the Uplands. This tendency, which was expected, is a by-product of higher elevations having more areas that promote snow removal, while lower elevations have more depressions that enhance snow accumulation. For example, the mountains in the Upland region normally have more hilltops, ridges, steep slopes, and less vegetation, all of which characteristically are sites of snow erosion, while the Lowlands have more valley bottoms, surface water bodies, and vegetation for the snow to accumulate on and around. By using all of the SWE measurements, the snowpack distribution patterns can be obscured by local-scale influences. The removal of survey sites that represent local-scale anomalies provides a more accurate representation of the regional snowpack.

1.6.2 Yearly trend lines

Yearly trend lines were plotted to evaluate the stability of the snowpack in time and space (Fig. 1.7). The lower elevations illustrate a tighter grouping of average SWEs, while an increase in elevation results in greater yearly variability. The greater variability at higher elevations results from increased complexity in slope and topography, while lower elevations are generally more uniform. Nine of the fourteen surveyed years had negative sloping trend lines, while five years had positive sloping trends.

1.7 Discussion

Numerous experimental studies have been done on the distribution of snow (Martinec & Rango, 1981; Elder et al., 1991; Benson & Sturm, 1993; Sturm et al., 1995; Konig & Sturm, 1998; Anderton et al., 2004; Stuefer et al., 2014). Most snowpack spatial distribution studies in mountainous catchments, such as Anderton et al. (2004) and Elder et al. (1991), suggest that topographic controls are the most important influence on snow distribution. This study also suggests that topography plays an important role in the distribution of snow within Alaska's Central Arctic. Within the study area, findings indicated that spatial variability greatly increases with increasing elevation. What was not found, however, was a linear increase of winter

precipitation with increasing elevation, which is found in many regions (Golding et al., 1968; Singh & Kumar, 1997; Hanson, 2001). On the contrary, this study found a slight overall decrease in SWE from the Coastal Plain to the Mountains. Initially, an increase in winter precipitation occurs with increases in elevation, but that increase in precipitation is interrupted at 225 m. Above this level the amount of winter precipitation decreases with increasing elevation, which is analogous to increasing distance from the ocean. This finding correlates well with previous work which has shown moisture content to decrease with distance from the ocean (Liston & Sturm, 2002; Kane et al., 2012). Together these results suggest that in this region, winter precipitation is more dependent on available moisture rather than topographic controls and is under investigation for a subsequent paper.

In an attempt to identify snowpack distribution patterns and establish their stability in time and space at a watershed scale in Alaska's Central Arctic, small-scale anomalies were differentiated from regional-scale snowpack characteristics. Many of the snow-surveyed sites constantly represent either regional or local-scale snowpacks. The point-source sampling strategy was improved by sampling only locations that consistently provided SWEs that characterize the regional average snowpack, thus more representative data were collected.

1.8 Conclusions

The presently collected long-term snow dataset provides a rare opportunity to explore spatial- and temporal-scale variations over a large-scale area in the Alaska Arctic. Using this dataset allowed the identification of a snowpack distribution pattern at a regional scale. More specifically, it was determined that SWE measurements are affected by the location in which the surveys were conducted. Some locations consistently produce either extreme high or low SWE values and represent local-scale snowpack irregularities. Through survey site descriptions and classifications, these local-scale high and low SWE representative sites were identified and removed. The remaining snow survey sites were left to represent what was classified as the regional snowpack. The removal of local-scale SWE measurements had little effect on the record average SWE, which, as concluded was relatively independent of elevation on Alaska's Central North Slope, with roughly an average of 10 cm from the Coastal Plain to the Mountains. At the smaller scale, however, slight elevation-based snowpack patterns were identified above and below 225 m elevation. At the watershed scale, the overall lack of variability in SWE with

change in elevation was unexpected and inconsistent with summer precipitation patterns within this region and snow accumulation in most other regions. It is the authors' opinion that the discrepancy comes from this region being extremely moisture deprived during the frozen winter months and, therefore, that snowfall is dependent on moisture availability rather than topography.

1.9 Acknowledgments

This work was funded by the Alaska Department of Transportation and Public Facilities (ADOT&PF), National Science Foundation (NSF Snow-Net) OPP-0632160, Inland Northwest Research Alliance (INRA), and Alaska Department of Natural Resources (ADNR). We would like to thank all the faculty, staff, and graduate students who have assisted in collecting data over the years.

1.10 References

Anderton, S.P., White, S.M. & Alvera, B. 2004 Evaluation of spatial variability in snow water equivalent for a high mountain catchment. Hydrological Processes 18(3), 435-453. doi:10.1002/hyp.1319

Benson, C.S. 1982 Reassessment of winter precipitation on Alaska's Arctic slope and measurement on the flux of wind blown snow: Report UAG R-288, Geophysical Institute, University of Alaska, 26 pp.

Benson, C.S. & Sturm, M. 1993 Structure and wind transport of seasonal snow on the Arctic Slope of Alaska. Annals of Glaciol. 18, 261-267.

Cavm Team 2003 Circumpolar Arctic Vegetation Map. Scale 1 : 7,500,000. Conservation of Arctic Flora and Fauna (CAFF) Map No. 1. U.S. Fish and Wildlife Service, Anchorage, Alaska.

Debeer, C.M. & Pomeroy, J.W. 2009 Modelling snow melt and snowcover depletion in a small alpine cirque, Canadian Rocky Mountains. Hydrological Processes 23(18), 2584-2599.

Elder, K., Dozier, J. & Michaelsen, J. 1991 Snow accumulation and distribution in an alpine watershed. Water Resources Research 27(7), 1541-1552.

Golding, D.L., Branch, C.F. & Laboratory, F.R. 1968 Snow Measurement on Marmot Creek Experimental Watershed: Forestry Branch.

Hall, D., Chang, A. & Foster, J. 1986 Detection of the depth-hoar layer in the snow-pack of the Arctic coastal plain of Alaska, USA, using satellite data. Journal of Glaciology 32(110), 87-94.

Hall, J.V., Wilen, B.O., Frayer, W.E., US Fish & Wildlife Service 1994 Status of Alaska wetlands. Anchorage, Alaska: U.S. Fish & Wildlife Service, Alaska Region.

Hanson, C.L. 2001 Long-Term Precipitation Database, Reynolds Creek Experimental Watershed, Idaho, United States. Water Resources Research 37(11), 2831-2834.

Hinzman, L.D., Kane, D.L. & Gieck, R.E. 1991 Regional snow ablation in the Alaskan Arctic. In: Northern Hydrology: Selected Perspectives, Proceeding of Northern Hydrology Symposium (T.D. Prowse & C.S.L Ommanney, eds.). Saskatoon, Saskatchewan, CAN, pp.121-139.

Homan, J.W., Luce, C.H., Mcnamara, J.P. & Glenn, N.F. 2010 Improvement of distributed snowmelt energy balance modeling with MODIS-based NDSI-derived fractional snow-covered area data. Hydrological Processes. doi:10.1002/hyp.7857

Kane, D.L. & Hinzman, L.D. 1988 Permafrost hydrology of a small arctic watershed. In: Proceedings: Fifth International Conference on Permafrost (K. Senneset, ed.). Trondheim, Norway, pp. 590-595.

Kane, D.L., Hinzman, L.D., Benson, C.S. & Liston, G.E. 1991 Snow hydrology of a headwater arctic basin. 1. Physical measurements and process studies. Water Resources Research 27(6), 1099-1109.

Kane, D.L., Hinzman, L.D., Mcnamara, J.P., Zhang, Z. & Benson, C.S. 2000 An overview of a nested watershed study in Arctic Alaska. Nordic Hydrology 31(4-5), 245-266.

Kane, D.L., Gieck, R.E., Kitover, D.C., Hinzman, L.D., Mcnamara, J.P. & Yang, D.Q. 2004 Hydrological cycle on the North Slope of Alaska. In: Northern Research Basins Water Balance (D.L. Kane & D. Yan, eds.). IAHS Publ. 290. IAHS, Wallingford, UK, pp. 224-236.

Kane, D.L., Gieck, R.E. & Hinzman, L. 2008a Water balance for a low-gradient watershed in Northern Alaska. In: Proceedings Ninth International Conference on Permafrost (D.L. Kane & K.M. Hinkel, eds). UAF Press, Fairbanks, Alaska, USA, pp 883-888.

Kane, D.L., Hinzman, L.D., Gieck, R.E., Mcnamara, J.P., Youcha, E.K. & Oatley, J.A. 2008b Contrasting extreme runoff events in areas of continuous permafrost, Arctic Alaska. Hydrology Research 39(4), 287-298.

Kane, D.L., Youcha, E.K., Stuefer, S., Toniolo, H., Schnabel, W., Gieck, R.E., Myerchin-Tape, G., Homan, J.W., Lamb, E. & Tape, K. 2012 Meteorological and Hydrological Data and Analysis Report for the Foothills/Umiat Corridor and Bullen Projects: 2006-2011. University of Alaska Fairbanks, Water and Environmental Research Center, Report INE/WERC 12.01, Fairbanks, Alaska, p 260.

Kojima, K. 1966 Densification of seasonal snow cover. International Conference on Low Temperature Science, vol. 1(2)Institute of Low Temperature Science, Hokkaido University, Sapporo, Japan, pp. 929–952.

Konig, M. & Sturm, M. 1998 Mapping snow distribution in the Alaskan Arctic using aerial photography and topographic relationships. Water Resources Research 34(12), 3471-3483. doi:1029/98WR02514.

Liston, G.E. & Sturm, M. 2002 Winter precipitation patterns in arctic Alaska determined from a blowing-snow model and snow-depth observations. Journal of Hydrometeorology 3(6), 646-659.

Martinec, J. & Rango, A. 1981 Areal Distribution of Snow Water Equivalent Evaluated by Snow Cover Monitoring. Water Resour. Res. 17. doi:10.1029/WR017i005p01480

McNamara, J.P., Kane, D.L. & Hinzman, L.D. 1998 An analysis of streamflow hydrology in the Kuparuk River basin, Arctic Alaska: A nested watershed approach. Journal of Hydrology 206(1-2), 39-57.

Osterkamp, T.E. 1984 Temperature measurements in permafrost. Report FHWQ-AK-RD-85-11, Alaska DOTPF. Fairbanks, Alaska, 87.

Pomeroy, J. & Gray, D. 1995 Snowcover accumulation, relocation and management. Bulletin of the International Society of Soil Science no 88(2).

Prasad, R., Tarboton, D.G., Liston, G.E., Luce, C.H. & Seyfried, M.S. 2001 Testing a blowing snow model against distributed snow measurements at Upper Sheep Creek, Idaho, United States of America. Water Resources Research 37(5), 1341-1356.

Rovansek, R.J., Kane, D.L. & Hinzman, L. 1993 Improving estimates of snowpack water equivalent using double sampling. Proceedings of the 61st Western Snow Conference, 157-163.

Seyfried, M.S. & Wilcox, B.P. 1995 Scale and the nature of spatial variability - field examples having implications for hydrologic modeling. Water Resources Research 31(1), 173-184.

Singh, P. & Kumar, N. 1997 Effect of orography on precipitation in the western Himalayan region. Journal of Hydrology 199(1–2), 183-206.

Stuefer, S., Kane, D.L. & Liston, G.E. 2013 In situ snow water equivalent observations in the US Arctic. Hydrology Research 44(1), 21-34.

Stuefer, S.L., Homan, J.W., Kane, D.L., Gieck, R.E. & Youcha, E.K. 2014 Snow Survey Results for the Central Alaskan Arctic, Arctic Circle to Arctic Ocean: Spring 2013 Water and Environmental Research Center.

Sturm, M. & Stuefer, S. 2013 Wind-blown flux rates derived from drifts at arctic snow fences. Journal of Glaciology 59(213), 21-34.

Sturm, M. & Wagner, A.M. 2010 Using repeated patterns in snow distribution modeling: An Arctic example. Water Resour. Res. 46(12), W12549.

Sturm, M., Holmgren, J. & Liston, G.E. 1995 A Seasonal Snow Cover Classification System for Local to Global Applications. Journal of Climate 8(5), 1261-1283.

Sturm, M., Racine, C. & Tape, K. 2001 Climate change: Increasing shrub abundance in the Arctic. [10.1038/35079180]. Nature 411(6837), 546-547.

Sturm, M., Douglas, T., Racine, C. & Liston, G.E. 2005 Changing snow and shrub conditions affect albedo with global implications. J. Geophys. Res. 110(G1), G01004.

Sturm, M., Taras, B., Liston, G.E., Derksen, C., Jonas, T. & Lea, J. 2010 Estimating Snow Water Equivalent Using Snow Depth Data and Climate Classes. Journal of Hydrometeorology 11(6), 1380-1394.

Tape, K.E.N., Sturm, M. & Racine, C. 2006 The evidence for shrub expansion in Northern Alaska and the Pan-Arctic. Global Change Biology 12(4), 686-702.

Walker, D.A., Binnian, E., Evans, B.M., Lederer, N.D., Nordstrand, E. & Webber, P.J. 1989 Terrain, vegetation and landscape evolution of the R4D research site, Brooks-Range-Foothills, Alaska. Holarctic Ecology 12(3), 238-261.

Winstral, A., Elder, K. & Davis, R.E. 2002 Spatial Snow Modeling of Wind-Redistributed Snow Using Terrain-Based Parameters. Journal of Hydrometeorology 3(5), 524.

1.11 Figures

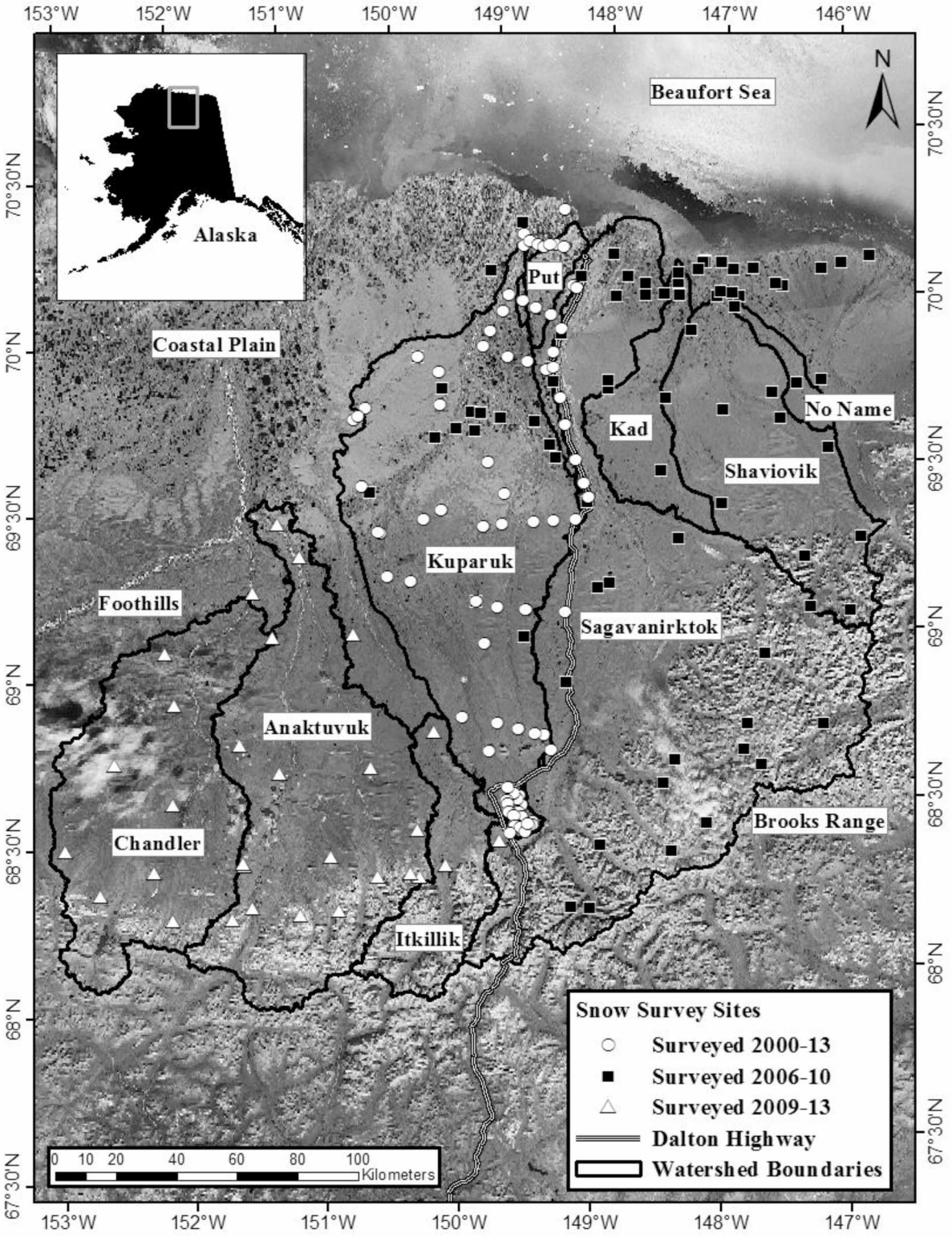

Figure 1.1: Site map showing snow survey locations within several Central Alaska North Slope watersheds.

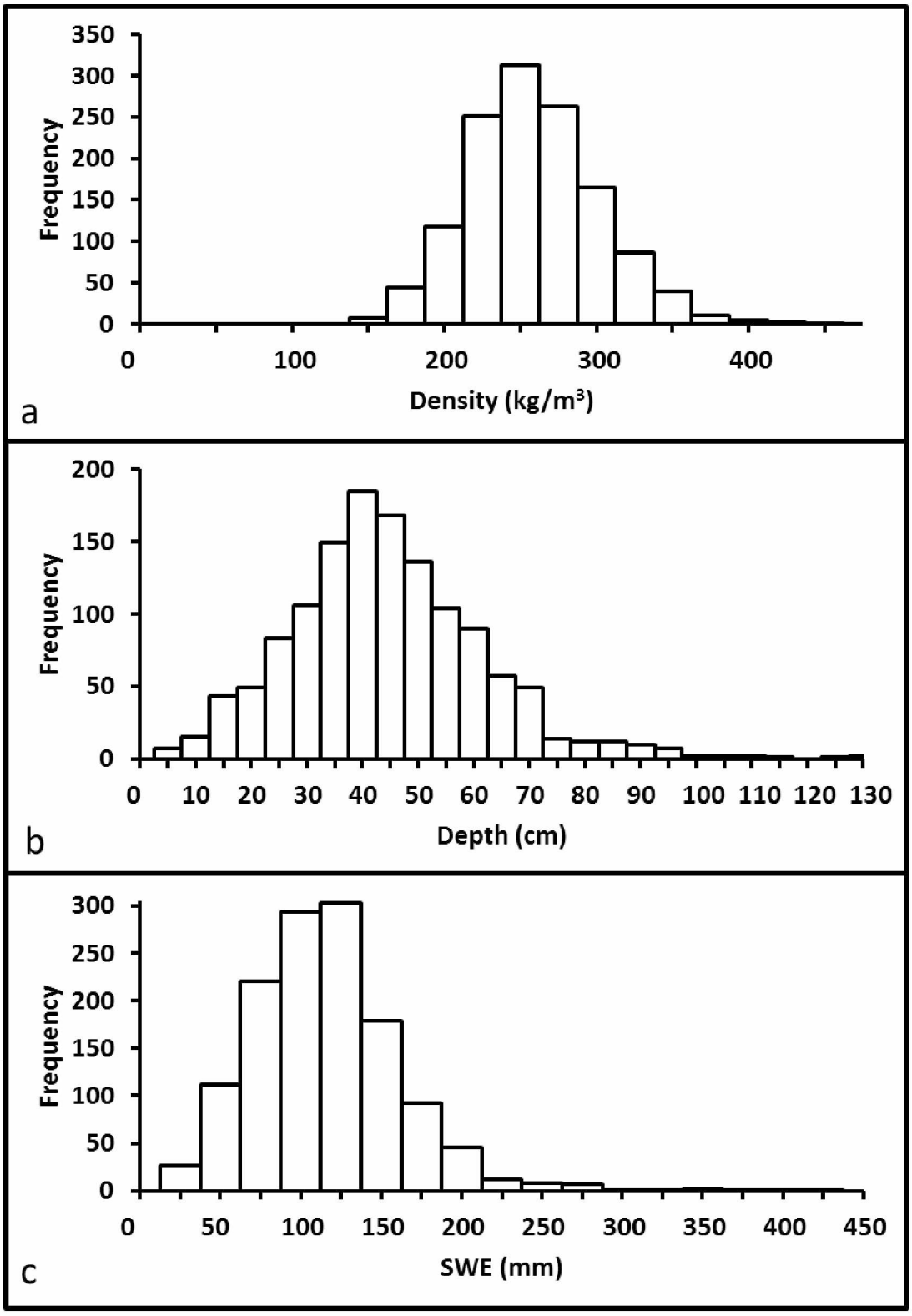

Figure 1.2: Frequency distributions for the complete record of snow densities, depths, and SWEs. Densities have a nearly symmetric distribution, while snow depth and SWE have asymmetric distributions.

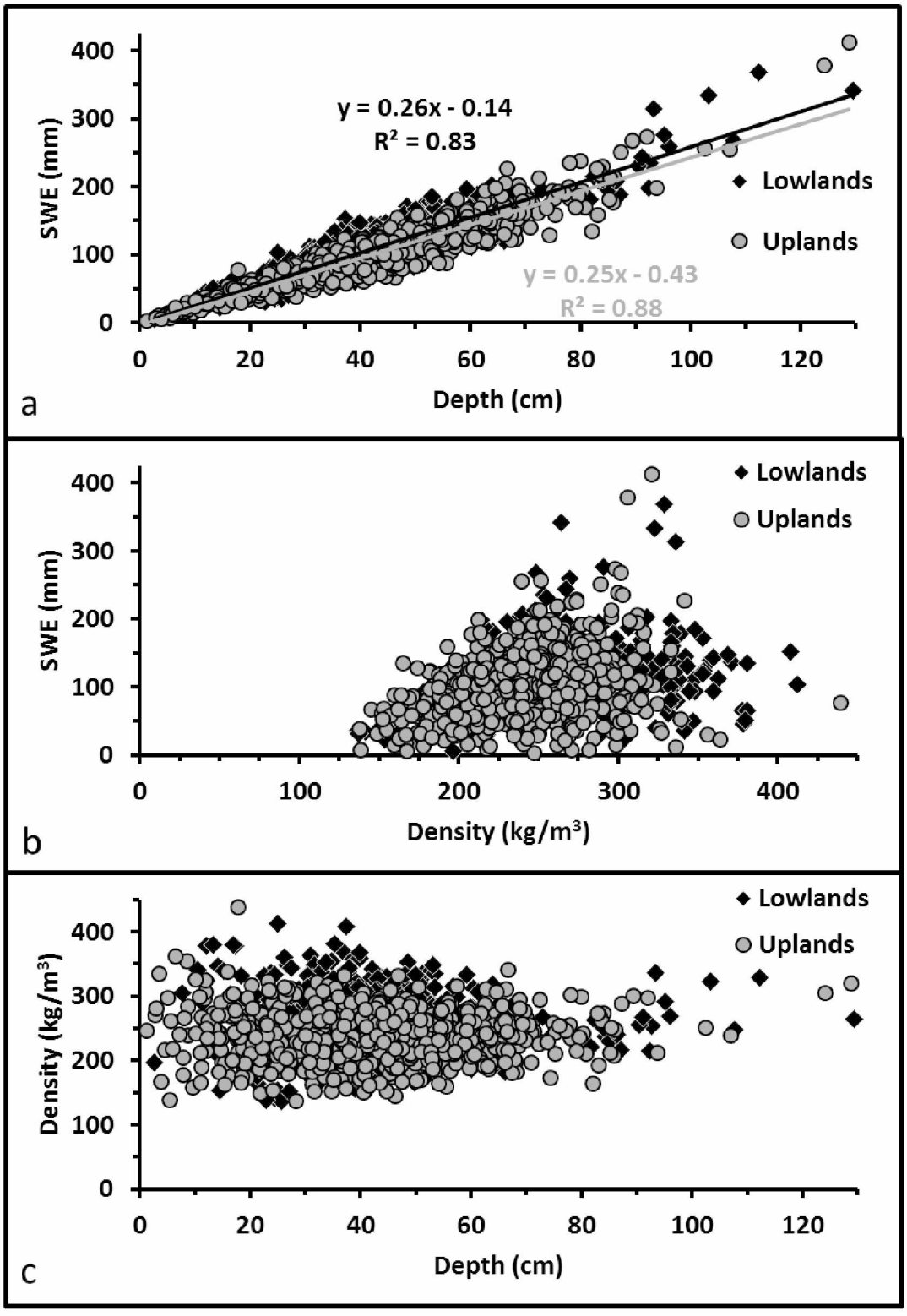

Figure 1.3: Scatter plots to assess similarity between SWE and snow depths compared with density.

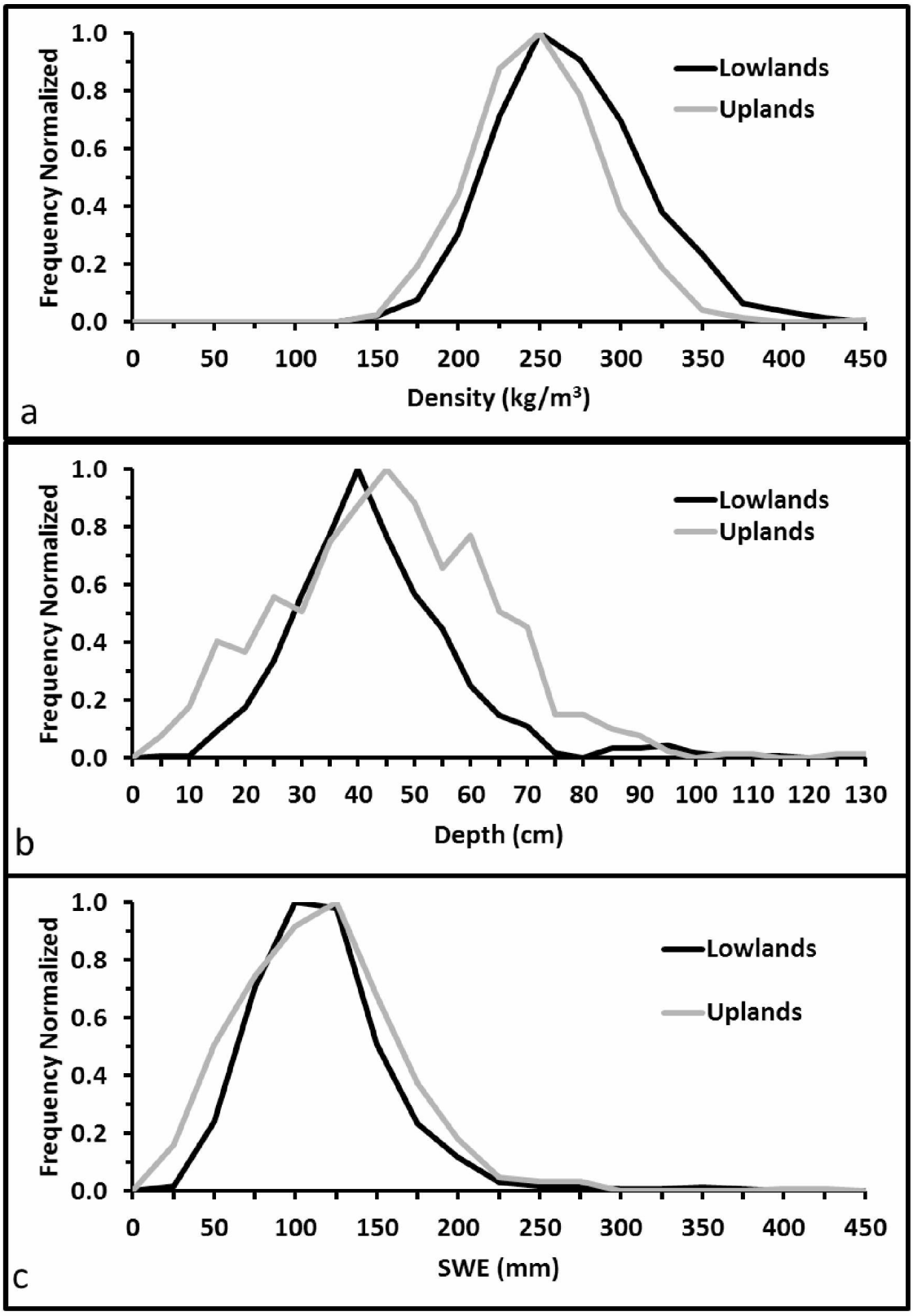

Figure 1.4: Probability distribution plots to demonstrate the differences in snow densities, depths, and SWEs between the Lowland and Upland regions.

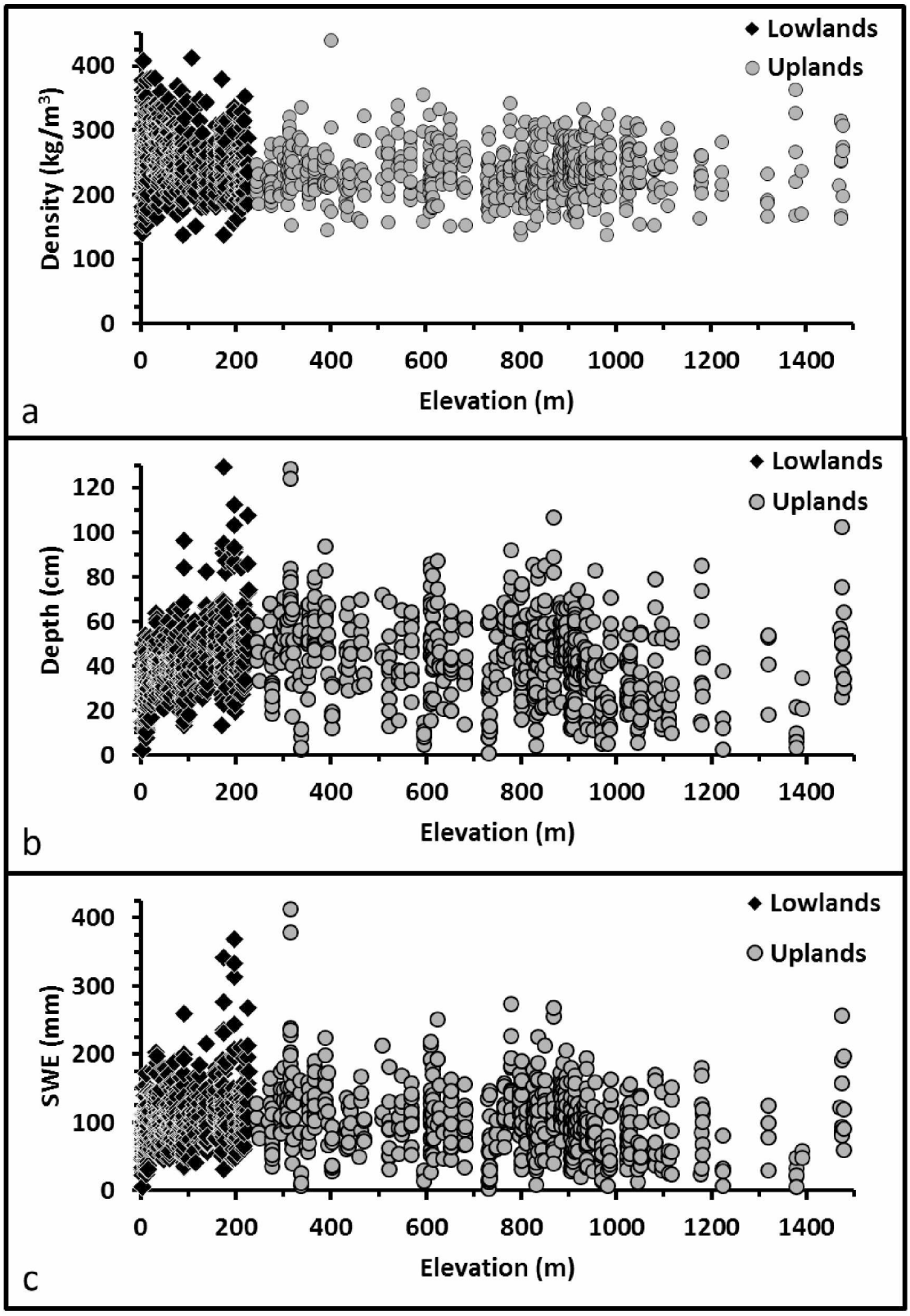

Figure 1.5: Distribution curves to illustrate the correlation between snow densities, depths, and SWEs to elevation.

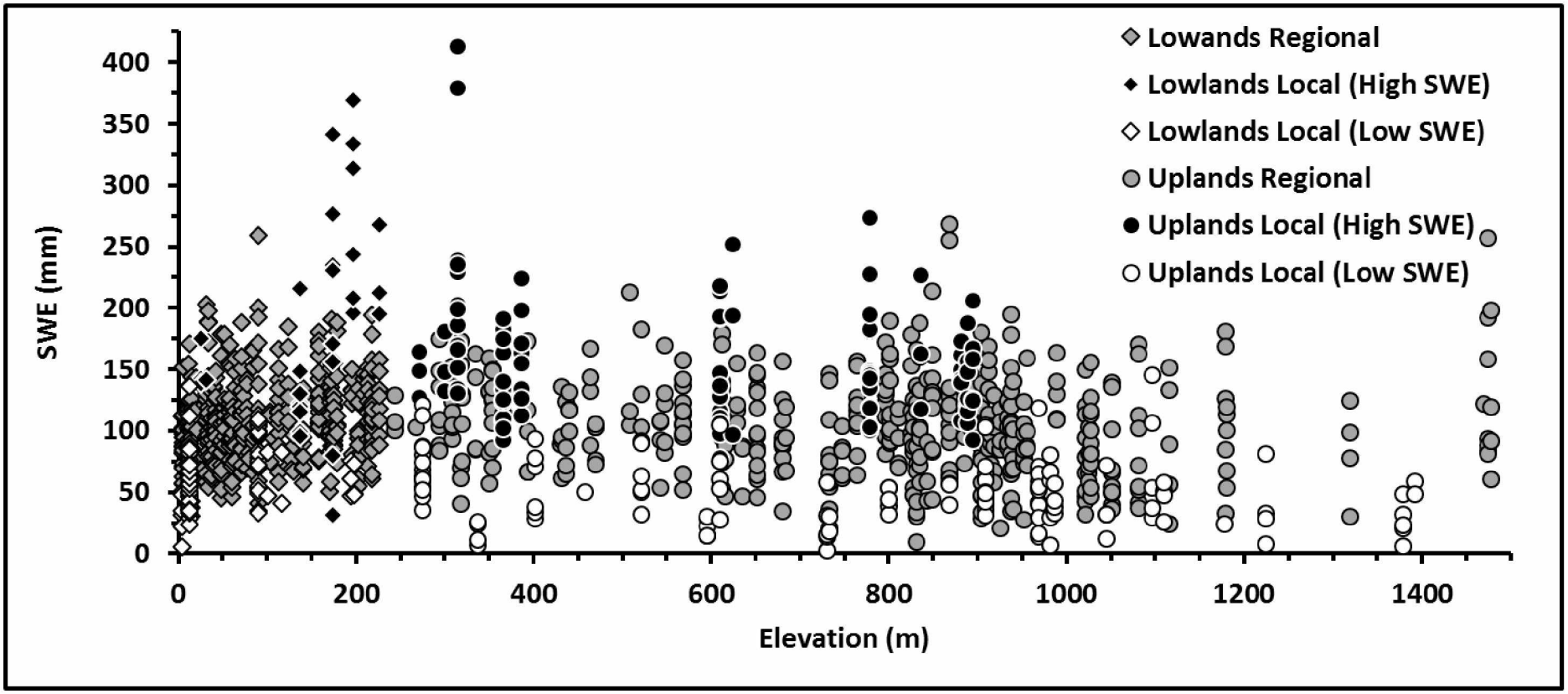

Figure 1.6: Classified (high and low SWE local-scale and regional-scale) SWE values plotted against snow survey site elevation. Differentiation between Lowlands and Uplands is also indicated by symbol changes at the 225 m elevation boundary. Record averaged SWE from the Coastal Plain to the Brooks Range is 103 mm, with only a 9.4 mm decrease in SWE over a 1000 m elevation change. With the removal of local-scale outliers the change in SWE was reduced to a 2.7 mm decrease for the same 1000 m elevation change.

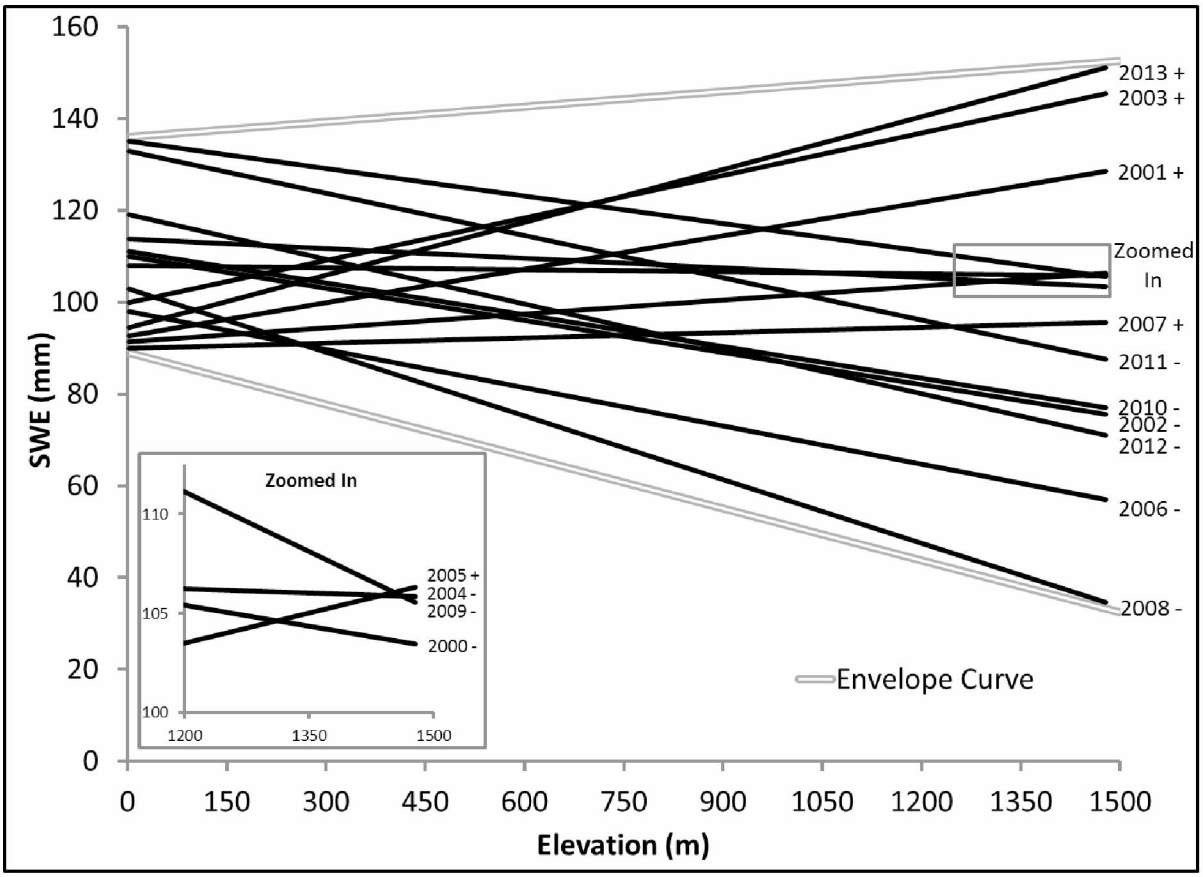

Figure 1.7: Yearly trend lines using annual datasets for the 14 year record illustrate the temporal and spatial variability of the snowpack. Yearly slope directions (positive (+) or negative (-)) are specified after year of trend line labels. Nine years have negative trends with elevation, while five have positive.

1.12 Tables

Table 1.1: Yearly (2000–2013) end-of-winter snowpack characteristics for the entire study domain; including sample size, mean, standard deviation (Stdev), range, minimum and maximum.

	Depth	Density	SWE	Depth	Density	SWE	Depth	Density	SWE	Depth	Density	SWE
	cm	kg/m^3	mm	cm	kg/m^3	mm	cm	kg/m^3	mm	cm	kg/m^3	mm
Year		2000			2001			2002			2003	
Sample Size		65			85			85			86	
Mean	47	236	111	44	237	103	43	238	100	43	264	113
Stdev	13	26	35	16	36	38	15	38	36	14	41	40
Range	70	167	181	79	198	205	82	208	160	78	260	210
Min	14	168	30	14	183	29	12	151	39	14	179	33
Max	84	335	210	93	380	235	94	359	199	91	439	243
Year		2004			2005			2006			2007	
Sample Size		56			81			118			150	
Mean	42	259	107	38	251	96	38	231	88	39	238	92
Stdev	13	39	36	17	37	44	13	49	34	17	45	43
Range	69	190	191	75	202	218	75	242	186	92	237	311
Min	15	182	39	8	137	21	11	137	21	1	141	3
Max	84	371	230	82	339	239	87	380	208	93	378	314
Year		2008			2009			2010			2011	
Sample Size		106			143			104			77	
Mean	34	237	83	50	258	126	39	260	101	47	248	119
Stdev	16	49	46	22	48	61	15	40	41	22	39	65
Range	101	269	328	122	255	399	73	187	221	118	210	356
Min	3	138	5	8	157	14	5	155	15	6	153	23
Max	103	408	334	129	412	413	78	342	236	124	363	380
Year					2012			2013				
Sample Size					73			76				
Mean				40	258	104	47	237	112			
Stdev				15	39	42	18	36	47			
Range				72	203	221	84	177	240			
Min				3	152	6	4	159	12			
Max				75	356	228	87	336	252			

Table 1.2: Record average end-of-winter (2000–2013) snowpack characteristics for the entire study domain, Lowlands and Uplands; including sample size, mean, standard deviation, range, maximum and minimum.

	Study Domain			Lowlands (<225 m)			Uplands (>225 m)		
	Depth	Density	SWE	Depth	Density	SWE	Depth	Density	SWE
	cm	kg/m^3	mm	cm	kg/m^3	mm	cm	kg/m^3	mm
Sample Size		1305			631			674	
Mean	42	246	103	41	256	104	43	237	102
Standard Deviation	17	43	47	15	45	44	19	39	50
Range	128	302	410	127	275	364	128	301	410
Min	1	137	3	3	137	5	1	138	3
Max	129	439	413	129	412	369	129	439	413

Table 1.3: Record snow survey information for the entire study domain, regional-scale and local-scale (high and low water contents subdivisions) representative areas; including number of survey sites and surveys, percentage of survey in each subdivision along with SWE averages and ranges.

	Total / Average	Regional-Scale	Local-scale	
			High SWE	Low SWE
# Survey Sites	186	136	18	32
# Surveys	1250	940	124	186
% of Total Surveys		75%	10%	15%
Average SWE (mm)	103	105	168	53
Range (mm)	410	259	381	143

Chapter 2 Warm Season Precipitation Patterns in the Alaska Central Arctic[1]

2.1 Abstract

Environmental change currently stimulates much of the interest in high-latitude hydrologic studies, as northern areas are expected to be strongly impacted by warming. Most published evidence for changes in Arctic precipitation patterns results from reanalysis and climate model simulations. In an effort to determine both temporal variability and spatial distribution of warm season precipitation based on field measurements, data from 31 meteorological stations, ranging in record length from 2 to 29 years and distributed throughout the Alaska Central Arctic, were analyzed. This data illustrates a strong spatial relationship, with warm season precipitation linearly increasing from approximately 80 mm near the Arctic Ocean to 300 mm at the continental divide of the Brooks Range. No discernible trends in warm season precipitation were found during somewhat limited 29-year period; however, years of very low (2007) and high (1999 and 2002) precipitation occurred during the study period (1985–2013). Monthly, warm season precipitation patterns show that maximum precipitation generally occurs in July, followed by August and June. May and September are transitional months when both rain and snow can occur. We conclude that a longer record is required before long-term trends can be examined for warm season precipitation.

---

[1] Homan, J.W., Kane, D.L. & Stuefer, S.S., Warm season precipitation patterns in the Alaska Central Arctic, Submitted to *Arctic, Antarctic, and Alpine Research*.

2.2 Introduction

The global hydrologic cycle is a complex web of continuous fluxes of water among its major reservoirs. There are three major features of the global hydrologic cycle: (1) the oceans lose more water by evaporation then they gain by precipitation; (2) the land surfaces receive more water as precipitation than they lose by evapotranspiration; and (3) the excess of water on the land returns to the oceans as runoff, balancing the deficit in the ocean-atmosphere exchange. In order to produce hydrologically significant rates of precipitation in the second feature of the global hydrologic cycle, air containing water vapor must be cooled to its dew point. A parcel of air can lose heat in several ways, but only vertical uplift of the air can cause rates of cooling high enough to produce significant precipitation. Therefore, regions characterized by rising air tend to have relatively high average precipitation, and those characterized by descending air tend to have low precipitation.

Large-scale atmospheric circulation patterns are known to exist and vary depending on latitude and time of year. Based on general circulation patterns, the Earth's atmosphere has these relatively fixed regions characterized by large-scale rising air and other regions with descending air. Because precipitation rates are also influenced by topography, air temperature, frontal activity, and wind directions in relation to moisture sources, global precipitation patterns show significant deviations from the idealistic general latitudinal distribution patterns. The major causes of these deviations are mountain ranges, such as the Himalayas, Alps, and Rocky Mountain–Andean chain. Mountain ranges induce high rates of precipitation in their immediate vicinity and typically produce "rain-shadow" zones of reduced precipitation over significant areas leeward of the prevailing winds.

Northern Alaska is a good example of the complex climatology of precipitation. Undoubtedly, geographical latitude is the main factor determining the weather and climate in the Arctic. Being located at such high latitudes significantly limits the magnitude of incoming solar energy, which subjects the area to climate extremes. The Arctic receives no solar radiation during the winter solstice, with the polar night lasting between 23 and 176 days (68° and 90°, respectively), and receives continuous solar energy over the summer solstice, with the polar day persisting between 40 and 189 days (68° and 90°, respectively).

The climate of northern Alaska is not well documented owing to the sparsity of meteorological stations and the discontinuity in observations. It is known that the mean annual temperatures are well below freezing. Winters are long and cold, with high winds and blowing snow in essentially a treeless environment. Summers are cool and cloudy along the coast, but are warmer further inland. The climate is strongly influenced by the ocean, not only during the summer months, but also during the winter months (Haugen and Brown, 1980; Zhang et al., 1996, 1997).

Along with latitudinal and oceanic influences, the climate of Alaska's Arctic is also greatly affected by topography. The Brooks Range provides a natural barrier that separates the Arctic climatically from the rest of Alaska. This east–west-oriented barrier greatly reduces moisture availability from storms that otherwise would bring precipitation from the south. The blockage of moisture from the south by both the Brooks Range and the Alaska Range results in a rain shadow effect across the Alaska Arctic, which contributes to it having the least amount of precipitation in the state (Perica et al., 2012).

During the winter, about eight months of the year, the Arctic Ocean along the northern coast of the Alaska Arctic has ice cover. During the summer, however, the Arctic Ocean becomes an available local source of moisture for precipitation. The combination of open water (Screen and Simmonds, 2010) and higher temperatures (Screen and Simmonds, 2010; Kane et al., 2012) allows for greater atmospheric moisture content compared with other seasons, making summer the time of year with greatest amounts of precipitation (Shulski and Wendler, 2007; Kane et al., 2012). Precipitation is at a minimum in late winter to spring (March, April, and May), when temperatures are low and there is a lack of significant open water as a moisture source for snow-producing storms.

Multiple studies indicate that the Arctic is warming (i.e. Serreze et al., 2000; Hinzman et al., 2005; Wendler and Shulski, 2009; Rawlins et al., 2010). How will this warming impact the annual precipitation pattern in the Arctic? Possible scenarios include less snowfall and greater warm season precipitation due to longer summers and shorter winters (IPCC, 1996, 2001), a larger ice-free area of the Arctic Ocean with a longer ice-free duration (Maslanik et al., 1999; Vinnikov et al., 1999; Cavalieri et al., 2003), and more extreme summer precipitation events (Kane et al., 2008). We cannot confidently predict what this impact will be. Presently, large

swings in annual precipitation occur in this extreme environment; changes in the magnitude and timing of this component of the hydrologic cycle could have significant ecological impacts (Kane et al., 2008). Past observational studies of warm season precipitation in the Arctic are limited in duration and scale. The sparsity of meteorological stations and the discontinuity in observations is primarily responsible for our inadequate knowledge base. In order to make future precipitation pattern comparisons, a comprehensive assessment of warm season precipitation must be made. This case study reported here is of warm season precipitation observations mainly from a number of research projects in the Alaska Central Arctic using the most homogeneous dataset available. Both temporal variability and spatial distribution of warm season precipitation are examined and quantified using data collected from a combined network of meteorological stations during the past three decades. All liquid precipitation data used in this investigation was collected using shielded rain gauges to ensure the highest reliability of data.

2.3 Background

Long-term hydrologic studies in the Arctic are notoriously limited and therefore of short duration. Historically, the collection of hydrologic and meteorological datasets has been in response to resource development. While hydrologic activity in the Alaska Arctic is limited spatially and temporally, a few data collection efforts and hydrologic studies have been carried out since the early 1970s (Kane et al., 2000; Kane et al., 2014). The logistical cost of installing, maintaining, and accessing these unstaffed sites is the main impediment that results in a minimal hydrologic network. The first sustained hydrologic data-collection effort north of the Brooks Range began after oil was discovered in Prudhoe Bay in November 1968. The U.S. Geological Survey (USGS) established three stream gauging stations along the Dalton Highway and on the oilfield (Kuparuk, Sagavanirktok, and Putuligayuk Rivers). Unfortunately, additional complementary data, such as precipitation (both solid and liquid) from the coast south into the Brooks Range, were almost completely lacking, which deterred precipitation/runoff studies. In the mid-1980s, some small hydrologic research studies were initiated north of the Brooks Range, and this effort expanded during the next three decades.

Currently, concerns about climate change have motivated much of the interest in high-latitude hydrologic studies, as northern areas are expected to be more strongly impacted by climate warming (ACIA, 2005). Evidence indicates ongoing changes to many aspects that impact

the hydrologic cycle in the Arctic: shorter seasonal snow cover season (Robinson, 1993; Curtis et al., 1998; Brown, 2000; Robinson and Frei, 2000), increases in surface air temperature (Stafford et al., 2000; Johannessen et al., 2004; Wendler and Shulski, 2009), later freeze-up and earlier breakup of lake and river ice (Magnuson et al., 2000), permafrost warming (Lachenbruch and Marshall, 1986; Romanovsky et al., 2010), increased active-layer thickness (Overduin and Kane, 2006), accelerated wasting of glacier mass (Arendt et al., 2002), increased river discharge (Peterson et al., 2002; ACIA, 2005), reduction of sea ice cover (IPCC, 1996; Vinnikov et al., 1999; Cavalieri et al., 2003), and rise in sea level (IPCC, 2001). Because these high-latitude data records are generally of short duration, it is frequently difficult to distinguish statistically sound trends. All these data records, however, do illustrate the same trend (Serreze et al., 2000; Hinzman et al., 2005; Rawlins et al., 2010): the system is in a warming phase, and intensification of the hydrologic cycle is ongoing.

Not conclusive are trends involving precipitation and evapotranspiration. The Intergovernmental Panel on Climate Change (IPCC, 1996, 2001) has consistently reported twentieth-century precipitation increases in northern high latitudes (55°–85°N). For the period since 1960, the gauge-adjusted and basin-averaged data of Serreze et al. (2002) show no discernible trends in mean annual precipitation over the Ob, Yenisey, Lena, and Mackenzie Basins. However, summer precipitation over the Yenisey Basin decreased by 5 to 10% over the four decades since 1960 (Serreze et al., 2002). Trends of annual evapotranspiration reanalyzed by the National Centers for Environmental Prediction/National Center for Atmospheric Research (NCEP/NCAR) are negative in the Ob Basin and positive in the Yenisey and Mackenzie Basins. The uncertainties concerning precipitation and evapotranspiration emphasize the sparse short-term network of *in situ* measurements and the compounding effects of elevation in topographically complex regions of the Arctic, where the distribution of observing stations is biased toward low elevations and coastal regions.

Based on a summary of numerous studies, McAfee et al. (2013) noted different conclusions (both increasing and decreasing) on precipitation trends in Alaska. What is known about the Alaska Arctic is that precipitation in the form of snow plays a dominate role in the hydrologic cycle. Snow may accumulate on the ground for nine months with little to no melt and then ablate in a relatively short time, typically 10 to 14 days just before the summer solstice (Kane et al., 2008). The total water content of the snowpack at the end of winter is on average

100 to 110 mm across the Alaska Central Arctic (Stuefer et al., 2013; Homan and Kane, 2015) and comprises 30 to 40% of the annual precipitation (Kane et al., 2008). The distribution of snowfall is relatively independent of elevation (Homan and Kane, 2015), while warm season precipitation varies considerably from the coast to the headwaters in the Brooks Range (Kane et al., 2000). This rainfall study by Kane et al. (2000) was of data with a short duration, however, prohibiting any meaningful statistical analyses; the longevity of basin studies in the Alaska Arctic pales in comparison with the longevity of basin studies in temperate climates.

2.4 Study Domain

The study domain consists of a 200 by 240 km region of the Alaska Central Arctic that is bound by the Brooks Range on the south and the Arctic Ocean on the north, and includes the Chandler, Anaktuvuk, Itkillik, Kuparuk, Putuligayuk (Put), Sagavanirktok (Sag), Kadleroshilik (Kad), and Shaviovik River watersheds (Fig. 2.1, Table 2.1). All of the watersheds drain north and eventually empty into the Arctic Ocean or another stream that ultimately discharges into the Arctic Ocean. The Putuligayuk lies entirely within the Coastal Plain region; the Kuparuk and Kadleroshilik Rivers emanate from the Foothills and cross the Coastal Plain; the Sagavanirktok, Shaviovik, Kavik, Itkillik, Anaktuvuk, and Chandler Rivers originate in the Brooks Range and cross both the Foothills and Coastal Plain. The southern and northern boundaries of the domain are between 68°N and 70°N latitude, while the western and eastern boundaries are between 153°W and 146°W longitude. Elevation within the study area ranges from sea level to 2675 m. The topography of the area is characterized by a flat northern portion (generally referred to as Coastal Plain), by gently rolling hills and valleys (Foothills), and by mountain ridges (Mountains) of the Brooks Range to the south.

The entire study area is underlain by continuous permafrost (250 to 300 m in the Brooks Range and up to 600 m along the coast (Osterkamp, 1984)) and, on average, is snow-covered 8 to 9 months of the year. The region is mostly treeless with some patches of trees in the riparian areas in the Foothills. Vegetation consists of alpine plant communities in the Mountains, tussock tundra in the Foothills, and sedge tundra on the Coastal Plain (Walker et al., 1989; CAVM Team, 2003). Willow and birch shrubs are common in riparian areas, and shrub height is variable, from approximately 0.3 to over 1 m. In response to climate warming in the Arctic, shrubs in tundra

areas are increasing in abundance and extent (Sturm et al., 2001; Sturm et al., 2005; Tape et al., 2006).

2.5 Meteorological Stations

In order to obtain good spatial and temporal precipitation patterns, a network of widespread meteorological stations is required for an informative duration. Consequently, this project used meteorological stations from a collection of different organizations and research projects (Fig. 2.1, Table 2.1). Initially, meteorological stations were logistically established across the Alaska Central Arctic based on the ease of access from the Dalton Highway. At the summit of Atigun Pass, the U.S. Department of Agriculture (USDA), National Resources Conservation Service (NRCS) installed a station in 1983. Subsequently, during the 1980s and 1990s, the University of Alaska Fairbanks (UAF), Water and Environmental Research Center (WERC) installed several more stations along the road from the Foothills to the Coastal Plain (mostly in the Kuparuk River Basin). In addition to the road stations, WERC installed stations in the Bullen/Sagavanirktok area (east of the Dalton Highway to the Canning River) and the Umiat Corridor/Kuparuk Foothills area (west of the Dalton Highway to the Umiat area) from 2006–2011 and 2009–2013, respectively. Meteorological data from the U.S. Bureau of Land Management (BLM) station (2008–2012) located in Umiat were also used in this investigation of the spatial and temporal variability of warm season precipitation. Not all available meteorological stations were used in this study. For example, several stations in the Upper Kuparuk watershed were not used because of their proximity to each other relative to the overall network spacing described here. Only 7 of the 31 stations used in this investigation exist as of 2015, the others having been removed recently with the completion of research projects. Of the 31 meteorological stations, 30 of them measured hourly warm season precipitation with an 8-inch standard tipping-bucket gauge surrounded by an Alter (wind) shield. The remaining meteorological station (Atigun Pass) provided daily precipitation measurements using a Wyoming fence with 12-inch US precipitation gauge equipped with pressure transducer. All meteorological stations are unattended and only visited by technicians once or twice a year. A known problem with most precipitation gauges is the undercatch of precipitation. Though we recognize that precipitation undercatch is a potential source of error, we did not make corrections to the data used in this study.

2.6 Results

One of the goals of this study was to evaluate precipitation patterns using data collected from a combined network of meteorological stations across the Alaska Central Arctic. Specifically, the objective was to quantify spatial and temporal precipitation patterns during the warm season. Warm season precipitation is defined as precipitation that occurs after spring ablation (generally mid-May to early June) and before the initiation of winter snow accumulation (mid-September). Precipitation during this warm season mostly falls in the form of rain, but occasionally as snow that quickly melts or as a mixed precipitation event (Kane et al., 2008). For water balance calculations and hydrologic model input, it is important to accurately quantify all forms of precipitation at watersheds. Long-term data collections are imperative for the evaluation of frequency estimates and changing patterns (which are crucial indicators of climate change).

Using the network of meteorological stations, warm season precipitation can be examined over the entire Alaska Central Arctic. Ideally, all 31 stations would have the same collection duration, but that is not the case, unfortunately (Fig. 2.2, Table 2.1). The number of stations in the Alaska Central Arctic has ranged from as few as 2 (mid-1980s) to as many as 25 (2009); Franklin Bluffs, however, did not have a complete data record in 2009, making 24 working stations the largest annual record both in 2009 and 2010. We can still draw some conclusions from the limited dataset. Figure 2.3 shows the record mean warm season precipitation for each of the 31 stations plotted against elevation, while Figure 2.4 is an isohyetal map, where the record mean warm season precipitation data have been interpolated across the study domain using the Barnes (1964) convergent weighted-averaging interpolation scheme. The spatial patterns from both Figures 2.3 and 2.4 illustrate that less warm season precipitation occurs at lower elevations along the Coastal Plain, but increases linearly with increasing elevation (in the southerly direction). The maximum warm season precipitation gradient is generally south, but from year to year, it can deviate slightly to the east or west. Record mean warm season precipitation varies from less than 80 mm on the Coastal Plain to nearly 320 mm in the Mountains. Figure 2.5 shows the cumulative warm season precipitation for all stations available in 2009 (one of the years with the largest number of stations) and iterates the spatial variability of warm season precipitation and its increase with elevation.

The large orographic change in warm season precipitation is not what was found for the distribution of snow water equivalent (SWE) for the same study domain (Homan and Kane,

2015) (Fig. 2.6a, b). Figure 2.6a illustrates the accumulation of warm season precipitation for each station from 1985–2013, while Figure 2.6b shows end-of-winter SWE from over 1000 snow surveys conducted at roughly 200 locations from 2000–2013. Overall, for the same 1500 m change in elevation, warm season precipitation increases more than 240 mm, compared with a roughly 10 mm decrease in SWE.

Yearly trend lines were plotted to evaluate the stability of warm season precipitation in time and space (Fig. 2.7a). Each of the 29 years of study (1985–2013) had trend lines that increased with elevation. The lower elevations illustrate a tighter grouping of cumulative warm season precipitation, while an increase in elevation results in great yearly variability. The greater variability of warm season precipitation at higher elevation is a product of increased complexity in topography, while lower elevation topography is generally more uniform. Snow water equivalent was also found to increase in variability with elevation during a 14-year study (2000–2013) over the same study domain (Homan and Kane, 2015) (Fig. 2.7b). The variability of SWE may increase with elevation, but the average trend was found to be negligible and had inconsistent slope directions that flip-flopped between negative and positive trending. Overall, the variability of both SWE and warm season precipitation increased with elevation, but the amounts and trends differed significantly (Fig. 2.7c).

To assess the variability of warm season precipitation through time, annual values were plotted for the four stations (from the Coastal Plain to the continental divide in the Brooks Range) with the longest record durations (all being 26 years or greater) (Fig. 2.8). No discernible long-term trends in warm season precipitation were found. Two of the stations (Atigun Pass and Sagwon) have negative sloping trends, while the other two stations (Imnavait and Franklin Bluffs) have trends that slope positively. Furthermore, the opposing trends alternate with an increase in elevation (negative at 71 m, positive at 275 m, negative at 937 m, and positive at 1463 m). What can be seen in Figure 2.8, to reiterate, is that warm season precipitation increases with elevation. The main conclusion from evaluating warm season precipitation in the Alaska Central Arctic through time is that, from the Coastal Plain to the Mountains, the measurements in years with relatively high precipitation amounts are universally high, and the measurements in years with relatively low precipitation amounts are universally low.

Warm season precipitation in the Arctic is limited to three full months (June, July, and August) and two partial months (May and September). In the Arctic, snow can fall any day of the year, but snow accumulation typically begins in September and persists until May, making May and September months of transition, when either rain or snow can fall. Using the 7 years (2007–2013) that had the highest population of meteorological stations (Fig. 2.2), monthly warm season precipitation plots show maximum precipitation in July for all years except 2009 (Fig. 2.9). Generally, June is the month of least warm season precipitation, while August usually accounts for precipitation totals somewhere between June and July. In descending order, July accumulates on average 59 mm of warm season precipitation, August 43 mm, and June 31 mm (Table 2.2). Warm season precipitation can vary by a factor of two from dry to wet years, and no temporal monthly pattern changes were identified with the limited data record. Warm season precipitation can occur via many low-intensity events, a few major storms, or some combination of both. Convective storms are more common early in the summer in the Foothills, when incoming solar radiation is near its maximum, while frontal storms are more common for the remaining part of the warm season (IPCC, 2001).

Maximum warm season precipitation events were evaluated for five meteorological stations located from the Coastal Plain to the Mountains, and compared against NOAA precipitation frequency estimates (Fig. 2.10). Specifically, warm season precipitation maximum measurements were determined for durations of one hour, one day, two days, four days, and seven days for each of the five meteorological stations (Table 2.3). Using NOAA's Atlas 14 Point Precipitation Frequency Estimates data server (PFDS) for Alaska (Perica et al., 2012), precipitation frequency estimates for the five durations listed above were obtained for five selected meteorological stations. The frequency estimates were determined for six recurrence intervals (1, 2, 5, 10, 25, 50 years). Figure 2.10 illustrates precipitation frequency estimates for just the 10-year recurrence interval for each station and shows not only an increase in precipitation with extended durations, as should be expected, but also an increase in precipitation with elevation. The measured field data records for the five stations range from 16 to 31 years, so it would be assumed that the estimated recurrence intervals are generally within a range of 10 to 25 years. Table 2.3 provides the maximum observed recorded warm season precipitation values and the estimated recurrence intervals for those values. Ideally, the estimated recurrence intervals would closely match or bracket the extent of the record. The Upper Kuparuk and its 17-year

record is a model example of this. For each of the selected precipitation durations (1 hour, 1 day, 2 days, 4 days, and 7 days) the maximum accumulations of warm season precipitation had 10- to 25-year estimated recurrence intervals, which brackets the record duration of 17 years. Betty Pingo consistently had estimated recurrence intervals between 5 and 10 years, which is in range of the short 16-year record (Table 2.3). Franklin Bluffs and Sagwon Hill, both with 26-year records, reliably had estimated recurrence intervals of between 5 and 25 years. Atigun Pass, with the longest record of 31 years, had the largest estimated recurrence intervals, extending from 10 to 50 years. In summary, for each precipitation duration and at all locations, the estimated recurrence intervals were in the range expected for maximum measured warm season precipitation, with the shortest measurement record having the smallest estimated recurrence intervals, and the longest measurement record having the largest estimated recurrence intervals (Table 2.3).

2.7 Discussion

Hydrological and meteorological networks in sparsely populated high-latitude permafrost environments were established later than the networks in more temperate climates (Woo et al., 2008). Precipitation gauges are generally located at populated centers, but in the Alaska Arctic, where population centers are few, precipitation gauges are located where they are easily accessible—at low elevations on major stream tributaries and in coastal areas. The location of these gauges is unfortunate, since more precipitation falls and more runoff is generated at higher elevations. Initially, precipitation data were collected for day-to-day river runoff and flood forecasting. Recently, interest in precipitation trends related to climate change has increased. Hydrologic cycle intensification of precipitation, evapotranspiration, and stream runoff is anticipated in a warming climate (Rawlins et al., 2010). However, the reality is that these data networks, when conceived and installed, were not envisioned for use in the study of climate change. There are many challenges to collecting quality precipitation data, with undercatch (Goodison et al., 1997; Yang et al., 2005) by all gauges the most significant, making trend analysis difficult. Challenges presented by changes in location, instrumentation, and observer (McAfee et al., 2013) may cloud the issue of direction and magnitude of precipitation change.

The use of observations to delineate precipitation trends (McAfee et al., 2013) creates challenges related to limited spatial coverage, short duration records, and uncertain and marginal

quality data (Kane and Stuefer, 2015). Still, it is generally accepted that with a warmer climate, more precipitation will occur in the Arctic (Kattsov and Walsh, 2000; Bintanja and Selten, 2014), although disagreement remains about the source of the moisture (enhanced poleward migration versus intensified local surface evaporation). Published evidence for increased precipitation is the result of modeling scenarios (Kattsov and Walsh, 2000; Bintanja and Selten, 2014).

McAfee et al. (2013) attempted to evaluate precipitation trends in Alaska using 29 meteorological stations with largely complete monthly records for two analysis periods (1950–2010 and 1980–2010). There is, however, only one station (Barrow) north of the Brooks Range with a complete record, so it is difficult to verify the direction of precipitation trends in this region. In the end, the study did not paint a particularly compelling and consistent picture of precipitation trends for the Alaska Central Arctic. Even if a trend were identified, it is uncertain whether the trend reflects regional changes in climate or peculiarities of that particular location, since it is the only one with an acceptable record duration. The state's precipitation network recently has expanded significantly (Perica et al., 2012; Kane and Stuefer, 2015), but the length of data collection must be extended and only time can produce that change. Even with the need for longer data records, meteorological stations are being removed with the completion of projects, which illustrates the necessity for the installation of stations with climate change in mind (Young et al., 2006).

While there is considerable interest globally in the increasing amount of predicted precipitation generated by climatic warming, this study was directed at the current spatial and temporal pattern of measured warm season precipitation over the Alaska Central Arctic. In this region of Alaska, warm season precipitation measurements are few and of poor quality in comparison with those from more temperate regions. In the last three decades, we have had the opportunity, through the combination of several research projects, to install numerous precipitation gauges in the Alaska Central Arctic. In each case, gauge installation has been done with the intention that the data collected would complement the data from the existing gauge network. In this treeless, windy, and remote environment, we installed shielded precipitation gauges that would minimize undercatch. Note that we only measure warm season precipitation at these gauges. Solid precipitation (less sublimation) is measured at the end of winter, when the

snowpack is at a maximum. During winter, the snowpack is redistributed by wind in this treeless landscape and incurs sublimation losses.

2.8 Conclusion

This study used the results from the 31 meteorological stations of numerous research projects to investigate warm season precipitation patterns across the Alaska Central Arctic. We demonstrated that the spatial variability of warm season precipitation has a strong linear relationship with topography and that such precipitation increases with elevation from the Coastal Plain to the continental divide in the Mountains. The maximum gradient for warm season precipitation generally increases north to south, but from year to year, can deviate slightly to the east or west. Lower elevations illustrate a tighter grouping of cumulative warm season precipitation, while an increase in elevation results in great yearly variability as a product of increased complexity in slope and topography.

The temporal variability was less conclusive and no discernible long-term trends in warm season precipitation were found in the somewhat limited 29 year data set. Most of the published evidence for changes in precipitation in the Arctic is a result of modeling scenarios and we conclude a longer record of data of improved quality is required before such statements can be made based on field measurements. We were, however, able to develop some monthly conclusions. Monthly warm season precipitation patterns show maximum precipitation generally occurs in July, followed by August, and finally by June. May and September are transitional months, when either rain or snow can fall, and thus were not included in this monthly evaluation.

A temporal trend in warm season precipitation may not be evident with our current dataset, but we quantified dry and wet years and that each year is consistent across the study domain. Dry years, such as 2007, are dry from the Coastal Plains to the Mountains, with consistently lower amounts of warm season precipitation: 9 mm (Franklin Bluffs) and 305 mm (Atigun Pass), respectively. While wet years, such as 1999, regularly have higher amounts of warm season precipitation from the Coastal Plains to the Mountains: 62 mm (Franklin Bluffs) and 470 mm (Atigun Pass), respectively.

2.9 Acknowledgments

The authors of this paper recognize the contributions made by all the faculty, staff, and graduate students who have assisted in collecting data over the years. We would like to specifically thank Robert Geick for his many years working on the meteorological stations and Glen Liston for sharing his codes for the interpolation. This work was supported by the Alaska Department of Transportation and Public Facilities (ADOT&PF), Alaska Department of Natural Resources (ADNR), National Science Foundation (NSF) and U.S. Fish and Wildlife Service (USFWS).

2.10 References

ACIA, 2005: Arctic climate impact assessment: Cambridge University Press, New York, NY.

Arendt, A. A., Echelmeyer, K. A., Harrison, W. D., Lingle, C. S., and Valentine, V. B., 2002: Rapid wastage of Alaska glaciers and their contribution to rising sea level. *Science,* 297(5580): 382-386.

Barnes, S. L., 1964: A technique for maximizing details in numerical weather map analysis. *Journal of Applied Meteorology,* 3(4): 396-409.

Bintanja, R. and Selten, F., 2014: Future increases in Arctic precipitation linked to local evaporation and sea-ice retreat. *Nature,* 509(7501): 479-482.

Brown, R. D., 2000: Northern Hemisphere snow cover variability and change, 1915–97. *Journal of Climate,* 13(13): 2339-2355.

Cavalieri, D., Parkinson, C., and Vinnikov, K. Y., 2003: 30-Year satellite record reveals contrasting Arctic and Antarctic decadal sea ice variability. *Geophysical Research Letters,* 30(18).

CAVM Team, 2003: Circumpolar Arctic Vegetation Map. Scale 1 : 7 500 000. Conservation of Arctic Flora and Fauna (CAFF) Map No. 1. U.S. Fish and Wildlife Service, Anchorage, Alaska.

Curtis, J., Wendler, G., Stone, R., and Dutton, E., 1998: Precipitation decrease in the western Arctic, with special emphasis on Barrow and Barter Island, Alaska. *International Journal of Climatology,* 18(15): 1687-1707.

Goodison, B., Louie, P., and Yang, D., 1997: The WMO solid precipitation measurement intercomparison. *World Meteorological Organization-Publications-WMO TD*65-70.

Haugen, R. K. and Brown, J., 1980: Coastal-inland distributions of summer air temperature and precipitation in Northern Alaska. *Arctic and Alpine Research,* 12(4): 403-412.

Hinzman, L. D., Bettez, N. D., Bolton, W. R., Chapin, F. S., Dyurgerov, M. B., Fastie, C. L., Griffith, B., Hollister, R. D., Hope, A., Huntington, H. P., Jensen, A. M., Jia, G. J., Jorgenson, T., Kane, D. L., Klein, D. R., Kofinas, G., Lynch, A. H., Lloyd, A. H., McGuire, A. D., Nelson, F. E., Oechel, W. C., Osterkamp, T. E., Racine, C. H., Romanovsky, V. E., Stone, R. S., Stow, D. A., Sturm, M., Tweedie, C. E., Vourlitis, G. L., Walker, M. D., Walker, D. A., Webber, P. J., Welker, J. M., Winker, K., and Yoshikawa, K., 2005: Evidence and implications of recent climate change in northern Alaska and other arctic regions. *Climatic Change,* 72(3): 251-298.

Homan, J. W. and Kane, D. L., 2015: Arctic snow distribution patterns at the watershed scale. *Hydrology Research,* 46(4): 507-520.

IPCC, 1996: Climate change 1995: The science of climate change. Contribution of Working Group 1 to the Third Assessment Report of the Intergovernmental Panel on Climate Change, Cambridge University Press, Cambridge, UK, and New York, USA.

IPCC, 2001: Climate change 2001: The scientific basis. Contribution of Working Group 1 to the Third Assessment Report of the Intergovernmental Panel on Climate Change, Cambridge University Press, Cambridge, UK, and New York, USA.

Johannessen, O. M., Bengtsson, L., Miles, M. W., Kuzmina, S. I., Semenov, V. A., Alekseev, G. V., Nagurnyi, A. P., Zakharov, V. F., Bobylev, L. P., and Pettersson, L. H., 2004: Arctic climate change: Observed and modelled temperature and sea-ice variability. *Tellus Series a-Dynamic Meteorology and Oceanography,* 56(4): 328-341.

Kane, D. L., Hinzman, L. D., McNamara, J. P., Zhang, Z., and Benson, C. S., 2000: An overview of a nested watershed study in Arctic Alaska. *Nordic Hydrology,* 31(4-5): 245-266.

Kane, D. L., Hinzman, L. D., Gieck, R. E., McNamara, J. P., Youcha, E. K., and Oatley, J. A., 2008: Contrasting extreme runoff events in areas of continuous permafrost, Arctic Alaska. *Hydrology Research,* 39(4): 287-298.

Kane, D. L., Youcha, E. K., Stuefer, S., Toniolo, H., Schnabel, W., Gieck, R. E., Myerchin-Tape, G., Homan, J. W., Lamb, E., and Tape, K., 2012: Meteorological and hydrological data and analysis report for the Foothills/Umiat Corridor and Bullen projects: 2006-2011. University of Alaska Fairbanks, Water and Environmental Research Center, Report INE/WERC 12.01, Fairbanks, Alaska, 260 pp.

Kane, D. L., Youcha, E. K., Stuefer, S., Myerchin-Tape, G., Lamb, E., Homan, J. W., Gieck, R. E., Schnabel, W., and Toniolo, H., 2014: Hydrology and meteorology of the central Alaskan Arctic: Data collection and analysis, University of Alaska Fairbanks, Water and Environmental Research Center, Report INE/WERC 14.05, Fairbanks, AK.

Kane, D. L. and Stuefer, S. L., 2015: Reflecting on the status of precipitation data collection in Alaska: a case study. *Hydrology Research,* 46(4): 478-493.

Kattsov, V. M. and Walsh, J. E., 2000: Twentieth-century trends of Arctic precipitation from observational data and a climate model simulation. *Journal of Climate,* 13(8): 1362-1370.

Lachenbruch, A. H. and Marshall, B. V., 1986: Changing climate: Geothermal evidence from permafrost in the Alaskan Arctic. *Science,* 234(4777): 689-696.

Magnuson, J. J., Robertson, D. M., Benson, B. J., Wynne, R. H., Livingstone, D. M., Arai, T., Assel, R. A., Barry, R. G., Card, V., and Kuusisto, E., 2000: Historical trends in lake and river ice cover in the Northern Hemisphere. *Science,* 289(5485): 1743-1746.

Maslanik, J. A., Serreze, M. C., and Agnew, T., 1999: On the record reduction in 1998 western Arctic sea-ice cover. *Geophysical Research Letters,* 26(13): 1905-1908.

McAfee, S. A., Guentchev, G., and Eischeid, J. K., 2013: Reconciling precipitation trends in Alaska: 1. Station-based analyses. *Journal of Geophysical Research: Atmospheres,* 118(14): 7523-7541.

Osterkamp, T. E., 1984: Temperature measurements in permafrost. Rep. FHWA-AK-RD-85-11, State of Alaska, Department of Transportation and Public Facilities, Division of Planning and Programming, Research Section87.

Overduin, P. P. and Kane, D. L., 2006: Frost boils and soil ice content: Field observations. *Permafrost and Periglacial Processes,* 17(4): 291-307.

Perica, S., Kane, D., Dietz, S., Maitaria, K., Martin, D., Pavlovic, S., Roy, I., Stuefer, S., Tidwell, A., Trypaluk, C., Unruh, D., Yekta, M., Betts, E., Bonnin, G., Heim, S., Hiner, L., Lilly, E., Narayanan, J., Yan, F., and Zhao, T., 2012: Precipitation-frequency atlas of

the United States. *In* vol. **7,** A., NOAA, National Weather Service, Silver Spring, MD (ed.), NOAA atlas 14. Silver Springs, MD.

Peterson, B. J., Holmes, R. M., McClelland, J. W., Vörösmarty, C. J., Lammers, R. B., Shiklomanov, A. I., Shiklomanov, I. A., and Rahmstorf, S., 2002: Increasing river discharge to the Arctic Ocean. *Science,* 298(5601): 2171-2173.

Rawlins, M. A., Steele, M., Holland, M. M., Adam, J. C., Cherry, J. E., Francis, J. A., Groisman, P. Y., Hinzman, L. D., Huntington, T. G., Kane, D. L., Kimball, J. S., Kwok, R., Lammers, R. B., Lee, C. M., Lettenmaier, D. P., McDonald, K. C., Podest, E., Pundsack, J. W., Rudels, B., Serreze, M. C., Shiklomanov, A., Skagseth, O., Troy, T. J., Vorosmarty, C. J., Wensnahan, M., Wood, E. F., Woodgate, R., Yang, D. Q., Zhang, K., and Zhang, T. J., 2010: Analysis of the Arctic System for Freshwater Cycle Intensification: Observations and Expectations. *Journal of Climate,* 23(21): 5715-5737.

Robinson, D. A., 1993: Hemispheric snow cover from satellites. *Annals of Glaciology,* 17367-367.

Robinson, D. A. and Frei, A., 2000: Seasonal Variability of Northern Hemisphere Snow Extent Using Visible Satellite Data. *The Professional Geographer,* 52(2): 307-315.

Romanovsky, V. E., Smith, S. L., and Christiansen, H. H., 2010: Permafrost thermal state in the polar Northern Hemisphere during the international polar year 2007–2009: a synthesis. *Permafrost and Periglacial Processes,* 21(2): 106-116.

Screen, J. A. and Simmonds, I., 2010: The central role of diminishing sea ice in recent Arctic temperature amplification. *Nature,* 464(7293): 1334-1337.

Serreze, M., Walsh, J., Chapin Iii, F., Osterkamp, T., Dyurgerov, M., Romanovsky, V., Oechel, W., Morison, J., Zhang, T., and Barry, R., 2000: Observational evidence of recent change in the northern high-latitude environment. *Climatic Change,* 46(1-2): 159-207.

Serreze, M. C., Bromwich, D. H., Clark, M. P., Etringer, A. J., Zhang, T., and Lammers, R., 2002: Large-scale hydro-climatology of the terrestrial Arctic drainage system. *Journal of Geophysical Research: Atmospheres (1984–2012),* 107(D2): ALT 1-1-ALT 1-28.

Shulski, M. and Wendler, G., 2007: The climate of Alaska: University of Alaska Press, Fairbanks, AK.

Stafford, J., Wendler, G., and Curtis, J., 2000: Temperature and precipitation of Alaska: 50 year trend analysis. *Theoretical and Applied Climatology,* 67(1-2): 33-44.

Stuefer, S., Kane, D. L., and Liston, G. E., 2013: In situ snow water equivalent observations in the US Arctic. *Hydrology Research,* 44(1): 21-34.

Sturm, M., Holmgren, J., McFadden, J. P., Liston, G. E., Chapin, F. S., and Racine, C. H., 2001: Snow-Shrub Interactions in Arctic Tundra: A Hypothesis with Climatic Implications. *Journal of Climate*, 14:336-344.

Sturm, M., Douglas, T., Racine, C., and Liston, G. E., 2005: Changing snow and shrub conditions affect albedo with global implications. *J. Geophys. Res.,* 110(G1): G01004.

Tape, K. E. N., Sturm, M., and Racine, C., 2006: The evidence for shrub expansion in Northern Alaska and the Pan-Arctic. *Global Change Biology,* 12(4): 686-702.

Vinnikov, K. Y., Robock, A., Stouffer, R. J., Walsh, J. E., Parkinson, C. L., Cavalieri, D. J., Mitchell, J. F., Garrett, D., and Zakharov, V. F., 1999: Global warming and Northern Hemisphere sea ice extent. *Science,* 286(5446): 1934-1937.

Walker, D. A., Binnian, E., Evans, B. M., Lederer, N. D., Nordstrand, E., and Webber, P. J., 1989: Terrain, vegetation and landscape evolution of the R4D research site, Brooks-Range-Foothills, Alaska. *Holarctic Ecology,* 12(3): 238-261.

Wendler, G. and Shulski, M., 2009: A Century of Climate Change for Fairbanks, Alaska. *Arctic,* 62(3): 295-300.

Woo, M. K., Kane, D. L., Carey, S. K., and Yang, D. Q., 2008: Progress in permafrost hydrology in the new millennium. *Permafrost and Periglacial Processes,* 19(2): 237-254.

Yang, D., Kane, D., Zhang, Z., Legates, D., and Goodison, B., 2005: Bias corrections of long-term (1973–2004) daily precipitation data over the northern regions. *Geophysical Research Letters,* 32(19).

Young, K. L., Bolton, W. R., Killingtveit, A., and Yang, D. Q., 2006: Assessment of precipitation and snowcover in northern research basins. *Nordic Hydrology,* 37(4-5): 377-391.

Zhang, T., Osterkamp, T. E., and Stamnes, K., 1996: Some characteristics of the climate in Northern Alaska, U.S.A. *Arctic and Alpine Research,* 28(4): 509-518.

Zhang, T., Osterkamp, T. E., and Stamnes, K., 1997: Effects of climate on the active layer and permafrost on the North Slope of Alaska, U.S.A. *Permafrost and Periglacial Processes,* 8(1): 45-67.

2.11 Figures

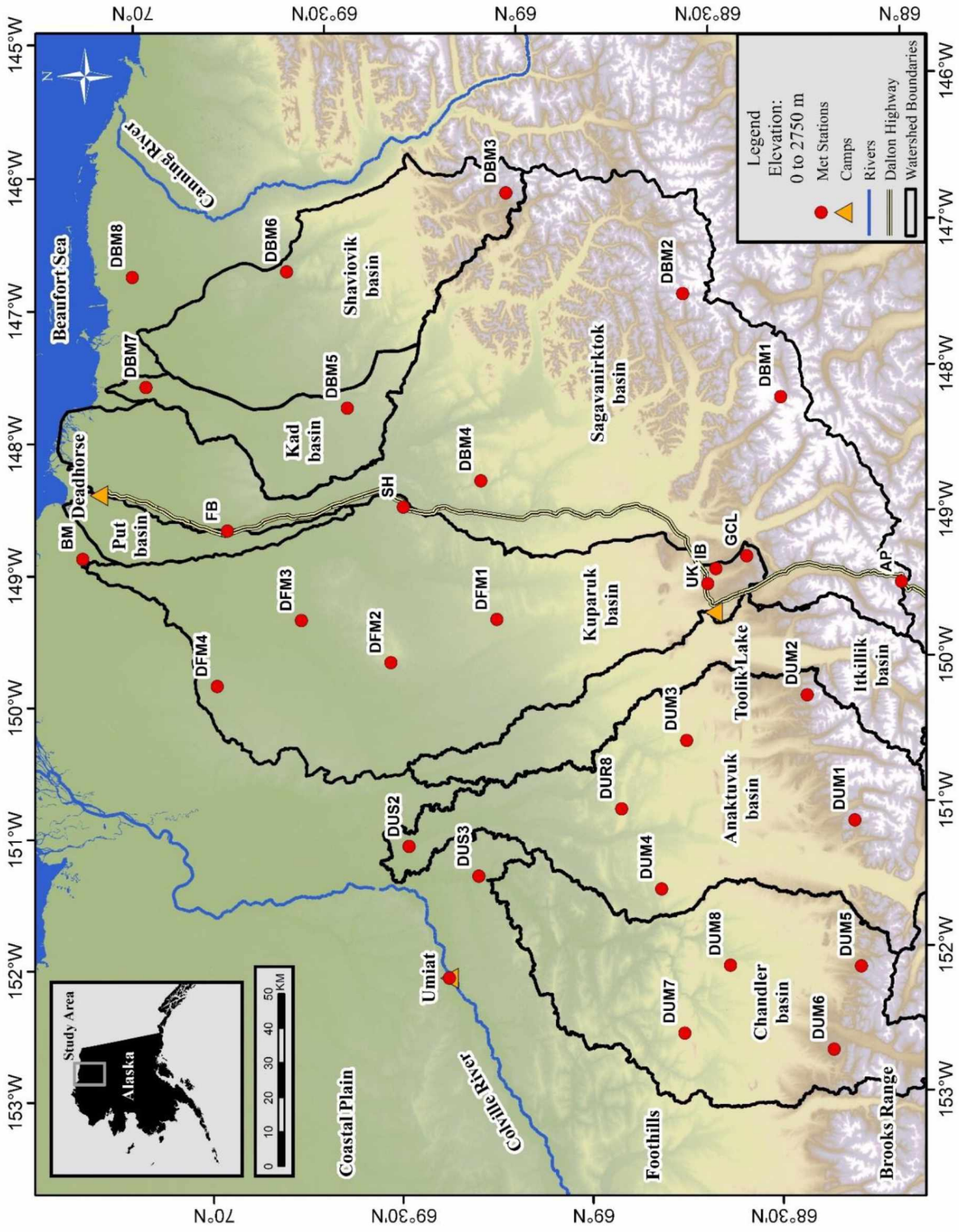

Figure 2.1: Study area and location map of meteorological stations for the Alaska Central Arctic. The duration of observations at each site varies, plus many have been removed.

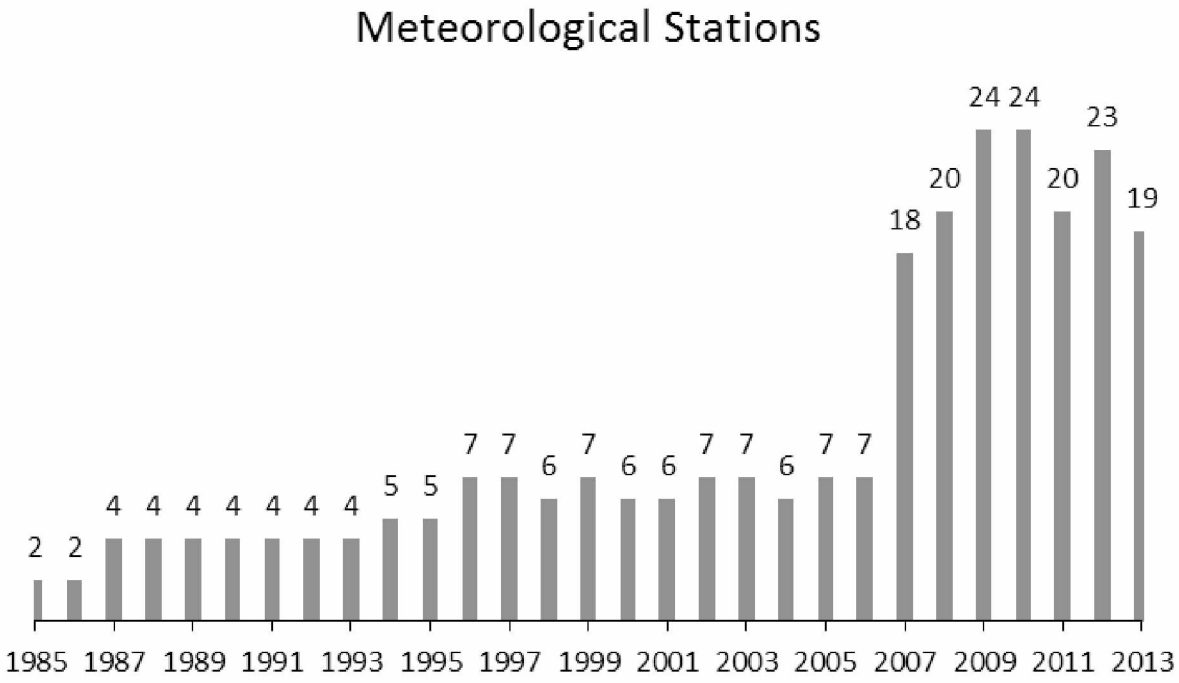

Figure 2.2: Number of meteorological stations each of the 29 years of study (1985–2013). In total, data from 31 different stations were used. Only seven stations currently exist today.

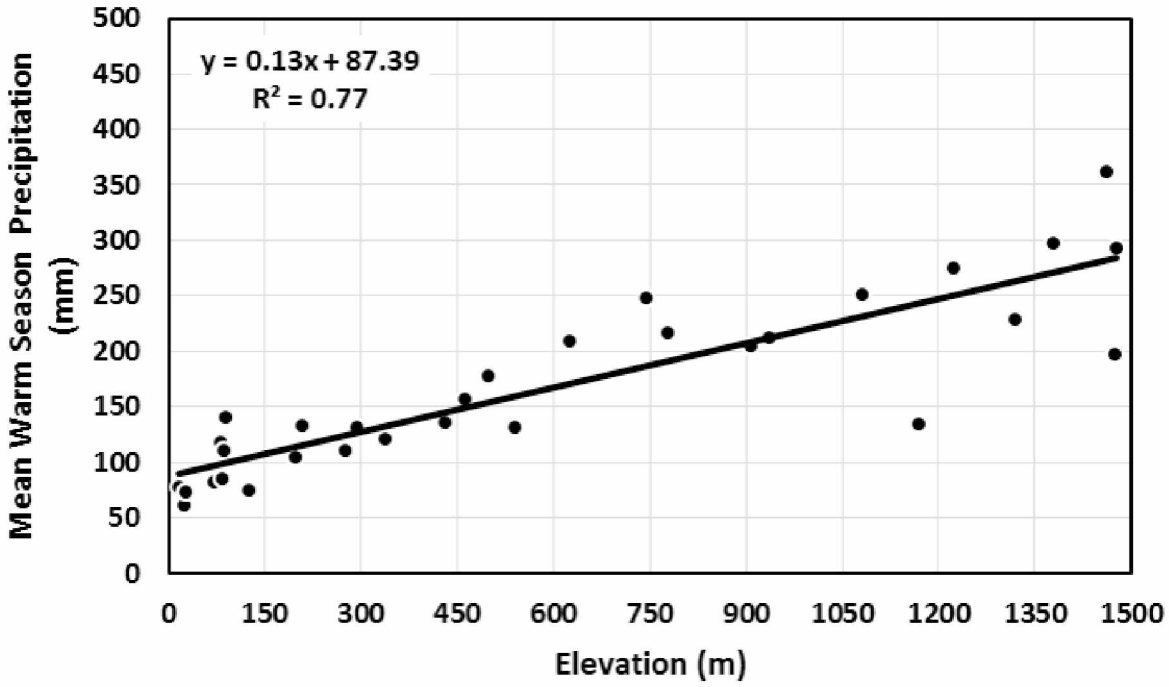

Figure 2.3: Record mean warm season precipitation versus elevation for the 31 meteorologic station, showing a strong linear relationship with greater precipitation at higher elevations.

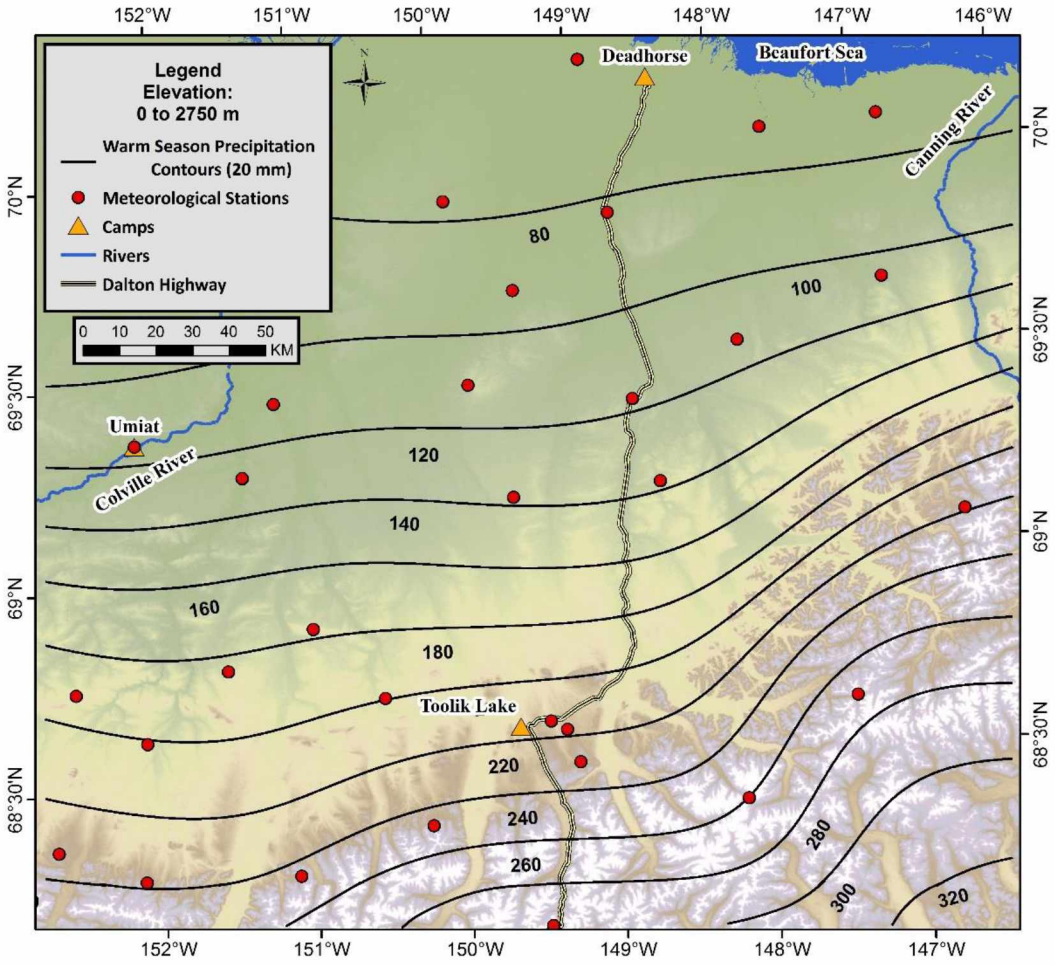

Figure 2.4: Contoured map of warm season precipitation in the Alaska Central Arctic. Point data were interpolated with Barnes (1964) interpolation method.

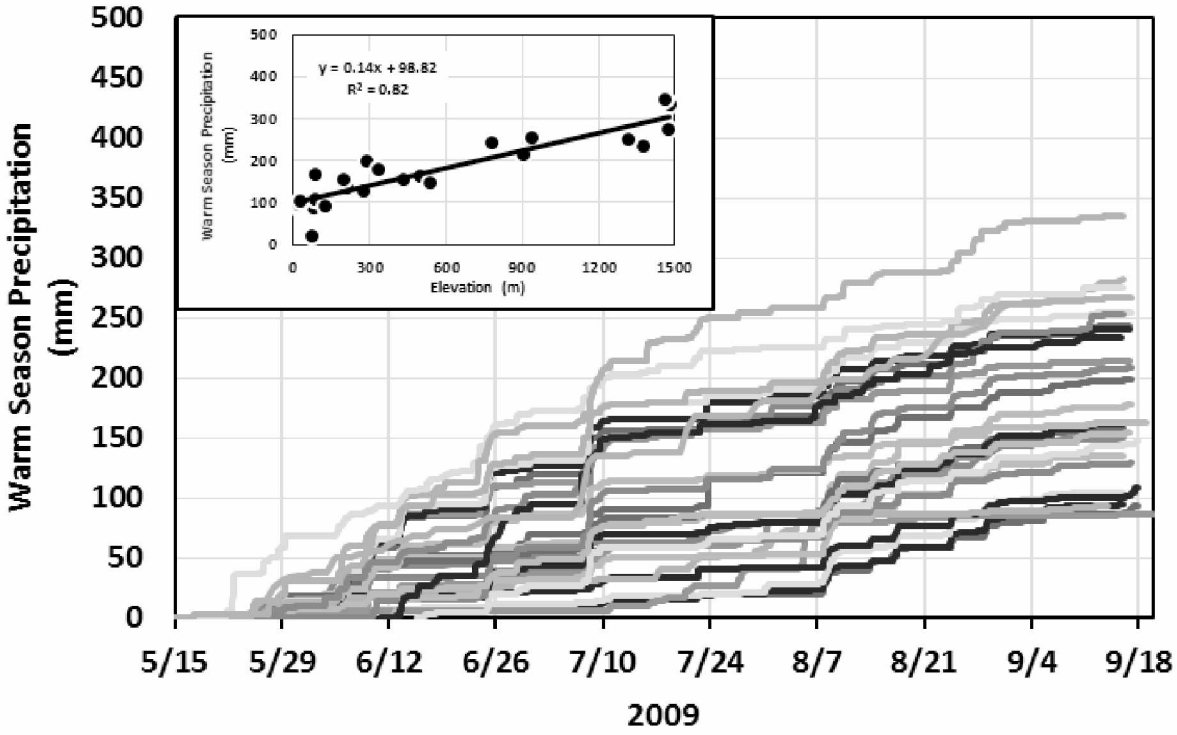

Figure 2.5: Cumulative warm season precipitation during 2009 for the 24 meteorological stations, showing spatial variations and a linear relationship (insert) with greater precipitation at higher elevations.

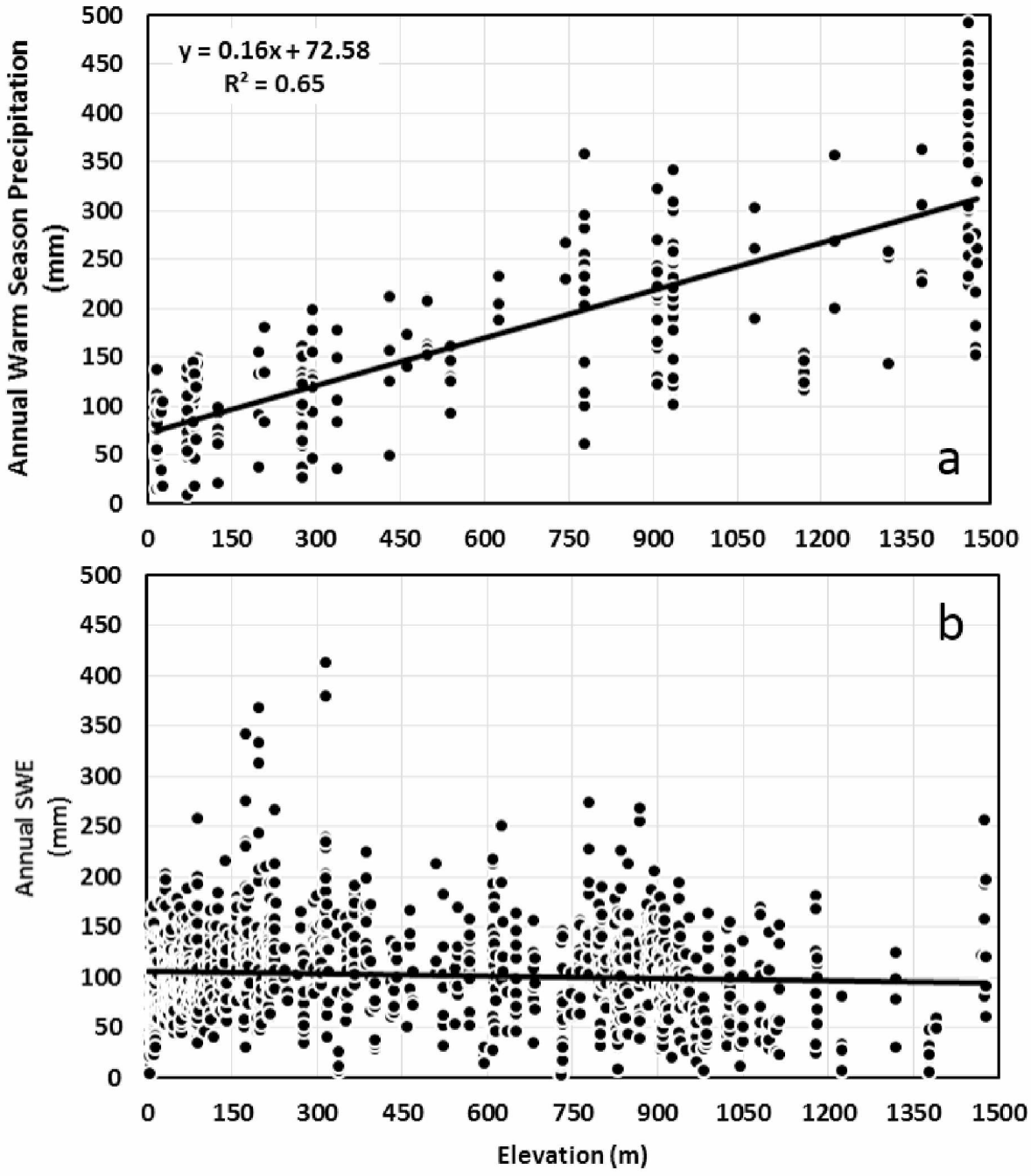

Figure 2.6: a) Warm season precipitation accumulation from all stations (1985–2013), and b) record end-of-winter SWE measurements (2000–2013) plotted versus elevation in the Alaska Central Arctic.

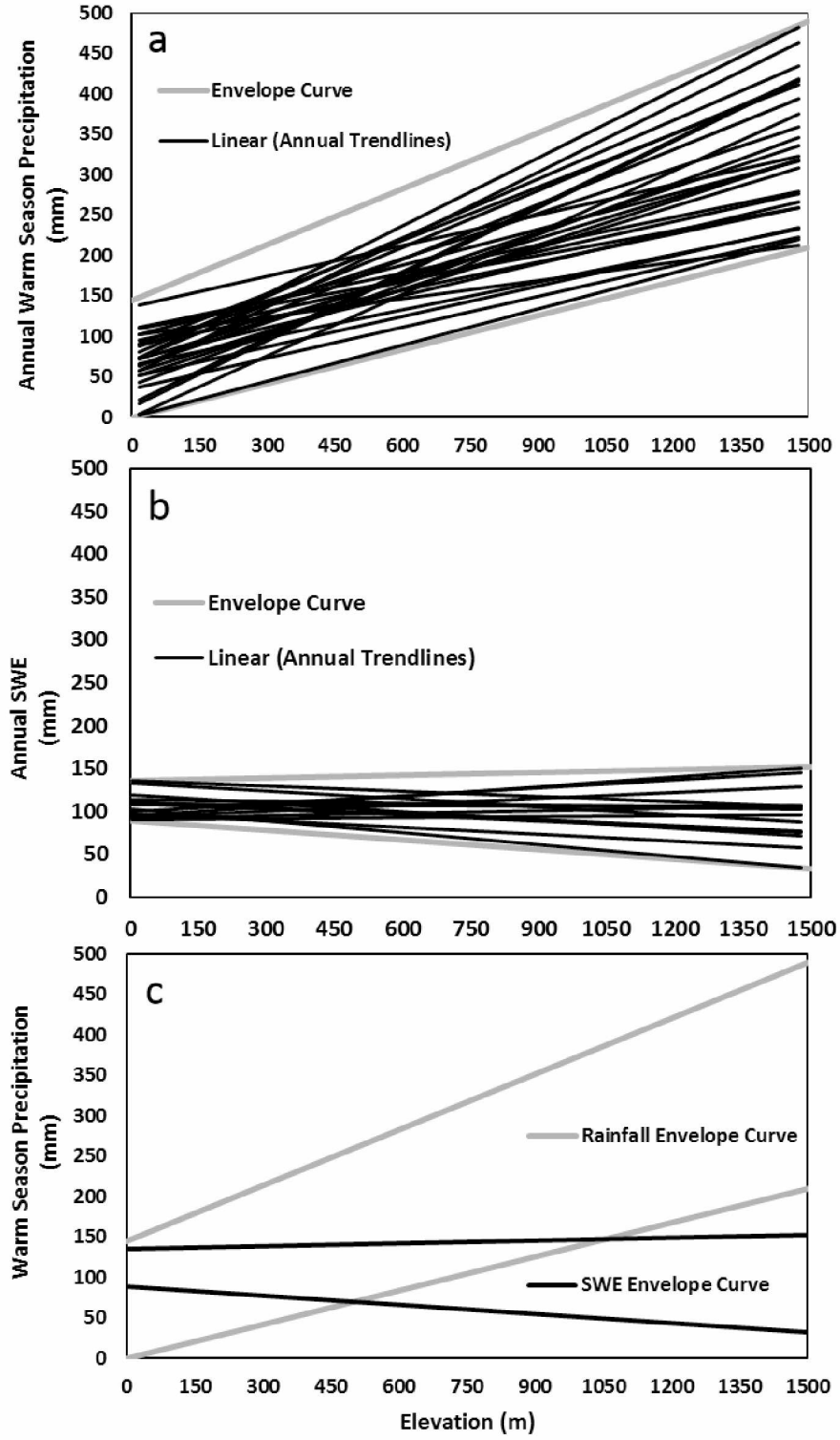

Figure 2.7: Yearly trend lines using annual datasets for the a) 29-year record (1985–2013) of warm season precipitation, and b) 14-year record (2000–2013) of end-of-winter SWE measurements plotted versus elevation. c) Overlapping envelope curves, which bracket the variability of the trend lines, for both datasets.

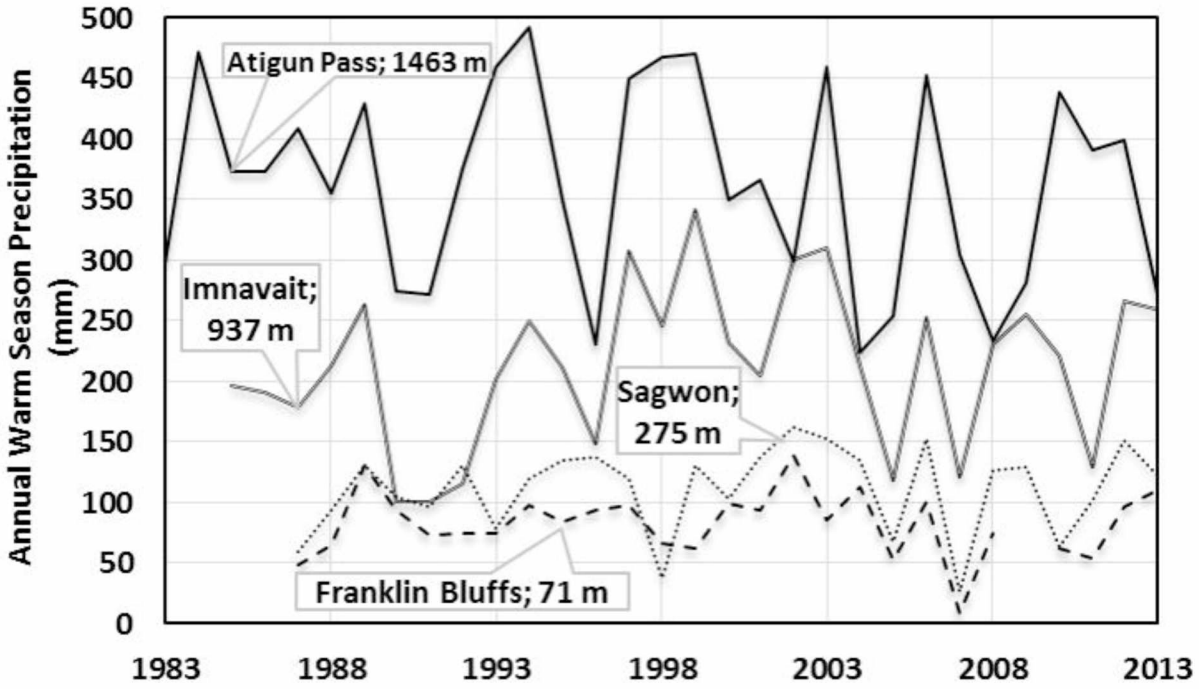

Figure 2.8: Annual cumulative warm season precipitation through time for four stations with a complete range of elevations and with the longest records. Franklin Bluffs had an incomplete data record in 2009 and is not included.

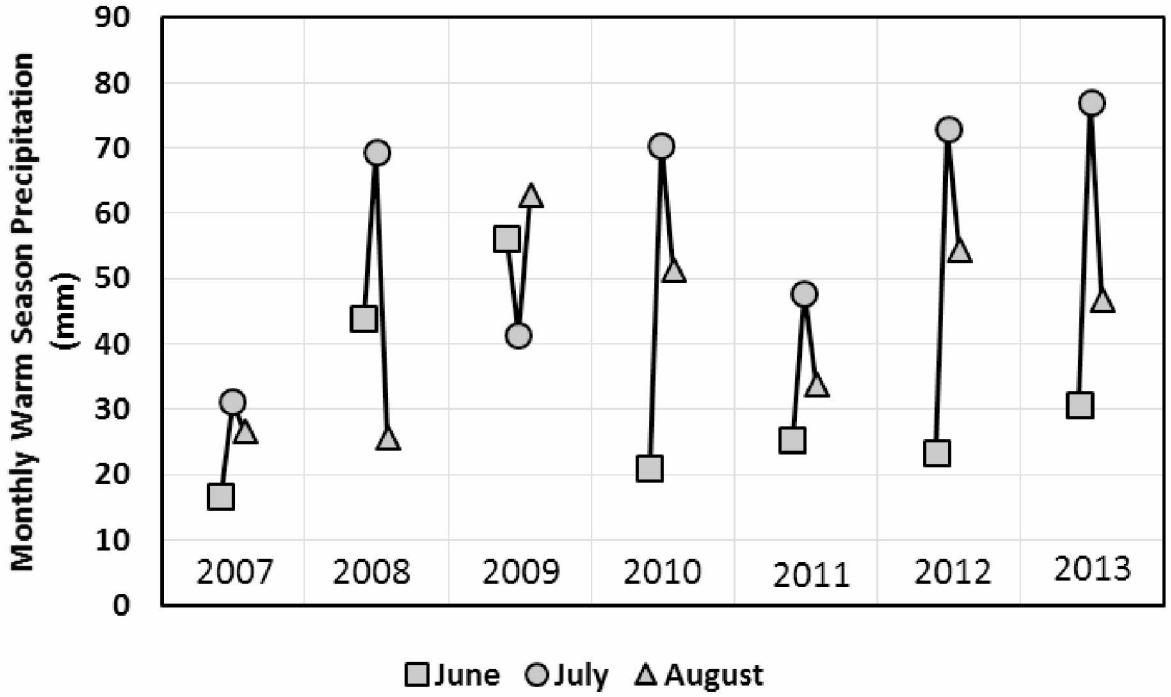

Figure 2.9: Monthly, average of all stations, warm season precipitation from 2007–2013, which were the years with the highest population of meteorological stations.

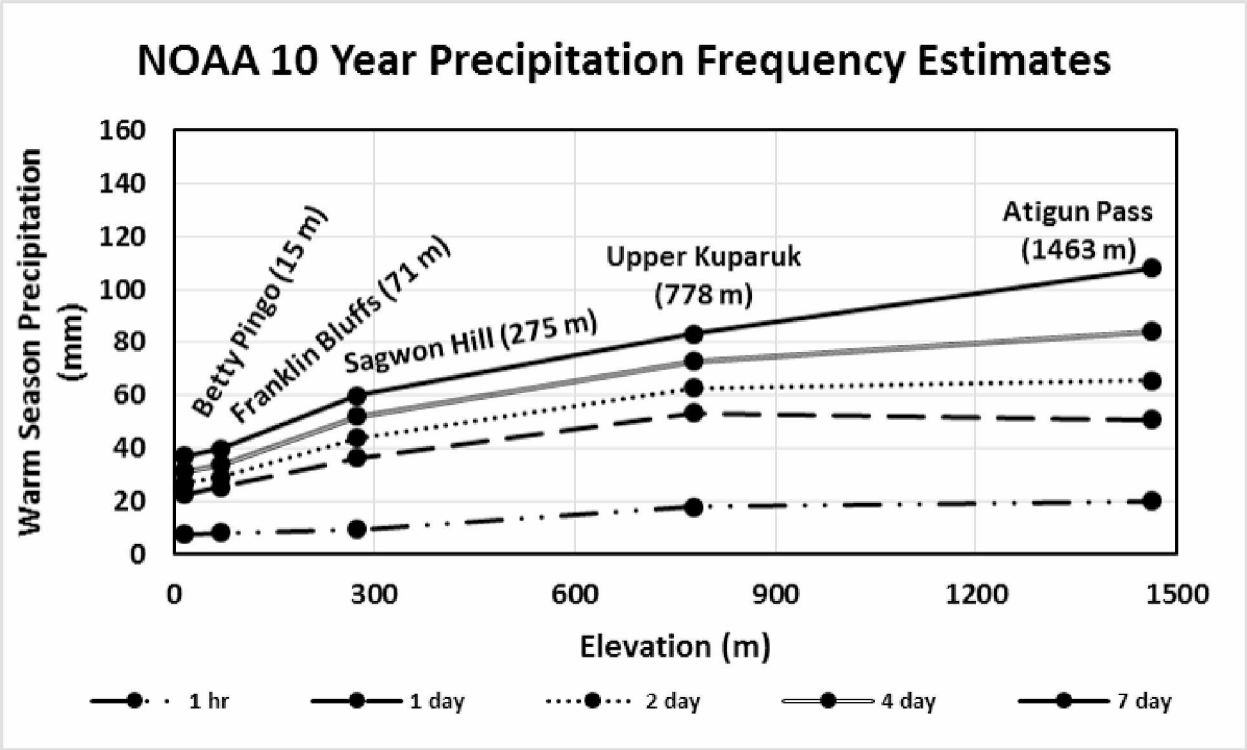

Figure 2.10: Warm season precipitation frequency estimates for a 10-year recurrence interval for five stations and precipitation durations of 1 hour, 1 day, 2 days, 4 days, and 7 days. Three of these stations were used in the Perica et al. (2012) precipitation frequency study: Betty Pingo, Sagwon Hill, and Atigun Pass. Franklin Bluffs and Upper Kuparuk were not used.

2.12 Tables

Table 2.1: Summary of meteorological stations utilized in this study. * These stations were used in the recent liquid precipitaiotn frequency analysis of Perica et al. (2012).

Station Name (Code)	Coordinates		Watershed	Record Duration/ # of Full Yrs	Elev. (m)	Warm Season Precipitation (mm)
*Betty Pingo (BM)	70° 16' 46" N	148° 53' 45" W	Kuparuk	1994-2011/ 16	15	78
Lower Kadleroshilik (DBM7)	70° 04' 24" N	147° 39' 00" W	Kadleroshilik	2007-2010/ 4	24	61
Bullen (DBM8)	70° 04' 47" N	146° 49' 09" W	No Name	2007-2009/ 3	26	73
Franklin Bluffs (FB)	69° 53' 32" N	148° 46' 05" W	Sagavanirktok	1987-2013/ 26	71	83
Anaktuvuk River (DUS2)	69° 27' 51" N	151°10' 07" W	Anaktuvuk	2009-2012/ 4	81	112
North White Hills (DFM3)	69° 42' 53" N	149° 28' 13" W	Kuparuk	2006-2013/ 7	84	80
Chandler River Bluff (DUS3)	69° 17' 00" N	151° 24' 16" W	Chandler	2011-2013/ 3	86	105
Umiat (BLM)	69° 22' 12" N	152° 08' 10" W	Colville	2008-2012/ 5	88	139
Northwest Kuparuk (DFM4)	69° 56' 51" N	149° 55' 00" W	Kuparuk	2006-2013/ 7	124	71
Kavik (DBM6)	69° 40' 24" N	146° 54' 02" W	Shaviovik	2007-2010/ 4	198	104
Upper Kadleroshilik (DBM5)	69° 32' 58" N	147° 56' 30" W	Kadleroshilik	2008-2010/ 3	209	133
*Sagwon (SH)	69° 25' 28" N	148° 41' 45" W	Sagavanirktok	1987-2013/ 26	275	114
South White Hills (DFM1)	69° 12' 02" N	149° 33' 30" W	Kuparuk	2006-2013/ 7	293	137
White Hills (DFM2)	69° 29' 11" N	149° 49' 17" W	Kuparuk	2006-2013/ 5	337	125
Sag-Ivishak (DBM4)	69° 12' 55" N	148° 33' 06" W	Sagavanirktok	2007-2010/ 4	431	136
Siksikpuk (DUM8)	68° 37' 48" N	152° 06' 08" W	Chandler	2011-2013/ 2	463	145
Tuluga (DUM4)	68° 48' 15" N	151° 32' 46" W	Anaktuvuk	2009-2013/ 5	497	179
Nanushuk (DUM3)	68° 43' 15" N	150° 30' 11" W	Anaktuvuk	2009-2013/ 5	540	131
Hatbox Mesa (DUM7)	68° 45' 16" N	152° 34' 23" W	Chandler	2011-2013/ 3	624	209
Rooftop Ridge (DUR8)	68° 54' 02" N	150° 57' 51" W	Anaktuvuk	2012-2013/ 2	745	249
Upper Kuparuk (UK)	68° 38' 25" N	149° 24' 23" W	Kuparuk	1994-2013/ 17	778	226
*Green Cabin Lake (GCL)	68° 32' 01" N	149° 13' 47" W	Kuparuk	1996-2013/ 18	908	205
*Imnavait Basin Met (IB)	68° 36' 59" N	149° 18' 13" W	Kuparuk	1985-2013/ 29	937	211
White Lake (DUM6)	68° 21' 47" N	152° 42' 25" W	Chandler	2011-2013/ 3	1081	251
Itikmalakpak (DUM1)	68° 17' 24" N	151° 06' 54" W	Anaktuvuk	2009-2013/ 5	1168	135
Encampment Creek (DUM5)	68° 17' 11" N	152° 07' 55" W	Chandler	2011-2013/ 3	1224	275
Juniper (DBM3)	69° 04' 34" N	146° 30' 17" W	Shaviovik	2007-2010/ 4	1319	228
Upper May Creek (DUM2)	68° 23' 55" N	150° 13' 40" W	Anaktuvuk	2009-2013/ 5	1378	298
*Atigun Pass (AP) (USDA/NRCS)	68° 08' 00" N	149° 29' 00" W	Sagavanirktok	1983-2013/ 31	1463	364
Accomplishment Creek (DBM1)	68° 24' 41" N	148° 08' 11" W	Sagavanirktok	2006-2013/ 5	1474	197
Ribdon (DBM2)	68° 38' 32" N	147° 21' 06" W	Sagavanirktok	2007-2010/ 4	1478	293

Table 2.2: Monthly average precipitation accumulation (mm) for June, July and August, for all available stations. May and September monthly values are not included because their precipitation accumulation generally consists of rain and snowfall, as they transition back and forth between the warm and cold seasons.

	Precipitation (mm)								
Year / # of Stations	2007 18	2008 20	2009 24	2010 24	2011 20	2012 23	2013 19	Mean	Std Dev
June Ave	17	44	56	21	25	23	31	31	13
July Ave	31	69	41	70	48	73	77	59	17
August Ave	27	26	63	51	34	54	47	43	13
Mean	25	46	53	48	36	50	52		
Std Dev	6	18	9	20	9	21	19		

Table 2.3: Maximum recorded warm season precipitation during one hour, one day, two days, four days and seven days from five stations on a north–south transect across the study area. Estimated recurrence intervals based on maximum measured values compared with results of Perica et al. (2012).

Site ID	Elev (m)	Sample Duration		1 hour	1 day	2 day	4 day	7 day
Betty Pingo	15	16 yr	Max Rainfall (mm)	8	19	23	29	34
			Date of Event	7/22/10	6/22/02	8/1/04	8/3/04	8/16/02
			Recurrence Estimate	10 yr.	5 yr.	5 yr.	5 - 10 yr.	5 - 10 yr.
Franklin Bluffs	71	26 yr.	Max Rainfall (mm)	9	31	32	32	38
			Date of Event	6/22/89	8/27/92	8/27/92	8/27/92	8/31/90
			Recurrence Estimate	10 - 25 yr.	10 - 25 yr.	10 - 25 yr.	5 - 10 yr.	5 - 10 yr.
Sagwon Hill	275	26 yr	Max Rainfall (mm)	12	44	51	51	51
			Date of Event	7/19/01	8/26/92	8/27/92	8/27/92	8/27/92
			Recurrence Estimate	25 yr	10 - 25 yr	10 - 25 yr	5 - 10 yr	5 yr
Upper Kuparuk	778	17 yr	Max Rainfall (mm)	19	59	78	79	101
			Date of Event	7/29/94	8/15/02	7/17/99	7/17/99	7/17/99
			Recurrence Estimate	10 - 25 yr	10 - 25 yr	10 - 25 yr	10 - 25 yr	10 - 25 yr
Atigun Pass	1463	31 yr	Max Rainfall (mm)	No Hourly Data	48	76	109	147
			Date of Event		8/26/94	8/26/94	8/27/94	8/27/94
			Recurrence Estimate		25 yr	10 - 25 yr	25 - 50 yr	50 yr

Chapter 3 Annual Precipitation Patterns in the Alaska Central Arctic

3.1 Abstract

Long-term datasets of solid and liquid precipitation were used to calculate the spatial and temporal variabilities of annual precipitation for the central area of the Alaska Arctic (referred to here as the Alaska Central Arctic). The solid precipitation dataset includes over 1000 end-of-winter snow water equivalent (SWE) surveys conducted from 2000-2013. The liquid precipitation dataset includes measurements from 31 meteorological stations, with collection durations that range from 2 to 31 years.

The combination of the datasets show that annual precipitation varies temporally and spatially over the Alaska Central Arctic. At the higher elevations of the foothills and mountains, annual precipitation is approximately 70% liquid and 30% solid, with a maximum liquid precipitation contribution of roughly 90% at some locations. On the coastal plain, the precipitation contribution is almost the opposite. Here, solid precipitation represents 60% of the annual precipitation budget, with a maximum contribution of 70% at one location. In general, therefore, at the lower foothills, the annual precipitation contribution consists of nearly equal amounts of liquid and solid precipitation, while at higher elevations in the mountains, the annual precipitation contribution is mostly from liquid precipitation. On the coastal plain, the primary annual precipitation contribution is from solid precipitation.

3.2 Introduction

Driven by the need to improve our understanding of the role Arctic hydrology plays in regional and global climate, and for the development and design of infrastructure (roads, airports, pipelines, etc.), several related hydrologic studies were initiated in the Alaska Arctic over the last four decades. These studies included developing a network of spatially distributed meteorological and hydrological stations where extensive field research was conducted. The goals were to collect quality hydrologic data throughout the year, monitor and study as many hydrologic processes as possible, address issues of temporal and spatial variability, and examine hydrologic responses at various scales. Reported here are the annual precipitation estimates, both solid and liquid, for the Alaska Central Arctic.

The Alaska Central Arctic is one of the most intensely studies areas in the circumpolar Arctic as a result of oil discovery in Prudhoe Bay in November 1968. Prior to successful oil exploration and development of this region, hydrological and meteorological measurements in this area were rare and research was essentially non-existent. Early measurements significantly underestimated annual precipitation, particularly the cumulative impact of trace amounts and under-catch of precipitation (mainly snowfall) during windy events. True precipitation is two to three time greater then what was reported by the National Weather Service and other federal agencies (Benson, 1982; Yang et al., 1998). Currently, concerns about environmental change motivates much of the interest in high-latitude hydrologic studies, as northern areas are expected to be more strongly impacted by climate warming (ACIA, 2005).

Indications are that the Arctic is generally warming (Serreze et al., 2000; Hinzman et al., 2005; Rawlins et al., 2010). How will a warming climate impact annual precipitation patterns and hydrologic runoff response? Possible scenarios include longer summers with more warm season precipitation, and less snow during the shorter winters (Houghton, 1996; Griggs and Noguer, 2002), a reduction in Arctic Ocean sea-ice, both in size and duration of cover (Maslanik et al., 1999; Vinnikov et al., 1999; Cavalieri et al., 2003), and more extreme summer precipitation events (Kane et al., 2008). We presently cannot confidently predict what this impact will be. At this time, large swings in annual precipitation occur in this extreme environment; changes in the magnitude and timing of this hydrologic input could have significant ecological impacts (Kane et al., 2008). This case study reports annual precipitation inputs, both warm season precipitation observations and snowpack distribution patterns, in the Alaska Central

Arctic. Temporal variability, as well as the spatial distribution of annual precipitation are examined and quantified using relatively long-term datasets.

3.3 The Alaska Central Arctic

3.3.1 Geographical Setting and Local Characteristics

Generally, the Arctic is defined as the region north of the Arctic Circle—the imaginary line at latitude 66°33′45.8″ N, but the Alaska Arctic is topographically bisected by the Brooks Range, which runs east to west, isolating what is generally referred to as the "North Slope" from the rest of Alaska. On directly opposing sides of the Arctic Circle, there is no stark climate contrast. On either side of the Brooks Range though, significant climate divergence occurs (Przybylak, 2003). For the purpose of this paper, the area north of the Brooks Range continental divide will be classified as the Arctic. The area of study for this report, consists of a 200 by 240 km region within the Alaska Central Arctic that is bounded by the Brooks Range in the south and the Arctic Ocean in the North (Fig. 3.1). It includes the Chandler, Anaktuvuk, Itkillik, Kuparuk, Putuligayuk (Put), Sagavanirktok (Sag), Kadleroshilik (Kad), and Shaviovik River basins. All of the watersheds drain north and eventually empty into the Arctic Ocean or another stream that eventually discharges to the ocean. The Putuligayuk lies entirely within the coastal plain region; the Kuparuk and Kadleroshilik Rivers emanate from the foothills and cross the coastal plain; the Sagavanirktok, Shaviovik, Kavik, Itkillik, Anaktuvuk, and Chandler Rivers originate in the Brooks Range and cross both the foothills and coastal plain. The southern and northern boundaries of the domain are at between 68°N and 70°N latitude, while the western and eastern boundaries are between 153°W and 146°W longitude. Elevation within the study area ranges from sea level to 2675 m. The topography is characterized by a flat northern portion (generally referred to as 'Coastal Plain') and by gently rolling hills and valleys ('Foothills') and mountain ridges ('Mountains') of the Brooks Range to the south.

This high latitude region has a mean annual air temperature well below freezing, at around −12°C (Shulski and Wendler, 2007). The entire study area is underlain by continuous permafrost (250 to 300 m think in the Brooks Range and up to 600 m think along the coast (Osterkamp, 1984)) and, on average, is snow-covered 8 to 9 months of the year. The region is mostly treeless with some patches of trees in the riparian areas in the Foothills. Vegetation consists of alpine plant communities in the Mountains, tussock tundra in the Foothills, and sedge

tundra on the Coastal Plain (Walker et al., 1989; CAVM Team, 2003). Willow and birch shrubs are common in riparian areas, and shrub height is variable, from approximately 0.3 to over 1 m. In response to climate warming in the Arctic, shrubs in tundra areas are increasing in abundance and extent (Sturm et al., 2001; Sturm et al., 2005; Tape et al., 2006).

3.3.2 Climate

The Alaska Arctic has continuous daylight during summer and little sunlight in winter. In addition to the extreme daylight cycles, because of the high latitudes, the sun crosses the horizon at a low angle and is primarily responsible for why the Arctic receives a lower income of solar energy (on an annual basis) compared with lower latitudes. Compounding factors in the Arctic's reduced net radiation balance are the high albedo of the extended winter snowpack (Przybylak, 2003; Zhang et al., 2003). The combination of extreme swings in daylight duration, shallow sun angles, and long periods of snow cover with high albedo results in a markedly lower radiation balance in the Arctic than in equatorial regions.

Because of the diminished amounts of energy and subsequent low air temperatures that follow, water vapor content is limited in the Arctic (Przybylak, 2003; Serreze and Barry, 2014). Only a small amount of water vapor can be held by cold air (for every 10°C drop in temperature, the ability of air to hold moisture is reduced by about half), and limited moisture is gained from evaporation/sublimation. The annual cycle of water vapor is therefore linked to that of air temperature, with the lowest water vapor pressures occurring during winter months when temperatures are lowest (Przybylak, 2003). If moisture content alone were considered, the Alaska Arctic would be classified as arid. In the Arctic, moisture, like incoming solar radiation and air temperatures, is relatively low and usually increases in a southerly direction (Woo, 2012).

3.4 Precipitation Inputs

Acquiring good precipitation data is challenging not only because most of the Alaska Arctic is remote, but also because from 8 to 9 months of the year the precipitation there is in solid form and extensively redistributed in the windy environment. In addition, sublimation can significantly reduce the snow water equivalent (SWE) on the ground at the end-of-winter. To get around some of the challenges involved with acquiring good snow distribution measurements, the actual accumulation of snow is not measured, instead field surveys were conducted to acquire SWE on the ground at winters end just prior to ablation. Warm season precipitation is typically

easier to measure, using shielded tipping bucket rain gauges at meteorological stations. The end-of-winter SWE measurements and the accumulation of rain captured in tipping buckets are the precipitation inputs into the hydrologic cycle. Below, the distribution of end-of-winter SWE and warm season precipitation inputs into the Alaska Central Arctic are outlined individually, then combined to calculate annual precipitation.

3.4.1 Distribution of End-of-winter SWE

The distribution of snow at winters end for the Alaska Central Arctic has been shown to be relatively independent of elevation, with roughly an average SWE of 100 mm from the Coastal Plain to the Mountains (Fig. 3.2a) (Homan and Kane, 2015). Homan and Kane (2015) quantified SWE on the ground at winters end by measuring both the depth and density of the snowpack at numerous, widely scattered, and representative sites. The idea behind this approach is to capture the spatial distribution of SWE after redistribution by the wind and most of the sublimation has taken place. The main problem with this approach is that snow surveys can be performed too early, with the possibility of additional snowfall before ablation. An additional concern is whether the measurement sites picked are truly representative of the general snow conditions of the surrounding areas. The long-term snow dataset presented by Homan and Kane (2015), which included over 1000 snow surveys conducted at roughly 200 locations from 2000-2013 (Fig. 3.1), is used in this investigation for the calculation of annual precipitation.

3.4.2 Warm Season Precipitation

The spatial variability of cumulative warm season precipitation within the Alaska Central Arctic has a strong linear relationship with topography and such precipitation increases with elevation from the Coastal Plain to the continental divide of the Mountains (Fig. 3.2b) (Homan et al., 2015). The maximum gradient for cumulative annual mean warm season precipitation generally increases north to south, but from year to year, can deviate slightly to the east or west. Warm season precipitation varies from less than 80 mm on the Coastal Plain to more than 320 mm in the Mountains (Fig. 3.3). Homan et al. (2015) analyzed warm season precipitation data from 31 meteorological stations (Fig. 3.1), ranging in record length from 2 to 31 years and distributed throughout the Alaska Central Arctic. Ideally, all 31 stations would have the same collection duration, but that is not the case, unfortunately. The standard NOAA/NWS 8-inch-orifice tipping bucket gauges were primarily used for measuring the liquid precipitation, and they

generally performed well except for occasional periods when either the weather (solid precipitation or wind) or wildlife (mostly bears) caused the gauges to be inoperable for a time. Warm season precipitation (liquid) was intended to be measured from the end of spring ablation to fall freeze up, generally from mid-May into September, with the warm season being shorter during the shoulder seasons (spring and fall) farther north. In the Arctic, snow can however fall any day of the year. During summer, solid precipitation captured in tipping bucket gauges eventually melts and the amount of precipitation is recorded, but the timing of deposition is offset. The transition seasons (spring and fall), with a likelihood of combined solid and liquid precipitation events is thus highly problematic for poor data quality. Spring time precipitation measurement are less of a concern because the spring is a drier time of the year. The fall, however, is a much wetter season and presents data quality measurement challenging. The long-term warm season precipitation dataset presented by Homan et al. (2015) is used in this investigation for the calculation of annual precipitation.

3.5 Annual Precipitation

Annual precipitation is the combined accumulation of end-of-winter SWE and warm season precipitation. The solid and liquid precipitation inputs for this study were acquired from Homan and Kane (2015) end-of-winter SWE measurements and Homan et al. (2015) warm season precipitation recordings. The two long term data records did not perfectly match, however. At one of the meteorological stations, Rooftop Ridge, no end-of-winter SWE measurements were conducted, so the station was removed from the data collection. In an attempt to improve the spatial distribution of meteorological stations in the northwest corner of the study domain, one additional station was additionally added. The Fish Creek station from the Fish Creek Arctic Freshwater Ecosystem (Fish CAFÉ) Circum-Arctic Lakes Observation Network (CALON) (Whitman et al., 2011) had both solid and liquid precipitation data, and was added into the long term datasets. Table 3.1 lists the name, geographic location, watershed name, and elevation of the 31 meteorological stations used in this investigation. Stations are arranged from lowest to highest elevation. Table 3.2 presents the record average end-of-winter SWE and cumulative mean warm season precipitation measurements at each of the meteorological stations, and states the time frame the averaged values are based on. Note that the period of record ranges from just 2 years (Siksikpuk) to 31 years (Atigun Pass); those stations with a longer record give a clearer picture of what can be expected hydrologically in this area. The end-of-winter SWE at the

31 stations range from 17 (White Hills, elev. 337 m) to 140 mm (Upper Kadleroshilik, elev. 209 m), but on average is roughly 100 mm from the Coastal Plain to the Mountains, and relatively independent of elevation. The warm season precipitation, however, has a large orographic variation, and ranges from roughly 40 mm on the coastal plain to 360 mm in the Brooks Range. Annual precipitation for each of the 31 meteorological stations were calculated by averaging the annual end-of-winter SWE and warm season precipitation values (Table 3.2). Because the end-of-winter SWE is roughly an average of 100 mm throughout the study domain, the annual precipitation pattern closely matches the warm season precipitation linear relationship with topography, but with roughly an additional 100 mm of water. The annual precipitation ranges from 136 mm on the Coastal Plain to 490 mm in the Brooks Range. A contoured map of annual precipitation over the Alaska Central Arctic is present in Figure 3.4.

Annual precipitation varies temporally and spatially over the Alaska Central Arctic. In the higher elevation of the Foothills and Mountains, annual precipitation is made up of approximately 70% liquid precipitation and 30% solid precipitation, which is almost exactly what Kane et al. (2004) found using a reduced sample size and duration. Liquid precipitation reached a maximum contribution of roughly 90% at two Mountains stations (88 % at Encampment, and 92% at Upper May Creek) (Table 2). On the Coastal Plain, the contribution of precipitation types is almost the opposite, with solid precipitation (SWE) on average representing 60% of the annual precipitation budget. Solid precipitation reached a maximum contribution of 70% at Fish Creek. In general, the Coastal Plain's primary precipitation contributor is end-of-winter SWE. With an increase in elevation to the lower Foothills, the precipitation contribution becomes almost equal amounts between liquid and solid. At even higher elevation, in the Mountains, the contribution of precipitation becomes largely from warm season precipitation.

Our field based measurements of annual precipitation compares well with the 30 year (1961-1990) average annual precipitation maps provided by PRISM (Parameter-elevation Regressions on Independent Slopes Model) model, which was developed by the Spatial Climate Analysis Service at Oregon State University (PRISM, 2000) (Fig. 3.5). Not only does PRISM modeled annual precipitation increase with elevation, the precipitation amounts are very comparable to our dataset, with roughly 200 mm on the Coastal Plain and upwards of 400 mm in the Mountains. Both the modeled and ground based results also show precipitation to wrap around to the northeast with the curve of the Brooks Range.

3.6 Conclusion

This study used the results from two relatively long term precipitation datasets, end-of-winter SWE and warm season precipitation, to illustrate that annual precipitation varies temporally and spatially over the Alaska Central Arctic. Annual precipitation is composed of the accumulation of both solid and liquid precipitation inputs, and the contribution of each type of precipitation varies with elevation. At high elevations, in the Mountains, annual precipitation is made up of approximately 70% liquid precipitation, while on the Coastal Plain, low elevations, warm season precipitation only accounts for roughly 40% of the annual precipitation budget.

A study by Kane et al. (2008) shows the total water content of the snowpack at the end of winter to comprise 30 to 40% of the annual precipitation. The current research found this to be true, but only at higher elevation. At lower elevation, end-of-winter SWE was found to represent an average of 60% of the annual precipitation budget, with a maximum contribution of 70% at one location.

Overall, annual precipitation has a strong linear relationship with elevation, and ranges from 136 mm on the Coastal Plain to 490 mm in the Brooks Range. The temporal variability was less conclusive and no discernible long-term trends in annual precipitation were found, primarily as a result of lacking evidence in the somewhat limited 29 year warm season precipitation dataset.

3.7 Acknowledgments

This paper is an outcome of numerous funded research projects in Arctic Alaska. Agencies that had some input into the precipitation data collection effort included the Alaska Department of Transportation and Public Facilities, National Science Foundational, and U.S. Fish and Wildlife Service. We thank all of the people who assisted in collecting precipitation data used in this study for the 31 sites analyzed: WERC, BLM, USDA NRCS, and Fish CAFÉ CALON.

3.8 References

ACIA, 2005: Arctic climate impact assessment: Cambridge University Press, New York, NY

Barnes, S. L., 1964: A technique for maximizing details in numerical weather map analysis. *Journal of Applied Meteorology,* 3(4): 396-409.

Benson, C. S., 1982: Reassessment of winter precipitation on Alaskas arctic slope and measurements on the flux of wind-blown snow. Research Report UAG R-288. Geophysical Institute.

Cavalieri, D., Parkinson, C., and Vinnikov, K. Y., 2003: 30-Year satellite record reveals contrasting Arctic and Antarctic decadal sea ice variability. *Geophysical Research Letters,* 30(18).

CAVM Team, 2003: Circumpolar Arctic Vegetation Map. Scale 1 : 7 500 000. Conservation of Arctic Flora and Fauna (CAFF) Map No. 1. U.S. Fish and Wildlife Service, Anchorage, Alaska.

Griggs, D. J. and Noguer, M., 2002: Climate change 2001: the scientific basis. Contribution of working group I to the third assessment report of the intergovernmental panel on climate change. *Weather,* 57(8): 267-269.

Hinzman, L. D., Bettez, N. D., Bolton, W. R., Chapin, F. S., Dyurgerov, M. B., Fastie, C. L., Griffith, B., Hollister, R. D., Hope, A., Huntington, H. P., Jensen, A. M., Jia, G. J., Jorgenson, T., Kane, D. L., Klein, D. R., Kofinas, G., Lynch, A. H., Lloyd, A. H., McGuire, A. D., Nelson, F. E., Oechel, W. C., Osterkamp, T. E., Racine, C. H., Romanovsky, V. E., Stone, R. S., Stow, D. A., Sturm, M., Tweedie, C. E., Vourlitis, G. L., Walker, M. D., Walker, D. A., Webber, P. J., Welker, J. M., Winker, K., and Yoshikawa, K., 2005: Evidence and implications of recent climate change in northern Alaska and other arctic regions. *Climatic Change,* 72(3): 251-298.

Homan, J. W. and Kane, D. L., 2015: Arctic snow distribution patterns at the watershed scale. *Hydrology Research,* 46(4): 507-520.

Homan, J. W., Kane, D. L., and Stuefer, S. L., 2015: Warm season precipitation patterns from low to high elevation in the Alaska Central Arctic. *Arctic, Antarctic, and Alpine Research,* submitted, 2015.

Houghton, J. T., 1996: Climate change 1995: The science of climate change: contribution of working group I to the second assessment report of the Intergovernmental Panel on Climate Change: Cambridge University Press.

Kane, D. L., Gieck, R. E., Kitover, D. C., Hinzman, L. D., McNamara, J. P., and Yang, D., 2004: Hydrological cycle on the North Slope of Alaska. In: Northern Research Basins Water Balance (D.L. Kane & D. Yang, eds.). Publ. 290. IAHS, Wallingford, UK, pp. 224-236.

Kane, D. L., Hinzman, L. D., Gieck, R. E., McNamara, J. P., Youcha, E. K., and Oatley, J. A., 2008: Contrasting extreme runoff events in areas of continuous permafrost, Arctic Alaska. *Hydrology Research,* 39(4): 287-298.

Maslanik, J. A., Serreze, M. C., and Agnew, T., 1999: On the record reduction in 1998 western Arctic sea-ice cover. *Geophysical Research Letters,* 26(13): 1905-1908.

Osterkamp, T. E., 1984: Temperature measurements in permafrost. *Rep. FHWA-AK-RD-85-11, State of Alaska, Department of Transportation and Public Facilities, Division of Planning and Programming, Research Section* 87.

PRISM, 2000: Western Region Climate Center, PRISM precipitation maps-1961-90, Mean Annual Precipitation, Alaska-Yukon: Western Regional Climate Center, accessed July 13, 2011 at http://www.wrcc.dri.edu/pcpn/ak.gif.

Przybylak, R., 2003: The climate of the Arctic. Kluwer Academic Publishers, Dordrecht, 270 pp.
Rawlins, M. A., Steele, M., Holland, M. M., Adam, J. C., Cherry, J. E., Francis, J. A., Groisman, P. Y., Hinzman, L. D., Huntington, T. G., Kane, D. L., Kimball, J. S., Kwok, R., Lammers, R. B., Lee, C. M., Lettenmaier, D. P., McDonald, K. C., Podest, E., Pundsack, J. W., Rudels, B., Serreze, M. C., Shiklomanov, A., Skagseth, O., Troy, T. J., Vorosmarty, C. J., Wensnahan, M., Wood, E. F., Woodgate, R., Yang, D. Q., Zhang, K., and Zhang, T. J., 2010: Analysis of the Arctic System for Freshwater Cycle Intensification: Observations and Expectations. *Journal of Climate,* 23(21): 5715-5737.
Serreze, M., Walsh, J., Chapin Iii, F., Osterkamp, T., Dyurgerov, M., Romanovsky, V., Oechel, W., Morison, J., Zhang, T., and Barry, R., 2000: Observational evidence of recent change in the northern high-latitude environment. *Climatic Change,* 46(1-2): 159-207.
Serreze, M. C. and Barry, R. G., 2014: The Arctic climate system: Cambridge University Press.
Shulski, M. and Wendler, G., 2007: The climate of Alaska: University of Alaska Press, Fairbanks, AK.
Sturm, M., Holmgren, J., McFadden, J. P., Liston, G. E., Chapin, F. S., and Racine, C. H., 2001: Snow-Shrub Interactions in Arctic Tundra: A Hypothesis with Climatic Implications. *Journal of Climate*, 14:336-344.
Sturm, M., Douglas, T., Racine, C., and Liston, G. E., 2005: Changing snow and shrub conditions affect albedo with global implications. *J. Geophys. Res.,* 110(G1): G01004.
Tape, K., Sturm, M., and Racine, C., 2006: The evidence for shrub expansion in Northern Alaska and the Pan-Arctic. *Global Change Biology,* 12(4): 686-702.
Vinnikov, K. Y., Robock, A., Stouffer, R. J., Walsh, J. E., Parkinson, C. L., Cavalieri, D. J., Mitchell, J. F., Garrett, D., and Zakharov, V. F., 1999: Global warming and Northern Hemisphere sea ice extent. *Science,* 286(5446): 1934-1937.
Walker, D. A., Binnian, E., Evans, B. M., Lederer, N. D., Nordstrand, E., and Webber, P. J., 1989: Terrain, vegetation and landscape evolution of the R4D research site, Brooks-Range-Foothills, Alaska. *Holarctic Ecology,* 12(3): 238-261.
Whitman, M. S., Arp, C. D., Jones, B., Morris, W., Grosse, G., Urban, F., and Kemnitz, R., 2011: Developing a long-term aquatic monitoring network in a complex watershed of the Alaskan Arctic Coastal Plain. Pages 15-20 in C. N. Medley, G. Patterson, and M. J. Parker, editors. Proceedings of the Fourth Interagency Conference on Research in Watersheds: Observing, Studying, and Managing for Change. USGS, Reston.
Woo, M.-k., 2012: Permafrost hydrology: Springer Science & Business Media.
Yang, D., Goodison, B., Benson, C., and Ishida, S., 1998: Adjustment of daily precipitation at 10 climate stations in Alaska: Application of WMO intercomparison results. *Water Resour. Res,* 34(2): 241-256.
Zhang, T., Scambos, T., Haran, T., Hinzman, L. D., Barry, R. G., and Kane, D. L., 2003: Ground-based and satellite-derived measurements of surface albedo on the North slope of Alaska. *Journal of Hydrometeorology,* 4(1): 77-91.

3.9 Figures

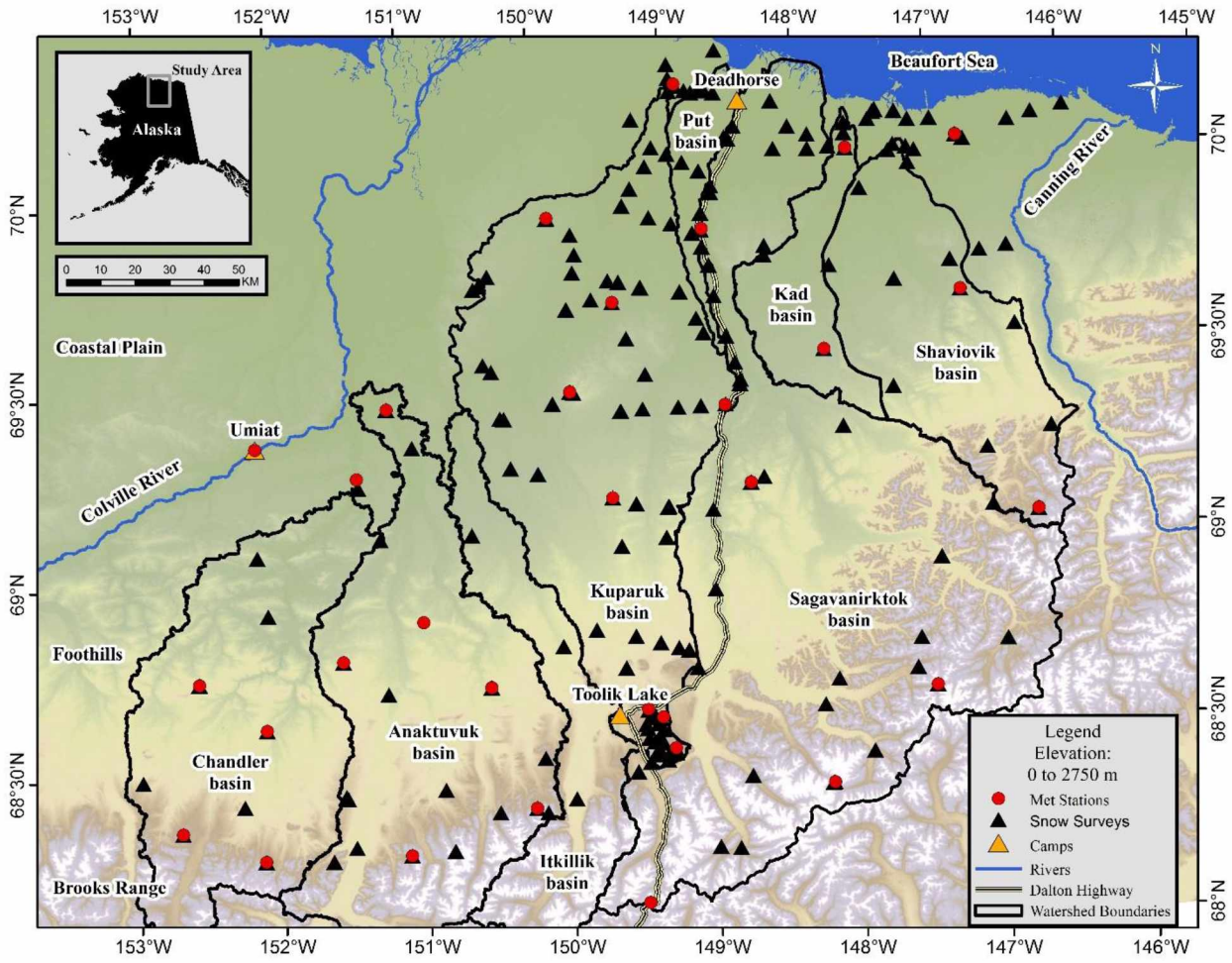

Figure 3.1: Site map showing snow survey and meteorological (Met) station locations within several Alaska Central Arctic watersheds.

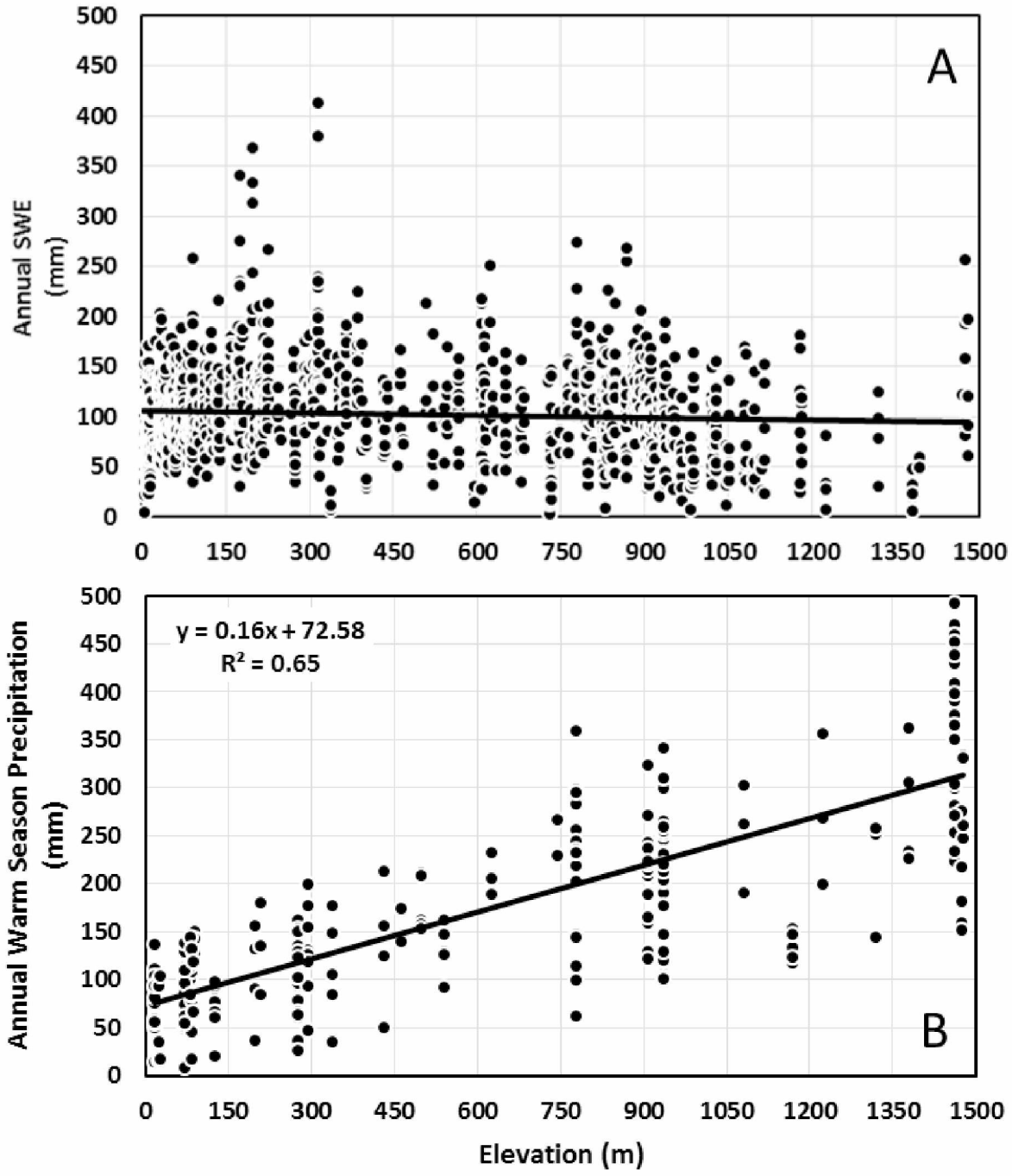

Figure 3.2: A) End-of-winter SWE measurements (2000–2013), and B) Warm season precipitation accumulation from all 31 stations (1985–2013) plotted versus elevation in the Alaska Central Arctic.

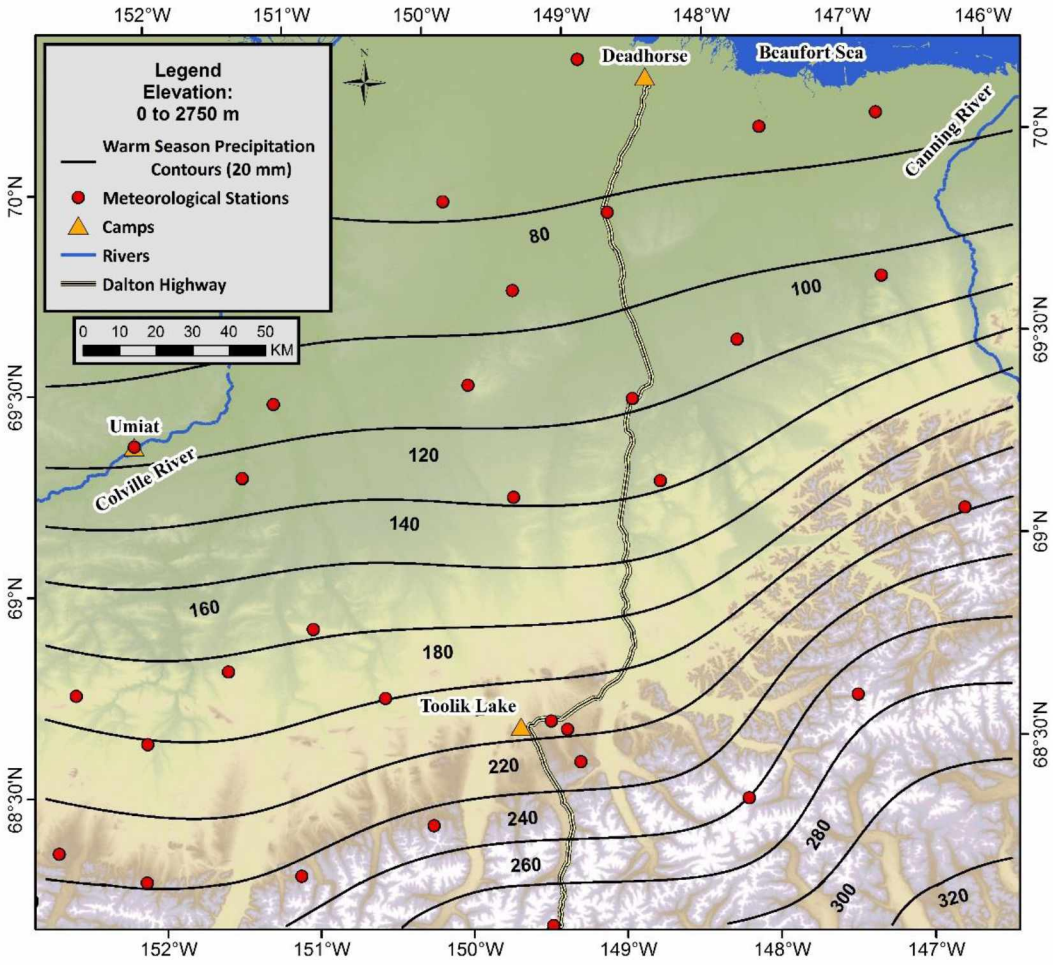

Figure 3.3: Contoured map of station average warm season precipitation in the Alaska Central Arctic. Point data were interpolated with Barnes (1964) interpolation method.

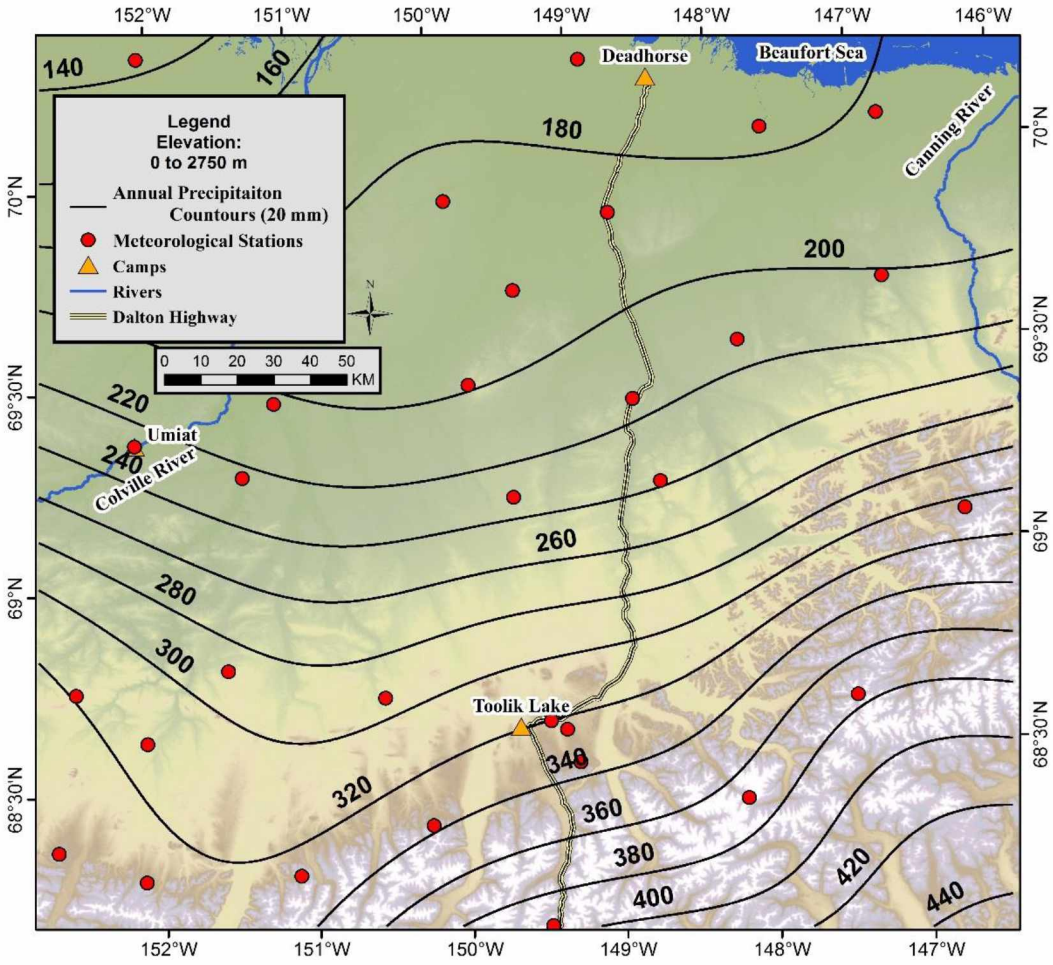

Figure 3.4: Contoured map of station average annual precipitation in the Alaska Central Arctic. Point data were interpolated with Barnes (1964) interpolation method.

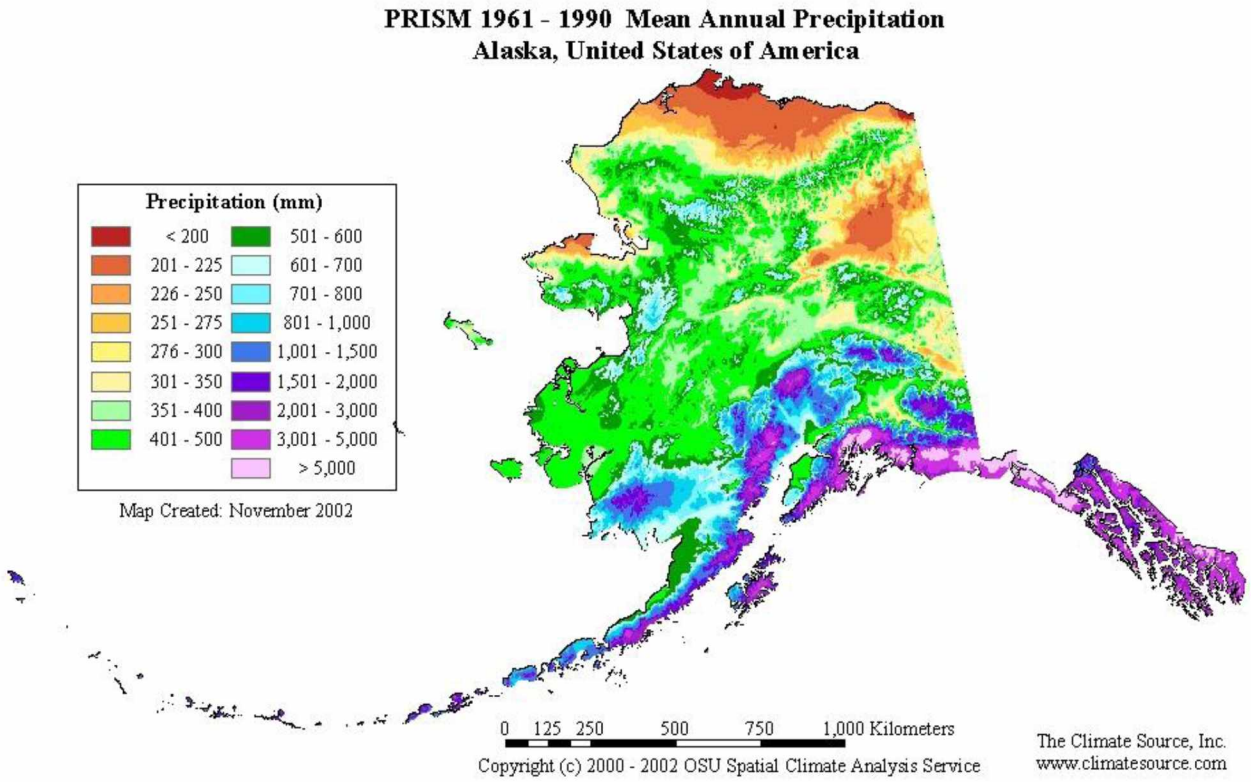

Figure 3.5:Mean annual precipitation modeled by PRISM climate group for the state of Alaska (PRISM, 2000).

3.10 Table

Table 3.1: Name, geographic coordinates, watershed name and elevation of the 31 meteorological stations used for annual precipitaiton measurements.

Station Name (Code)	Coordinates		Watershed	Elev. (m)
Betty Pingo (BM)	70° 16' 46" N	148° 53' 45" W	Kuparuk	15
Lower Kadleroshilik (DBM7)	70° 04' 24" N	147° 39' 00" W	Kadleroshilik	24
Bullen (DBM8)	70° 04' 47" N	146° 49' 09" W	No Name	26
Fish Creek (Fish) (USGS)	70° 20' 07" N	152° 03' 07" W	Fish	31
Franklin Bluffs (FB)	69° 53' 32" N	148° 46' 05" W	Sagavanirktok	71
Anaktuvuk River (DUS2)	69° 27' 51" N	151°10' 07" W	Anaktuvuk	81
North White Hills (DFM3)	69° 42' 53" N	149° 28' 13" W	Kuparuk	84
Chandler River Bluff (DUS3)	69° 17' 00" N	151° 24' 16" W	Chandler	86
Umiat (BLM)	69° 22' 12" N	152° 08' 10" W	Colville	88
Northwest Kuparuk (DFM4)	69° 56' 51" N	149° 55' 00" W	Kuparuk	124
Kavik (DBM6)	69° 40' 24" N	146° 54' 02" W	Shaviovik	198
Upper Kadleroshilik (DBM5)	69° 32' 58" N	147° 56' 30" W	Kadleroshilik	209
Sagwon (SH)	69° 25' 28" N	148° 41' 45" W	Sagavanirktok	275
South White Hills (DFM1)	69° 12' 02" N	149° 33' 30" W	Kuparuk	293
White Hills (DFM2)	69° 29' 11" N	149° 49' 17" W	Kuparuk	337
Sag-Ivishak (DBM4)	69° 12' 55" N	148° 33' 06" W	Sagavanirktok	431
Siksikpuk (DUM8)	68° 37' 48" N	152° 06' 08" W	Chandler	463
Tuluga (DUM4)	68° 48' 15" N	151° 32' 46" W	Anaktuvuk	497
Nanushuk (DUM3)	68° 43' 15" N	150° 30' 11" W	Anaktuvuk	540
Hatbox Mesa (DUM7)	68° 45' 16" N	152° 34' 23" W	Chandler	624
Upper Kuparuk (UK)	68° 38' 25" N	149° 24' 23" W	Kuparuk	778
Green Cabin Lake (GCL)	68° 32' 01" N	149° 13' 47" W	Kuparuk	908
Imnavait Basin Met (IB)	68° 36' 59" N	149° 18' 13" W	Kuparuk	937
White Lake (DUM6)	68° 21' 47" N	152° 42' 25" W	Chandler	1081
Itikmalakpak (DUM1)	68° 17' 24" N	151° 06' 54" W	Anaktuvuk	1168
Encampment Creek (DUM5)	68° 17' 11" N	152° 07' 55" W	Chandler	1224
Juniper (DBM3)	69° 04' 34" N	146° 30' 17" W	Shaviovik	1319
Upper May Creek (DUM2)	68° 23' 55" N	150° 13' 40" W	Anaktuvuk	1378
Atigun Pass (AP) (USDA/NRCS)	68° 08' 00" N	149° 29' 00" W	Sagavanirktok	1463
Accomplishment Creek (DBM1)	68° 24' 41" N	148° 08' 11" W	Sagavanirktok	1474
Ribdon (DBM2)	68° 38' 32" N	147° 21' 06" W	Sagavanirktok	1478

Table 3.2: Average SWE, warm season precipitation, and annual precipitation for each of the 31 metorological station locations. Druation of record for both SWE and warm seasoin precipitation are also provided and range from 2 to 31 years.

Station Name (Code)	Elev. (m)	SWE Record Duration/ # of Full Yrs	SWE (mm)	Warm Season Precipitation Record Duration/ # of Full Yrs	Warm Season Precipitation (mm)	Annual (mm)
Betty Pingo (BM)	15	2000-2013/ 14	96	1994-2011/ 16	78	174
Lower Kadleroshilik (DBM7)	24	2009-2010/ 2	72	2007-2010/ 4	61	133
Bullen (DBM8)	26	2008-2010/ 3	152	2007-2009/ 3	73	225
Fish Creek (FC) (USGS)	31	2012-2014/3	95	2007-2010/ 4	41	136
Franklin Bluffs (FB)	71	2000-2013/ 14	110	1987-2013/ 26	83	193
Anaktuvuk River (DUS2)	81	2010-2013/ 4	86	2009-2012/ 4	112	198
North White Hills (DFM3)	84	2007-2013/ 7	120	2006-2013/ 7	80	200
Chandler River Bluff (DUS3)	86	2010-2013/ 3	101	2011-2013/ 3	105	206
Umiat (BLM)	88	2008-2012/ 5	91	2008-2012/ 5	139	230
Northwest Kuparuk (DFM4)	124	2007-2013/ 7	130	2006-2013/ 7	71	201
Kavik (DBM6)	198	2007-2010/ 3	56	2007-2010/ 4	104	160
Upper Kadleroshilik (DBM5)	209	2007-2010/ 3	140	2008-2010/ 3	133	273
Sagwon (SH)	275	2000-2013/ 14	72	1987-2013/ 26	114	186
South White Hills (DFM1)	293	2007-2013/ 7	121	2006-2013/ 7	137	258
White Hills (DFM2)	337	2007-2013/ 4	17	2006-2013/ 5	125	142
Sag-Ivishak (DBM4)	431	2007-2010/ 4	97	2007-2010/ 4	136	233
Siksikpuk (DUM8)	463	2010-2013/ 4	133	2011-2013/ 2	145	278
Tuluga (DUM4)	497	2009-2013/ 5	120	2009-2013/ 5	179	299
Nanushuk (DUM3)	540	2009-2013/ 5	119	2009-2013/ 5	131	250
Hatbox Mesa (DUM7)	624	2010-2013/ 4	184	2011-2013/ 3	209	393
Upper Kuparuk (UK)	778	2000-2013/ 14	159	1994-2013/ 17	226	385
Green Cabin Lake (GCL)	908	2000-2013/ 14	58	1996-2013/ 18	205	263
Imnavait Basin Met (IB)	937	2000-2013/ 14	113	1985-2013/ 29	211	324
White Lake (DUM6)	1081	2010-2013/ 4	82	2011-2013/ 3	251	333
Itikmalakpak (DUM1)	1168	2009-2013/ 5	91	2009-2013/ 5	135	226
Encampment Creek (DUM5)	1224	2010-2013/ 4	38	2011-2013/ 3	275	313
Juniper (DBM3)	1319	2007-2010/ 4	83	2007-2010/ 4	228	311
Upper May Creek (DUM2)	1378	2009-2013/ 5	27	2009-2013/ 5	298	325
Atigun Pass (AP) (USDA/NRCS)	1463	2000-2013/ 14	126	1983-2013/ 31	364	490
Accomplishment Creek (DBM1)	1474	2007-2013/ 7	137	2006-2013/ 5	197	334
Ribdon (DBM2)	1478	2007-2010/ 4	118	2007-2010/ 4	293	411

Chapter 4 Winter Moisture Sources and Pathways in the Alaska Arctic[3]

4.1 Abstract

The Alaska Arctic snowpack and its annual spring melt is historically the most significant event of the hydrological cycle. Several factors affect the accumulation of this winter water storage, including proximity to oceanic water sources, topography, and the Arctic's high latitude location, which result in diminished winter solar radiation and subsequent cold air temperatures. During fall when the Beaufort and Chukchi Seas are open or covered with relatively thin and fractured ice, the ocean is a substantial moisture source for snow-producing storms. We determined that snowfall events derived from the Arctic seas (north events) occur primarily during this time. In mid-winter, when the concentration of sea ice off Alaska's northern coast is at a maximum, snow-producing storms are advected from the Gulf of Alaska and the southern Bering Sea, which remain ice-free throughout winter, providing an open source of moisture. Starting after Spring Equinox, a second episode of northern storms occur, which is thought to be the result of the Arctic Ocean developing more leads and open water as solar radiation quickly increases. Data from this study indicate that the Brooks Range divide affects moisture availability throughout the Alaska Arctic by acting as a moisture passage barrier. More than twice as many snowfall events per meteorological station occur on the southern side of the continental divide as on the northern side. In the Alaska Arctic, where localized moisture sources can be ephemeral, both atmospheric circulation and sea ice cover are key components in the accumulation and amount of snow storage.

---

[3] Homan, J.W., and Kane, D.L., Winter moisture sources and pathways in the Alaska Arctic, Submitted to *American Meteorological Society*.

4.2 Introduction

The high geographical latitude of the Arctic creates unique hydrological conditions as a result of a low thermal energy state and, therefore, annual average air temperatures are low and winters long. Consequently, winter snow accumulation and snowmelt are the most important features of the hydrological cycle in cold regions. Snow accumulation may last for nine months and is then released in a relatively short time, typically 10 to 14 days just before summer solstice (Kane and Hinzman, 1988). Each year, for six months or more, Arctic water bodies are affected by ice because of the long duration of cold temperatures. The presence of ice affects overall streamflow, making it intensely seasonal or even ephemeral. Spring melting of snow and ice, when soils are frozen and infiltration is reduced, accentuates the amount of runoff and peak flow. The total water content of the snowpack within the Alaska Arctic at winter's end comprises 40% or more of the region's annual precipitation (Kane et al., 1991; Kane et al., 2008b); on average, about two-thirds of the snow water equivalent (SWE) leaves catchments as runoff (Kane et al., 2008a; Kane et al., 2000; Kane et al., 2004). On larger rivers in the Alaska Arctic, the breakup flood can account for about 40% of the annual discharge (Arnborg et al., 1967); on smaller streams, for as much as 90% (McCann et al., 1972).

With the snowpack being such a significant part of the Alaska Arctic hydrologic cycle, it may seem surprising that annual snowfall totals are generally quite low, on the order of 10 cm of snow water equivalent (SWE) per year (Benson, 1982; Homan et al., 2015; Liston and Sturm, 2002; Sturm and Liston, 2003). Cumulative low snowpack water content totals are a result of very low air temperatures (cold air masses cannot hold as much moisture as warm air masses) and ice, which covers many of the potential sources (lakes and seas) of moisture. In order for precipitation to occur, water vapor in the atmosphere can be (1) transported into a cold region through atmospheric circulation (advected), (2) recycled within the same region by either evaporation or sublimation (local), or (3) supplied by both processes (Serreze et al., 2005). During the long Arctic winter, however, there is limited energy to drive evaporation/sublimation. Excess in annual precipitation over evaporation and sublimation results from the inflow of moisture through atmospheric circulation, which for the Arctic in general, has a mean value of roughly 160 mm (Serreze et al., 2005). Identifying moisture sources and possible vapor flux pathways, which deliver the excess precipitation to the Arctic, would provide a better understanding of potential variations in the local hydrologic cycle. This is particularly true for

the winter precipitation that produces the snowpack. In this paper we examine the sources of moisture responsible for snow-producing storms in the energy-limited and arid Alaska Arctic and the pathways by which moisture is delivered. With the Arctic defined as the region north of the Arctic Circle (~ 66°33′45.8″ N), the area that comprises the Alaska Arctic is topographically bisected by the Brooks Range, which runs east to west, isolating what is generally referred to as the "North Slope" from the rest of Alaska. While evaluating the advected precipitation pathways to the Alaska Arctic, we will also assess the blocking influence of the Brooks Range.

4.3 The Alaska Arctic

4.3.1 Climate

The Alaska Arctic climate is controlled by three major factors; (1) extreme daylight cycles, (2) having oceans on three sides, one of which freezes over, and (3) being topographically bisected by a mountain range. The duration of daylight depends on latitude and time of year, but in general, the Alaska Arctic has continuous daylight during summer, and little sunlight in winter. In addition, because of the high latitudes, the sun crosses the horizon at a shallow angle and is primarily responsible for why the Arctic receives a lower income of solar energy (on an annual basis) compared with lower latitudes. Compounding factors in the Arctic's reduced net radiation balance are the high albedo of the extended winter snowpack (Przybylak, 2003; Zhang et al., 2003). The combination of extreme swings in daylight duration, shallow sun angles, and long periods of snow cover with high albedo results in a markedly lower radiation balance in the Arctic than in equatorial regions.

Alaska is surrounded by water on three sides and can be thought of as a large peninsula, with the Arctic Ocean to the north (Beaufort Sea, north; Chukchi Sea, northwest), the Bering Sea to the west and southwest, and the Pacific Ocean to the south. Alaska's climate is influenced by these vast water bodies and by the seasonal distribution of sea ice. The ability of oceans to absorb and release large amounts of energy has a moderating influence on the climate of coastal regions (maritime climates), which have warmer winters and cooler summers than interior areas (continental climates) (Haugen and Brown, 1980; Zhang et al., 1996, 1997). Areas along the coastline at the Beaufort Sea and Chukchi Sea are marginally considered maritime though, as conditions are closer to those of a polar desert, which consists of mean annual temperatures well below freezing and low annual precipitation. Liston and Sturm, (2002) did find, however, that

maritime temperature dampening patterns occur in the Alaska Arctic, along with increases in relative humidity and wind speed with proximity to the coast. When the seas are ice-covered, the maritime influence is significantly less than when the water is ice-free, due to a corresponding decrease in energy transfer to the atmosphere. Sea ice is present for much of the year in the Arctic Ocean and only retreats north for a short time in summer before forming again in autumn (Przybylak, 2003). The Bering Sea transitions from ice-covered winters in the north to ice-free winters in the south.

Along with latitude and ocean influences, the climate of the Alaska Arctic is affected by topography. On either side of the Brooks Range, significant climate divergence occurs (Przybylak, 2003). This barrier is hypothesized to greatly reduces moisture availability in the Alaska Arctic by blocking potential pathways for storms that otherwise would bring precipitation from the south to farther north.

Other than the three controlling factors for climate just mentioned, Alaska's climate is significantly affected by the large-scale circulation of the atmosphere. Because the Arctic has a lower thermal energy state, on an annual basis, it serves as the Northern Hemisphere "heat sink" and plays a fundamental role in the global climate system. To balance earth's energy budget, the Arctic imports heat (energy) from southerly latitudes and radiates it back to space (Serreze and Barry, 2014). This poleward energy transport is brought about by pressure gradients from an imbalance in pressure surface heights. Corresponding to uneven solar heating and related troposphere temperature differences that decrease poleward from equatorial regions is a poleward decrease in height of pressure surfaces that induces the pressure gradient. The atmosphere attempts to reduce the temperature gradient between the Equator and the poles, meanwhile balancing the energy budget. This process drives the global energy exchange and shapes our climate system (Serreze and Barry, 2014). Understanding these facts about the Alaska Arctic climate is crucial for comprehending the parameters that govern the moisture content and movement within this area.

4.3.2 Moisture Content

As a result of diminished amounts of energy and the low air temperatures that follow, water vapor content is limited in the Arctic (Przybylak, 2003; Serreze and Barry, 2014). Only a small amount of water vapor can be held by cold air (for every 10°C drop in temperature, the

ability of air to hold moisture is reduced by about half), and limited moisture is acquired from evaporation/sublimation. The annual cycle of water vapor is therefore linked to that of air temperature, with the lowest water vapor pressures occurring during winter months when temperatures are lowest (Przybylak, 2003). Serreze et al., (2005) analyzed aspects of Arctic water vapor and found that between 70°N and the North Pole, the perceptible water (which is depth of water obtained if all moisture in the atmosphere column is condensed) is only about 2.5 mm in winter, increasing to roughly 14 mm in summer. This amount compares to a global mean annual average of about 25 mm (Serreze and Barry, 2014). If moisture content alone were considered, the Alaska Arctic would be classified as arid. In the Arctic, moisture, like incoming solar radiation and air temperatures, is relatively low and usually increases in a southerly direction (Woo, 2012).

4.3.3 Precipitation

In general, the total annual precipitation in the Alaska Arctic amounts to only 100 to 400 mm of liquid water (Kane et al., 2000; Kane et al., 2012; Searby, 1971; Shulski and Wendler, 2007; Stuefer et al., 2012). If the total water content is separated into (1) water content in the snowpack at the end of winter (SWE) and (2) warm season precipitation, distinctly different distribution patterns are noticeable. The water content in the snowpack at the end of winter is on average 100 to 110 mm across the Alaska Central Arctic, with little to no orographic effect (Homan and Kane, 2015). Warm season precipitation, however, increases linearly with increasing elevation, with less than 80 mm on the Coastal Plain to nearly 320 mm in the Brooks Range (Homan et al., 2015). Overall, for the same 1500 m change in elevation, warm season precipitation increases more than 240 mm, while little or no change in SWE occurs. A considerable fraction of warm season precipitation results from regional recycling of water vapor when evapotranspiration rates are fairly high and are strongly affected by the land surface (Serreze and Barry, 2014). The sources of moisture responsible for snow-producing storms are still in question, however. During the middle of winter when ice limits moisture availability from the Arctic Ocean, lakes, and rivers, snow-producing storms are known to still occur. It is hypothesized that mid-winter moisture is delivered from non-local moisture sources through atmospheric advected circulation.

4.3.4 Geographical Setting and Local Characteristics

For the purpose of this paper, the area north of the Brooks Range will be classified as the Arctic, while the area between the continental divide of the Brooks Range and the Arctic Circle will be called the Subarctic. Regardless, both areas are at high latitudes with mean annual temperatures below freezing, at around −12°C and −4°C in the Arctic and Subarctic, respectively (Shulski and Wendler, 2007). The Subarctic has more of a continental climate though, with extreme temperature variability. The statewide high and low temperature records, 38°C and −62°C, respectively, have been set in the Subarctic, albeit north of the Arctic Circle (Shulski and Wendler, 2007). The high temperatures are the result of abundant summer solar heating and isolation from the moderating effect of the ocean. Subarctic winds are usually quite light, with annual averages less than 2 m/s. During winter, under anticyclonic patterns (high pressure) with clear skies and calm wind conditions, temperature inversions can develop and result in extreme cold air temperatures at low elevations. With the average annual temperature in the Subarctic only a few degrees below freezing and with its wide range, this area is underlain by discontinuous permafrost (Shulski and Wendler, 2007). Residing at yet higher latitudes with colder average annual temperatures, the area north of the Brooks Range is underlain by continuous permafrost (250 to 300 m in the Brooks Range and up to 600 m along the coast (Osterkamp, 1984). In the mostly treeless Arctic, average annual wind speeds can exceed 5 m/s and increase during the cold season (Shulski and Wendler, 2007).

4.4 Methods

In order to determine the sources of moisture responsible for snow-producing storms, we examined the timing of snowfall events using data from meteorological stations; next, we used an atmospheric model (HYSPLIT: HYbrid Single Particle Lagrangian Integrated Trajectory) (Draxler and Hess, 1997) to generate backward air particle trajectories based on the timing of the determined precipitation events. The trajectory model does not by itself indicate whether snow occurred; rather it suggests the possible pathways by which air particles traveled to our meteorological stations in order to arrive when there was recorded snowfall events. National Weather Service (NWS) surface analysis charts were acquired for the snowfall events. The surface analysis charts indicate the location of low (L) and high (H) pressure centers and show positions and types of fronts. In conjunction, the HYSPLIT back-trajectories and surface analysis

charts were used to determine whether the source of moisture for the snow-producing storms was local or whether the moisture was transported over long distances via atmospheric circulation.

4.5 Snowfall Events

Snowfall events were acquired from eight federal government metrological stations that are spatially distributed throughout Alaska's Arctic and Subarctic (Fig. 4.1). Additional stations exist within the study domain, but only stations with homogeneous data records between the years of 2000 and 2014 where used. Furthermore, the metrological data needed to include winter liquid precipitation or snow depth information, and air temperature data were also used if available. Daily measurements were used, or hourly values were converted to get daily values. Eight stations met the criteria of being spatially distributed, with mostly continuous winter liquid precipitation or snow depth data during the desired time frame. Five of the stations are located in the Arctic, north of the Brooks Range, with three at the coastline of the Chukchi and Beaufort Seas and two inland in the northern foothills. The three remaining stations are located in the Subarctic, south of the continental divide. These stations are operated by several federal agencies: two are from the U.S. Geological Survey (USGS) (Tunalik and Awuna2), two are from the Natural Resources Conservation Service (NRCS), U.S. Department of Agriculture (USDA) Snow Telemetry (SNOTEL) (Fort Yukon and Imnavait Creek), and four are from the National Climate Data Center (NCDC), National Oceanic and Atmospheric Administration (NOAA) (Barrow, Bettles, Kuparuk Airport, and Kotzebue).

The different agency stations used a variety of measurement instruments, sampling methods, and reporting units. Because our goal was to examine moisture, all snow measurements were re-calculated into units of liquid water (SWE, mm) (Table 4.1). Four different data treatments were implemented depending on the original data collection method and recording format. Treatment 1 – Precipitation data originally in units of liquid water (SWE) and air temperature (T) available: No calculations were performed and data were simply limited to below freezing air temperatures ($T < 0°C$). Treatment 2 – Precipitation data originally in units of liquid water are available, but air temperature data not available: No calculations were performed and data were restricted to below freezing air temperature periods based on neighboring stations. Treatment 3 – Precipitation data in units of snow depth (SD, mm) and air temperature data available: The data were converted into units of liquid water using $SWE = SD*(\rho_s / \rho_w)$, where

ρs is the density of snow (kg/m^3) and ρw is the density of water (1000 kg/m^3). Different snow densities were used based on different air temperatures (Judson and Doesken, 2000; Super and Holroyd, 1997; U.S. Department of Commerce, 1996). Treatment 4 – Precipitation data in units of snow depth and air temperature data not available: All snow depth measurements were converted into units of liquid water using SWE = SD*(ρ_s / ρ_w), with a fixed value for snow density (100 kg/m^3). Most of the snowfall events recorded with supplemental air temperature measurements occurred when air temperatures where between -2°C and -10°C, which typically produces a snow density of 100 kg/m^3, and is the reason that this density was used as the fixed value for treatment 4. All snow densities and depths used in treatments 3 and 4 were for newly fallen snow. Determining the exact amount of precipitated SWE was not important, as we were only interested in an indication that significant snow fell.

With all the snow data in units of liquid water (SWE, mm), criteria for what constitutes a snowfall event needed to be established. Each of the eight meteorological stations used in this investigation acquired snow measurements (liquid water or snow depth) by means of automated methods and reported the data as accumulation totals. Positive changes in accumulation thus correlate to the occurrence of additional snow. But how much snow accumulation defines a snowfall event? Using a snowfall event criterion consisting of a large addition in SWE (e.g., 10 mm) would result in very few snowfall events above that threshold, and to the contrary, a small addition in SWE requirement (e.g., 0.5 mm) would ensure a very high number of snowfall events and most likely pick up instrument noise and "Trace" snow events, which are highly prevalent in the Arctic (Benson, 1982; Black, 1954) A concern with randomly choosing criteria was whether any chosen value would affect the results. If only large snowfall events were evaluated, would that skew the source of moisture and the pathway results compared with looking at a wider range of event sizes? To alleviate this concern, a sensitivity analysis was conducted using four different criteria. The duration of snowfall events can last for multiple days or at least begin and end on different days. Therefore, the criteria defining a snowfall event needed to accept not only single day snowfalls that surpassed the SWE requirements, but also the accumulation of snow on consecutive days that collectively exceeded it. Table 4.2 provides the four criteria required and breaks down the changes in daily SWE (1 day) and consecutive accumulation of SWE (multi-day) that needed to be surpassed for consideration as a snowfall event. For the case of Criterion 1, a single day would need an accumulation of SWE greater than 10 mm and/or consecutive days

each having more than a 5 mm addition in SWE. The snowfall requirements decrease from Criteria 1 through 4. The results from this analysis would illustrate if the amount of snow accumulation during a given storm is a function of its moisture source and its travel pathway. To do this analysis, the occurrence of snowfall events for each criterion was evaluated through time. A graphical change in shape between criteria would indicate that different snowfall event sizes are related to different pathways and separate moisture sources, while a similar graphical shape for each criterion would illustrate consistent sources of moisture and make the criteria size selections unimportant.

4.5.1 HYSPLIT Air Trajectory Calculations

To reconstruct the transport trajectories of precipitating air associated with the historic snowfall events, we used the HYSPLIT modeling system developed by the National Oceanic and Atmospheric Administration's Earth System Research Laboratory (NOAA-ESRL). The HYSPLIT modeling system, in part, was designed to compute air parcel back-trajectories from gridded meteorological data fields (Draxler and Hess, 1997; Draxler and Rolph, 2015; Rolph, 2015). The meteorological data used are gridded on conformal map projections, and calculations of the motion of air parcels are performed in successive time steps from these data (Stohl, 1998). Trajectories can be computed sequentially on multiple meteorological grids and at different spatial resolutions. Reconstructed (archive) or forecasted (forward) air trajectories can then be plotted on maps. Archive trajectories are a useful tool to describe the most probable upwind path taken by an air mass (Stohl, 1998). Additional overview information on the HYSPLIT model can be found in Draxler and Hess (1998) and Draxler et al., (2012).

The HYSPLIT model was used to calculate and visualize the flow path of air parcels associated with historic snowfall events in Arctic Alaska. This method has been used in similar studies to determine the pathways of heavy precipitation, snow delivery, and extreme snow accumulation (e.g., Andin et al., 2014; Bednorz, 2013; Mesquita et al., 2010; Sinclair et al., 2010). In the present study, the gridded meteorological data used for the archive air parcel trajectory calculations were obtained from two different data sets: (1) Global Data Assimilation System (GDAS1) post December 1, 2004, and (2) Global Reanalysis Data prior to December 1, 2004. Air parcel trajectories were computed for each of the selected historic snowfall events using as starting locations the meteorological stations at which the events were recorded. The

model was set to run at 915 m (height of moisture bearing clouds) above ground level and back in time for 120 hours (5 days), which is the maximum run-time duration.

For each selected snowfall event, the HYSPLIT model was run to generate a map of archive air parcel trajectories. Because it was known to be snowing when the HYSPLIT modeled air parcels arrived at the meteorological stations, the archived trajectories illustrate the potential pathways to the sources of moisture responsible for the snow-producing storms. The trajectory model does not by itself indicate where the moisture was acquired and air flow trajectories can therefore be misleading. For example, dry cold air from the north could travel southward into a warmer localized moisture source and initiate precipitate by lowering the dew point. The back-trajectories for this example would suggest the moisture came from the north, while in reality the source of moisture was local or from the south. Consequently, surface analysis maps were used to produce a second criterion, which was whether the moisture was local, and if not where it had come from.

Because low-pressure systems are associated with high winds, warm air, and atmospheric lifting, lows are normally indicative of clouds and precipitation. In some places, lows are referred to as cyclones and move counterclockwise in the Northern Hemisphere (Bjerknes and Solberg, 1922). Conversely, high-pressure systems or anticyclones move clockwise and are normally correlated with air subsidence, evaporation, and clear skies. Using the shape of the back-trajectory travel pathways (clockwise or counterclockwise) in conjunction with the originating direction (north or south) from which the HYSPLIT trajectories approached the meteorological stations, the moisture source for the snowfall events was categorized as either originating from the north (Fig. 4.2) or from the south (Fig. 4.3). Back-trajectories were not required to follow counterclockwise travel pathways to be considered moisture barring, but when they did it provided the certainty as to the moisture source, and then surface analysis charts were not needed for validation.

4.5.2 Surface Analysis Charts

In the case of uncertain HYSPLIT back-trajectory pathways (i.e., trajectories simultaneously originating from multiple directions and/or not following a counterclockwise pathway), surface analysis chart information was utilized by evaluating the placement of low and high pressure systems, and frontal movement leading up to snowfall events. NWS surface

analysis charts were acquired for uncertain trajectories using the NOAA National Operational Model Archive and Distribution System (NOMADS), an archive and access system for NWS operational products maintained at the National Climatic Data Center (NCDC). Together, HYSPLIT back-trajectory maps and surface analysis charts were used to determine whether the source of moisture for the snow-producing storms was local or whether moisture was transported over long distances via atmospheric circulation. The surface analyses charts were not used in conjunction with every HYSPIT map, just when back-trajectory pathways were not convincingly clear.

Trajectory pathways and low-pressure systems originating from Siberia, the Arctic Ocean (Beaufort and Chukchi Seas), northern Canada, and the North Slope of Alaska were considered from the north, while pathways from the Bering Sea, Gulf of Alaska, and Pacific Ocean were considered from the south. Figure 4.2 provides four examples of HYSPLIT maps with back-trajectories from the north. Not only do the locations have back-trajectories solely from the north, but have counterclockwise travel pathways as well. Based on the shape of the trajectory travel pathways and originating direction, these example snowfall events were interpreted as having moisture sources from the north. Figure 4.3 provides four examples of HYSPLIT maps that were interpreted as having south originating moisture sources. The interpretations were based on the maps having south originating back-trajectories and because they follow counterclockwise travel pathways. Frequently, south originating snowfall events with low pressure systems located in the Bering Sea and/or Pacific Ocean are also accompanied by high pressures systems residing over the Gulf of Alaska or the Aleutian Island (Fig. 4.3A & B). This high and low pressure system arrangement works together to funnel moisture northward. Figure 4.4 provides four examples of HYSPLIT maps with unclear moisture sources. Additional pressure system information obtained from surface analysis charts was used to develop a more complete weather picture. HYSPLIT maps with unclear moisture sources were almost always a byproduct of opposing pressure systems. The combination of HYSPLIT back-trajectories and pressure system information allowed the source of moisture for the snow-producing storms to be interpreted. HYSPLIT maps exampled in Figure 4.4A-C were interpreted as having south originating moisture sources as a result of low pressure systems being located in the Bering Sea and/or Pacific Ocean, while Figure 4.4A was interpreted as having a north originating moisture source because the low pressure system resided over the Arctic Ocean.

4.6 Results

We identified 650 snowfall events using a combined network of eight meteorological stations across northern Alaska. Based on the timing of those events, 650 backward air parcel trajectory maps were developed using HYSPLIT, and over 1000 surface analysis charts were acquired from NOMADS. Using the HYSPLIT maps and the surface analysis charts, each snowfall event was categorized as either originating from the north (N) or from the south (S), and therefore the source of moisture responsible for the snow-producing storms.

4.6.1 Criteria Sensitivity Analysis for Defining Snowfall Events

To define what accumulation of SWE best constitutes a snowfall event, the effects of changing criteria sizes (Table 4.2) were evaluated. The results from four meteorological stations, two each from the Arctic and Subarctic, were selected as examples (Figs. 4.5 & 6). Among the Arctic stations, the Kuparuk provided a good example of the Arctic coast (Fig. 4.5A & B), while Awuna2 offered a sample of the Arctic interior (Fig. 4.5C & D). Criterion 1, which requires the largest accumulation of SWE, had the lowest number of snowfall events that met the criterion. As the accumulation of SWE requirements are reduced from Criteria 1 to 4, the number of snowfall events increases, but the timing and the pathway orientation remain relatively constant. This indicates consistent sources of moisture throughout the range of accumulated SWE evaluated and a stable travel pathway.

To evaluate the influence of selecting different amounts of SWE accumulation for the three Subarctic stations, the criteria were restricted to the three largest SWE accumulations (Criteria 1 to 3) because too many small snowfall events surpassed the lower threshold of 4 mm/day (Criterion 4). Even with the restricted criteria, the Subarctic stations still experienced almost twice as many snowfall events compared with stations located in the Arctic. Figure 4.6 (A–D) shows the snowfall criteria results for Kotzebue (Subarctic coast) and Fort Yukon (Subarctic interior). All four examples from Figure 4.5 and 4.6, the Arctic coast (Kuparuk) and interior (Awuna2), and Subarctic coast (Kotzebue) and interior (Fort Yukon), illustrate that a reduction in the amount of required SWE accumulation results in an increase in sample size but had little to no effect on the timing or orientation of the moisture source pathway. Consequently, lowering the amount of required SWE accumulation clarified the timing and orientation of

snowfall events and demonstrated that the amount of SWE accumulation used to define a snowfall event is of less concern than we originally imagined.

4.6.2 Pathway and Timing of Snowfall Events

For each of the defined snowfall events, HYSPLIT maps were developed and used in combination with surface pressure information to categorize the originating pathway of the snow-producing storms. Table 4.3 provides the number of snowfall events that took place from 2000 to 2014 at each of the eight meteorological stations and the travel pathways of the storms: from the north (N) or from the south (S). The snowfall events for the five Arctic stations were defined using Criterion 4, while snowfall events occurring at the three Subarctic stations were defined using Criterion 3. The layout of Table 4.3 has the meteorological stations positioned in the same geographic orientation as they are physically located (Fig. 4.1), with Tunalik residing in the northwest corner of the study domain and Fort Yukon in the southeast corner. The average snowfall event sizes are also listed in Table 4.3. The number of snowfall events at each station varied greatly, so in order to compare the data between stations, the data were normalized by rescaling the range of snowfall events (0 to 1). For each station, including both the north and south storm pathways, the normalized rescaling was accomplished by dividing each month's count of snowfall events by the largest monthly occurrence of events observed at that station. By standardizing the occurrence of snowfall events between 0 and 1, the different stations can be evaluated and compared with each other, and as a result, the pathway orientations can be evaluated and compared as well (Fig. 4.7).

As a whole, there are key consistencies between when and from where the north- and south-originating snow-producing storms occur. Most north-originating snowfall events occur in fall and early winter (Aug – Dec) and again in late spring (Apr – Jun) with a "dead" period in mid-winter. Snowfall events originating from the south arise throughout the winter and generally peak between December and February, when the northern storms are least prevalent. There are some important differences, however, between the stations on either side of the Brooks Range. To evaluate snowfall events as single entities on either side of the Brooks Range divide, the normalized snowfall events from the five Arctic stations were averaged to represent all Arctic events, and the three Subarctic stations were averaged to represent all Subarctic events (Fig. 4.8). Because Figure 4.8 represents an average of normalized values, the scale is no longer fixed

between 0 and 1, but ranges from less than 1 to 0. In the Arctic, north events are slightly more predominant (Fig. 4.8A), while in the Subarctic, the occurrence of northern events is significantly overshadowed by the number of southern snow storms (Fig. 4.8B). Snowfall events in the Arctic also begin earlier in the fall and extend later into spring.

4.6.3 Historical Comparison

For the 15 years of record (2000 to 2014), the snowfall events pattern is consistent in both originating pathways and timing. The record indicates that snow-producing storms approaching from the north generally occur in fall and spring, while storms approaching from the south occur in mid-winter (Fig. 4.8). It is almost impossible to know if these patterns are stable for an extended timeframe due to the lack of long-term data sets. The Barrow meteorological station is the sole location with sufficient long-term data to evaluate how the snowfall event patterns differ from the more recent 15 years (2000 to 2014) compared to past patterns. The preceding 15 years (1960 to 1974) of data were processed for historical comparison (Fig. 4.9). The two 15-year records reveal slightly different patterns. The 1960 to 1974 data record has fewer north originating storms, with an average of roughly 1.5 north storms per year and a record total of 44 % of the snowfall events, compared to an average of 2 north storms per year during the more recent 15 years and a record total of 51% of the snowfall events. The historical comparison also illustrates there has been a slight increase in storms with SWE accumulation greater than criterion 4 (4 mm/day), with 47 snowfall events occurring during 1960 to 1974, and 53 snowfall events occurring during 2000 to 2015. The more recent snowfall events are also larger, with an average of 8.9 mm of SWE per snowfall event verse 7.6 mm of SWE per snowfall event during 1960 to 1974. Overall, the more recent 15 year record has more snowfall events, which on average deposit a great amount of SWE and have a higher chance of originating from the north The transition to more north snowfall events is thought to be related to the longer duration of open water and an increase in ice-free area in recent years (Bhatt et al., 2014; Serreze et al. 2007; Stroeve et al., 2011; Stroeve et al., 2012).

4.7 Discussion and Conclusion

During the long and cold Alaska Arctic winters, most moisture is locked in a solid state, leaving little available in the atmosphere for precipitation. During the fall season when much of the Beaufort and Chukchi Seas remains open and/or the sea ice is relatively thin, the ocean is a

substantial heat and moisture source to the atmosphere (Zhang et al., 1996). The current investigation found that snowfall events originating from the north are three times more likely to occur during this time of year (fall) when sea ice is thin, broken by the movement of wind, or nonexistent (Figs. 4.7 & 4.8). From Table 4.3, the total number of fall (Aug – Nov), mid-winter (Dec – Mar), and spring (Apr – Jun) north originating snowfall events deposited at the five Alaska Arctic stations were 76, 21, and 25, respectively. National Weather Service records indicate that maximum monthly snowfall in the Alaska Arctic occurs during the fall season and that more than 50% of the annual snowfall occurs from September through November (Zhang, 1993). As winter continues to set in, sea ice thickness increases and ice concentration becomes higher, the heat flux from the ocean to the atmosphere is reduced significantly (Zhang et al., 1996). The maximum concentration of sea ice off the Arctic coast occurs during mid-February to late March (Dunbar, 1967; Overland and Pease, 1982; Zhang et al., 1996), which coincides with our finding of the fewest north-originating snowfall events (Figs. 4.7 & 4.8). At approximately the time of Spring Equinox, the radiation balance at the surface of the ice changes so that the ice begins to melt (Overland and Pease, 1982). The concentration of sea ice sharply decreases starting in April (Zhang et al., 1996). Leads and open water have been shown to occupy a considerable fraction of the ocean surface during spring, and heat and moisture transfer through these open leads to the atmosphere is much greater than through an ice-covered area (Maykut and Church, 1973). The second episode of springtime north-originating snowfall events (Figs. 4.7 & 4.8), in our opinion, is a result of this increase in leads and open water, which supports increases in evaporation and locally derived precipitation. Regardless of whether they occurred in fall or spring, local snowfall events were consistently represented by counterclockwise HYSPLIT trajectories descending from the north and accompanied by low-pressure systems over the Chukchi and/or Beaufort Seas (Fig. 4.2).

Between the fall and spring episodes of north-originating snowfall events, winter precipitation north of the Brooks Range transitions from primarily having localized northern moisture sources to being advected from the south through atmospheric circulation (Figs. 4.7 & 4.8). In response to high radiative losses from the winter snow cover (Keegan, 1958), anticyclones are common and often a persistent feature of the Arctic atmospheric circulation. Although anticyclones are frequent and strong over Alaska, the penetration of cyclone activity through the Bering Sea can bring warm, moist oceanic air masses to the Arctic (Serreze et al.,

1993). A typical North Pacific cyclone forms as a wave on the polar front and strengthens, matures, and decays over a period of several days, all while traveling several thousand kilometers (Graham and Diaz, 2001). Individual tracks vary considerably, but most intense lows in the North Pacific form west of the dateline between 30° and 40°N, tracking first to the east and then curving toward the north as they mature and decay (Anderson and Gyakum, 1989). This description of an idealized North Pacific cyclone pathway closely matches the HYSPLIT modeled air parcel trajectories produced for south-originating snowfall events (Fig. 4.3). For south-originating snowfall events, surface analysis charts also consistently illustrate low-pressure systems in the Bering Sea, which supports the availability of moisture and air parcel trajectory pathways. South-originating snowfall events occur throughout the winter at all eight of the meteorological stations (Fig. 4.7). From Table 4.3, the total number of fall (Aug – Nov), mid-winter (Dec – Mar), and spring (Apr – Jun) south originating snowfall events deposited at the five Alaska Arctic stations were 54, 88 and 29, respectively.

The Subarctic, not having a large localized moisture source like the Arctic Ocean, relies on atmospheric circulation patterns to receive most of its moisture. Winter precipitation deposited across the Subarctic is predominantly from south-originating snowfall events, while few snow-producing storms come from the north (Figs. 4.7 & 4.8). From Table 4.3, the Subarctic received a total of 28 north originating snowfall events, while receiving 329 from the south. The overall snowfall season is also slightly shorter on the south side of the divide because there are fewer days of sub-freezing air temperatures. It appears that the Brooks Range divide, which topographically bisects (east to west) the Alaska Arctic, limits precipitation tracks from traveling across the range. In the Subarctic, south-originating storms account for 92% of all snowfall events, while in the Arctic, they account for only 58% of the snowfall events. There are more than twice as many snowfall events per station on the south side of the divide (Table 4.3). This finding might result from there being a decrease in storms with latitude (Overland and Pease, 1982). Regardless, south-originating storms are the dominant contributor of snowfall events across the Subarctic and occur throughout the winter. The timing of snowfall events, however, remains the same on both sides of the Brooks Range divide, despite the differences in occurrence numbers. Thus, north-originating snowfall events, whether deposited in the Arctic or Subarctic, occur mostly during fall and spring, while south-originating snowfall events are more evenly distributed throughout winter on both sides of the continental divide (Fig. 4.7).

In the Alaska Arctic, slow rates of snowfall frequently result in "trace" events, which are precipitation events with less than 0.2 mm of water and cannot be easily measured (Benson, 1982). Benson (1982) observed 282 days with recorded precipitation at Barrow during the calendar year 1978, but 192 of those days (68%) were trace occurrences. Annually, the traces could amount to roughly 20% of the annual precipitation. The present study, however, had a minimum requirement of 2.5 mm/day of accumulated SWE per snowfall event (Criterion 4, Table 4.2) for the Arctic stations and a minimum requirement of 3.0 mm/day for the Subarctic stations (Criterion 3, Table 4.2). By restricting the amount of accumulated SWE so that it is easily measurable, we hoped to prevent erroneous snowfall events from being accidently modeled and assigned false air parcel trajectories. Requiring the accumulation of SWE to be larger than set thresholds means snowfall events that contributed to the snowpack were not accounted for, although the amount of SWE accumulated from those storms was small.

Based on the snowfall events with accumulated SWE greater than 2.5 mm/day for the Arctic stations and 3.0 mm/day for the Subarctic stations (Criterion 4 and 3 respectively, Table 4.2), the average event size (average SWE accumulation per storm) is consistent (Table 4.3). For the five Arctic meteorological stations, the record average snow accumulation per snowfall event was 8 mm of SWE, with a plus or minus 1 mm standard deviation. The snowfall depositions were similar among the different stations, and the accumulation amounts from south- and north-originating storms were nearly even, with roughly 1 mm of SWE difference between them for all five Arctic stations. The three Subarctic stations received an additional roughly 3 mm of SWE per snowfall event compared with the Arctic stations, with a record average of 11 mm. The additional water content per storm event in the Subarctic is thought to result from the slightly warmer air temperatures, which can hold more moisture. There is also a greater discrepancy between the three stations, with plus or minus 3 mm of SWE.

Of the 650 snowfall events evaluated during this study, the largest SWE accumulations were routinely deposited by south-originating storms and mostly south of the Brooks Range. In the Subarctic, 22 storms deposited more than 30 mm of SWE (from 30 to 57 mm of SWE), and of those storms, all but one originated from the south. These substantial advected storms are usually accompanied by low-pressures systems in the Bering Sea and high-pressure systems over the Gulf of Alaska (Fig. 4.10). In combination, the low- and high-pressure systems work together to funnel moisture northward. This unique pressure system arrangement also positions the storm

tracks west of the Alaska Range (located in southern Alaska), which avoids a significant topographic barrier. The largest snowfall of record (mm of SWE), which occurred at Bettles on February 2, 2011, took place during such a pressure system arrangement, but an additional high-pressure system was over the Arctic also (Fig. 4.10A). During this scenario, colder Arctic air masses ascended southward across the Brooks Range and cooled the relatively warm and moisture-filled Subarctic air. Bjerknes and Solberg (1922) describe our Subarctic maximum snowfall scenario as warm air being attacked by cold air masses, thereby lifting the warm air and causing precipitation to form (cold front precipitation).

North of the Brooks Range, moisture responsible for Arctic snowfall events can be (1) transported into the colder region via south-originating storms or (2) derived locally during times when sea ice is thin and broken by the movement of wind, or nonexistent. The largest snowfall events are from a combination of both scenarios. Of the 20 biggest Arctic snowfall events (from 15 to 33 mm of SWE), 9 of them occurred when moisture was transported in from the south, while 11 were derived from local northern moisture. Advected snowfall events from the south deposited in the Arctic generally occurred under very similar pressure system scenarios as those described for the large Subarctic snowfalls, which had high-pressure systems over the Gulf of Alaska that pushed the storm track farther west to skirt around the Alaska and Brooks Ranges (Fig. 4.3A & B). Upon reaching the colder north, the moisture-laden air from the south cooled past its dew point and precipitated relatively sizeable quantities of snow. The largest north derived Arctic snowfall events all occurred during fall and/or spring when moisture was available and when low-pressure systems resided over the Chukchi or Beaufort Seas.

Curiosity about the origin of moisture for snow-producing storms in the middle of winter across the frozen and moisture-limited Alaska Arctic sparked this investigation. It is now known that more than 50% of snowfall events that occur in the Alaska Arctic are the result of moisture transported in from the south through atmospheric circulation and that, in general, recycling of northern moisture is restricted to when the Arctic Ocean is a readily available source of moisture for evaporation. The Brooks Range divide is a topographic barrier that hinders southern cyclone activity from reaching the Arctic, but periodically, snow-producing storms from the west bypass this obstacle. The effect of the Brooks Range divide results in more than twice as many snowfall events occurring in the Subarctic as in the Arctic.

4.8 Acknowledgments

This paper is an outcome of numerous funded research projects in Arctic Alaska. Agencies that had some input into the precipitation data collection effort included the Alaska Department of Transportation and Public Facilities (ADOT&PF), National Science Foundational (NSF), and U.S. Fish and Wildlife Service (USFWS). We thank all of the people who assisted in collecting precipitation data used in this study for the eight sites analyzed: USGS, NRCS USDA SNOTEL, and NCDC NOAA. Additionally, we gratefully acknowledge the NOAA Air Resources Laboratory (ARL) for providing the HYSPLIT transport and dispersion model and/or READY website (http://www.ready.noaa.gov) used in this publication.

4.9 References

Anderson, J. R., and J. R. Gyakum, 1989: A diagnostic study of Pacific Basin circulation regimes as determined from extratropical cyclone tracks. *Monthly Weather Review*, **117,** 2672-2686.

Andin, C., C. Zdanowicz, and L. Copland, 2014: Synoptic variability of extreme snowfall in the St. Elias Mountains, Yukon, Canada.

Arnborg, L., H. J. Walker, and J. Peippo, 1967: Suspended load in the Colville River, Alaska, 1962. *Geografiska Annaler. Series A, Physical Geography*, **49,** 131-144.

Bednorz, E., 2013: Synoptic conditions of heavy snowfalls in Europe. *Geografiska Annaler: Series A, Physical Geography*, **95,** 67-78.

Benson, C. S., 1982: Reassessment of winter precipitation on Alaskas arctic slope and measurements on the flux of wind-blown snow. Research Report UAG R-288. Geophysical Institute.

Bhatt, U. S., and Coauthors, 2014: Implications of arctic sea ice decline for the earth system. *Annual Review of Environment and Resources*, **39,** 57-89.

Bjerknes, J., and H. Solberg, 1922: Life cycle of cyclones and the polar front theory of atmospheric circulation. Grondahl.

Black, R. F., 1954: Precipitation at Barrow, Alaska, greater than recorded. *Eos, Transactions American Geophysical Union*, **35,** 203-207.

Draxler, R., B. Stunder, G. Rolph, A. Stein, and A. Taylor, 2012: HYSPLIT 4 User Guide Overview, (http://ready.arl.noaa.gov/HYSPLIT.php).

Draxler, R. R., and G. Hess, 1997: Description of the HYSPLIT4 modeling system, *NOAA Technical Memorandum ERL ARL-224*, December, 24 pp., [Available from National Technical Information Service, 5285 Port Royal Road, Springfield, VA 22161.].

——, 1998: An overview of the HYSPLIT 4 modelling system for trajectories. *Australian Meteorological Magazine*, **47,** 295-308.

Draxler, R. R., and G. D. Rolph, 2015: HYSPLIT (HYbrid Single-Particle Lagrangian Integrated Trajectory) Model access via NOAA ARL READY Website (http://www.arl.noaa.gov/HYSPLIT.php). NOAA Air Resources Laboratory, College Park, MD.

Dunbar, M., 1967: The monthly and extreme limits of ice in the Bering Sea. Physics of Snow and Ice, Vol. 1, Inst. Low Temp. Sci., University of Hokkaido, Hokkaido, Japan**,** 687-703.

Graham, N. E., and H. F. Diaz, 2001: Evidence for intensification of North Pacific winter cyclones since 1948. *B Am Meteorol Soc*, **82,** 1869-1893.

Haugen, R. K., and J. Brown, 1980: Coastal-inland distributions of summer air temperature and precipitation in Northern Alaska. *Arctic and Alpine Research*, **12,** 403-412.

Homan, J. W., and D. L. Kane, 2015: Arctic snow distribution patterns at the watershed scale. *Hydrology Research*, **46,** 507-520.

Homan, J. W., D. L. Kane, and S. L. Stuefer, 2015: Warm season precipitation patterns from low to high elevation in the Alaska Central Arctic. *Arctic, Antarctic, and Alpine Research*, submitted, 2015.

Judson, A., and N. Doesken, 2000: Density of freshly fallen snow in the central Rocky Mountains. *B Am Meteorol Soc*, **81,** 1577-1587.

Kane, D. L., and L. D. Hinzman, 1988: Permafrost hydrology of a small arctic watershed. In: Proceedings: Fifth International Conference on Permafrost (K. Senneset, ed.). Trondheim, Norway, pp. 590-595.

Kane, D. L., L. D. Hinzman, and J. P. Zarling, 1991: Thermal Response of the Active Layer to Climatic Warming in a Permafrost Environment. *Cold Regions Science and Technology*, **19,** 111-122.

Kane, D. L., R. E. Gieck, and L. Hinzman, 2008a: Water balance for a low gradient watershed in Northern Alaska. Proceedings of the Ninth International Conference on Permafrost, edited by: Kane, DL and Hinkel, KM, University of Alaska Fairbanks, AK, 883-888.

Kane, D. L., L. D. Hinzman, J. P. McNamara, Z. Zhang, and C. S. Benson, 2000: An overview of a nested watershed study in Arctic Alaska. *Nordic Hydrology*, **31,** 245-266.

Kane, D. L., R. E. Gieck, D. C. Kitover, L. D. Hinzman, J. P. McNamara, and D. Q. Yang, 2004: Hydrological cycle on the North Slope of Alaska. In: Northern Research Basins Water Balance (D.L. Kane & D. Yan, eds.). IAHS Publ. 290. IAHS, Wallingford, UK, pp. 224-236.

Kane, D. L., L. D. Hinzman, R. E. Gieck, J. P. McNamara, E. K. Youcha, and J. A. Oatley, 2008b: Contrasting extreme runoff events in areas of continuous permafrost, Arctic Alaska. *Hydrology Research*, **39,** 287-298.

Kane, D. L., and Coauthors, 2012: Meteorological and hydrological data and analysis report for the Foothills/Umiat Corridor and Bullen projects: 2006-2011. University of Alaska Fairbanks, Water and Environmental Research Center, Report INE/WERC 12.01, Fairbanks, Alaska, 260 pp.

Keegan, T. J., 1958: Arctic synoptic activity in winter. *Journal of Meteorology*, **15,** 513-521.

Liston, G. E., and M. Sturm, 2002: Winter precipitation patterns in arctic Alaska determined from a blowing-snow model and snow-depth observations. *Journal of Hydrometeorology*, **3,** 646-659.

Maykut, G. A., and P. E. Church, 1973: Radiation climate of Barrow Alaska, 1962–66. *Journal of Applied Meteorology*, **12,** 620-628.

McCann, S. B., P. J. Howarth, and J. G. Cogley, 1972: Fluvial processes in a periglacial environment: Queen Elizabeth Islands, N. W. T., Canada. *Transactions of the Institute of British Geographers*, 69.

Mesquita, M. S., D. E. Atkinson, and K. I. Hodges, 2010: Characteristics and variability of storm tracks in the north pacific, Bering Sea, and Alaska. *Journal of Climate*, **23,** 294-311.

Osterkamp, T. E., 1984: Temperature measurements in permafrost. Rep. FHWA-AK-RD-85-11, State of Alaska, Department of Transportation and Public Facilities, Division of Planning and Programming, Research Section, 87.

Overland, J. E., and C. H. Pease, 1982: Cyclone climatology of the Bering Sea and its relation to sea ice extent. *Monthly Weather Review*, **110,** 5-13.

Przybylak, R., 2003: *The climate of the Arctic.* 270 pp.

Rolph, G. D., 2015: Real-time environmental applications and display system (READY) website (http://www.ready.noaa.gov). NOAA Air Resources Laboratory, College Park, MD.

Searby, H. W. H. M. U. S. N. W. S. R. H., 1971: *Climate of the North Slope, Alaska.* U.S. Dept. of Commerce, National Oceanic and Atmospheric Administration, National Weather Service, Alaska Region.

Serreze, M. C., and R. G. Barry, 2014: *The Arctic climate system.* Cambridge University Press.

Serreze, M. C., A. P. Barrett, and F. Lo, 2005: Northern high-latitude precipitation as depicted by atmospheric reanalyses and satellite retrievals. *Monthly Weather Review*, **133,** 3407-3430.

Serreze, M. C., M. M. Holland, and J. Stroeve, 2007: Perspectives on the Arctic's shrinking sea-ice cover. *Science*, **315,** 1533-1536.

Serreze, M. C., J. E. Box, R. G. Barry, and J. E. Walsh, 1993: Characteristics of Arctic synoptic activity, 1952-1989. *Meteorol Atmos Phys*, **51,** 147-164.

Shulski, M., and G. Wendler, 2007: *The climate of Alaska.* University of Alaska Press.

Sinclair, K., N. Bertler, and W. Trompetter, 2010: Synoptic controls on precipitation pathways and snow delivery to high-accumulation ice core sites in the Ross Sea region, Antarctica. *Journal of Geophysical Research: Atmospheres (1984–2012)*, **115**.

Stohl, A., 1998: Computation, accuracy and applications of trajectories—a review and bibliography. *Atmospheric Environment*, **32,** 947-966.

Stroeve, J. C., M. C. Serreze, A. Barrett, and D. N. Kindig, 2011: Attribution of recent changes in autumn cyclone associated precipitation in the Arctic. *Tellus A*, **63,** 653-663.

Stroeve, J. C., M. C. Serreze, M. M. Holland, J. E. Kay, J. Malanik, and A. P. Barrett, 2012: The Arctic's rapidly shrinking sea ice cover: a research synthesis. *Climatic Change*, **110,** 1005-1027.

Stuefer, S. L., J. W. Homan, E. K. Youcha, D. L. Kane, and R. E. Gieck, 2012: Snow Survey Data for the Central North Slope Watersheds: Spring 2012. *University of Alaska Fairbanks, Water and Environmental Research Center, Report INE/WERC 12.22, Fairbanks, Alaska*, 38 pp.

Sturm, M., and G. E. Liston, 2003: The snow cover on lakes of the Arctic Coastal Plain of Alaska, USA. *Journal of Glaciology*, **49,** 370-380.

Super, A. B., and E. W. Holroyd, 1997: *Snow accumulation algorithm for the WSR-88D radar: Second annual report.* River Systems and Meteorology Group, Water Resources Services, Technical Service Center, US Bureau of Reclamation.

U.S. Department of Commerce, 1996: National Weather Service observing handbook No. 7, surface observations. U.S. Government Printing Office.

Woo, M.-k., 2012: *Permafrost hydrology.* Springer Science & Business Media.

Zhang, T., 1993: Climate, seasonal snow cover and permafrost temperatures in Alaska north of the Brooks Range, Doctoral dissertation, University of Alaska Fairbanks.

Zhang, T., T. E. Osterkamp, and K. Stamnes, 1996: Some characteristics of the climate in Northern Alaska, U.S.A. *Arctic and Alpine Research*, **28,** 509-518.

——, 1997: Effects of climate on the active layer and permafrost on the North Slope of Alaska, U.S.A. *Permafrost and Periglacial Processes*, **8,** 45-67.

Zhang, T., T. Scambos, T. Haran, L. D. Hinzman, R. G. Barry, and D. L. Kane, 2003: Ground-based and satellite-derived measurements of surface albedo on the North slope of Alaska. *Journal of Hydrometeorology*, **4,** 77-91.

4.10 Figures

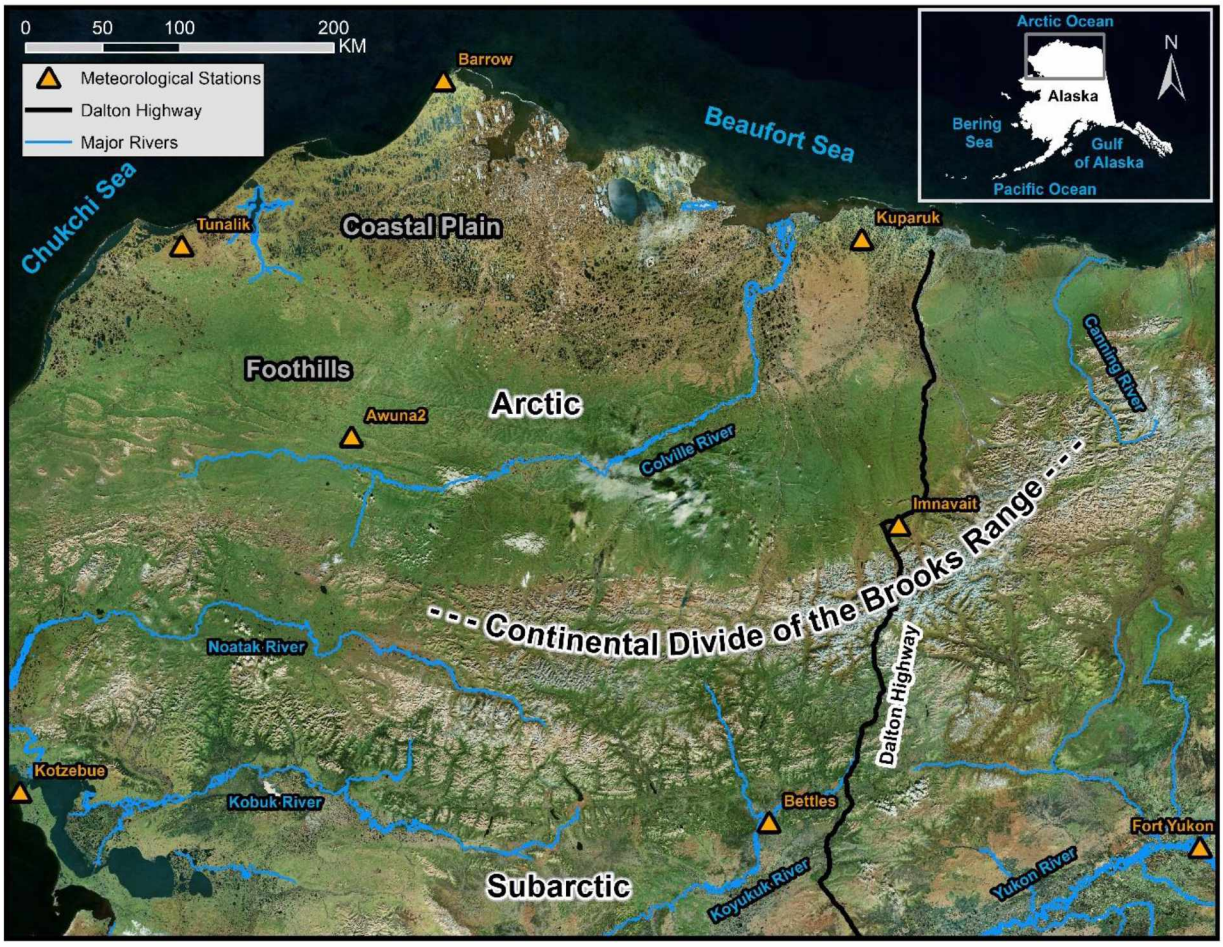

Figure 4.1: Site location map.

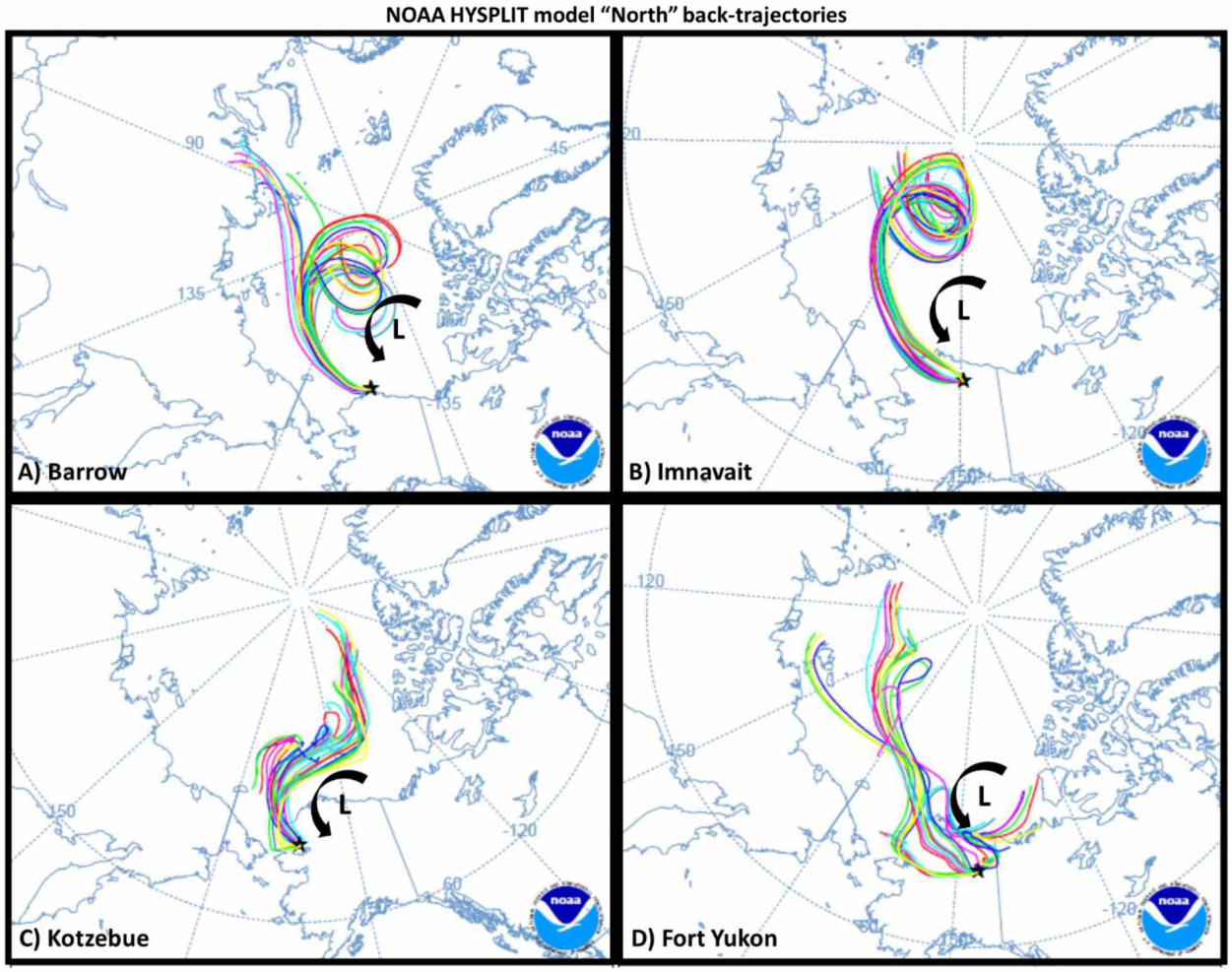

Figure 4.2: Typical NOAA HYSPLIT model back-trajectory maps for A) Barrow, B) Imnavait, C) Kotzebue, and D) Fort Yukon. All four examples are of "north" pathways. Each map has colored lines that represent 27 different back-trajectory ensembles, all starting at the same location, but calculated by offsetting the meteorological data by a fixed grid factor. The location of low-pressure (L) centers obtained from NOAA surface analysis weather maps is also provided.

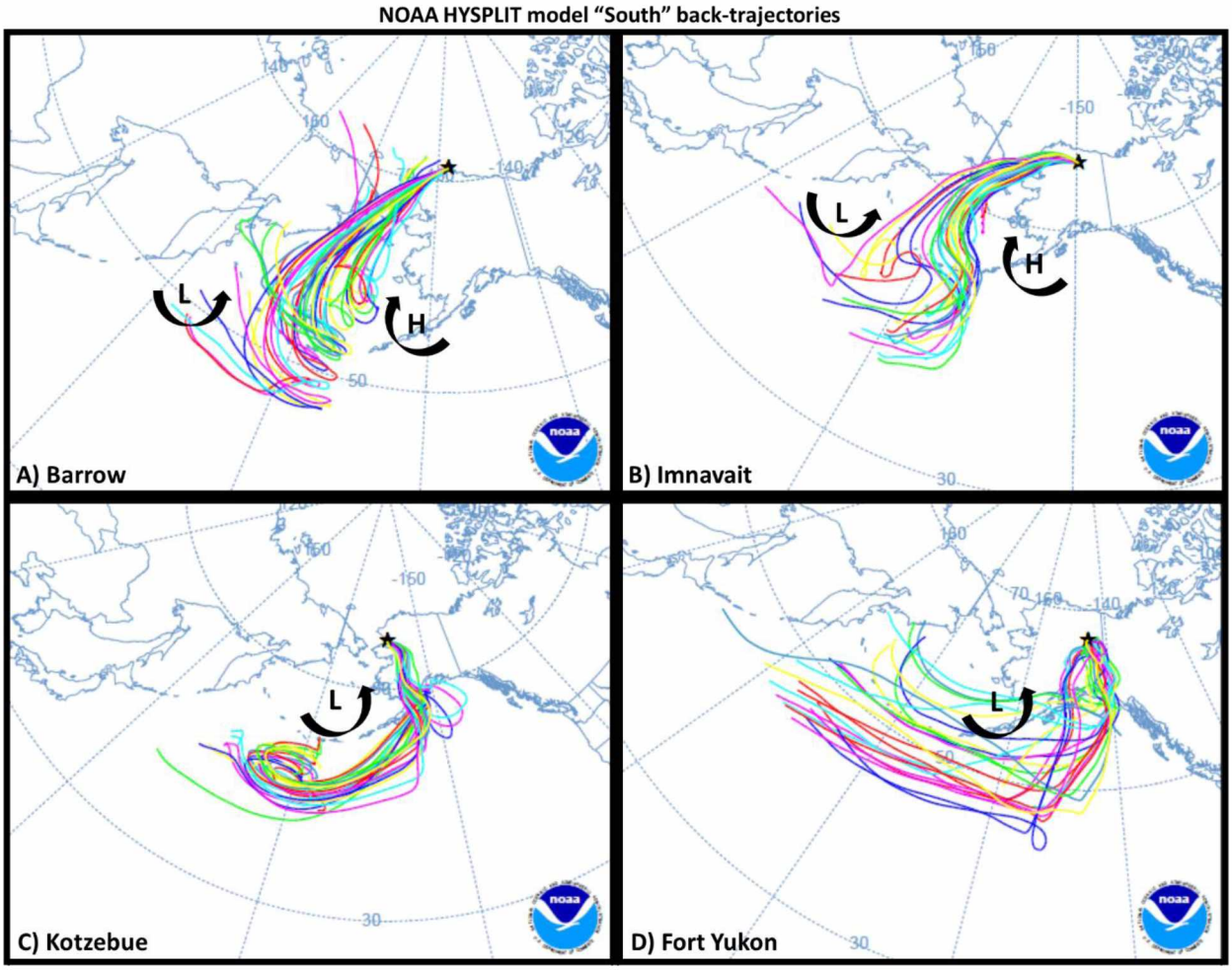

Figure 4.3: Typical NOAA HYSPLIT model back-trajectory maps for A) Barrow, B) Imnavait, C) Kotzebue, and D) Fort Yukon. All four examples are of "south" pathways. Each map has colored lines that represent 27 different back-trajectory ensembles, all starting at the same location, but calculated by offsetting the meteorological data by a fixed grid factor. The location of low (L) and high (H) pressure centers obtained from NOAA surface analysis weather maps is also provided.

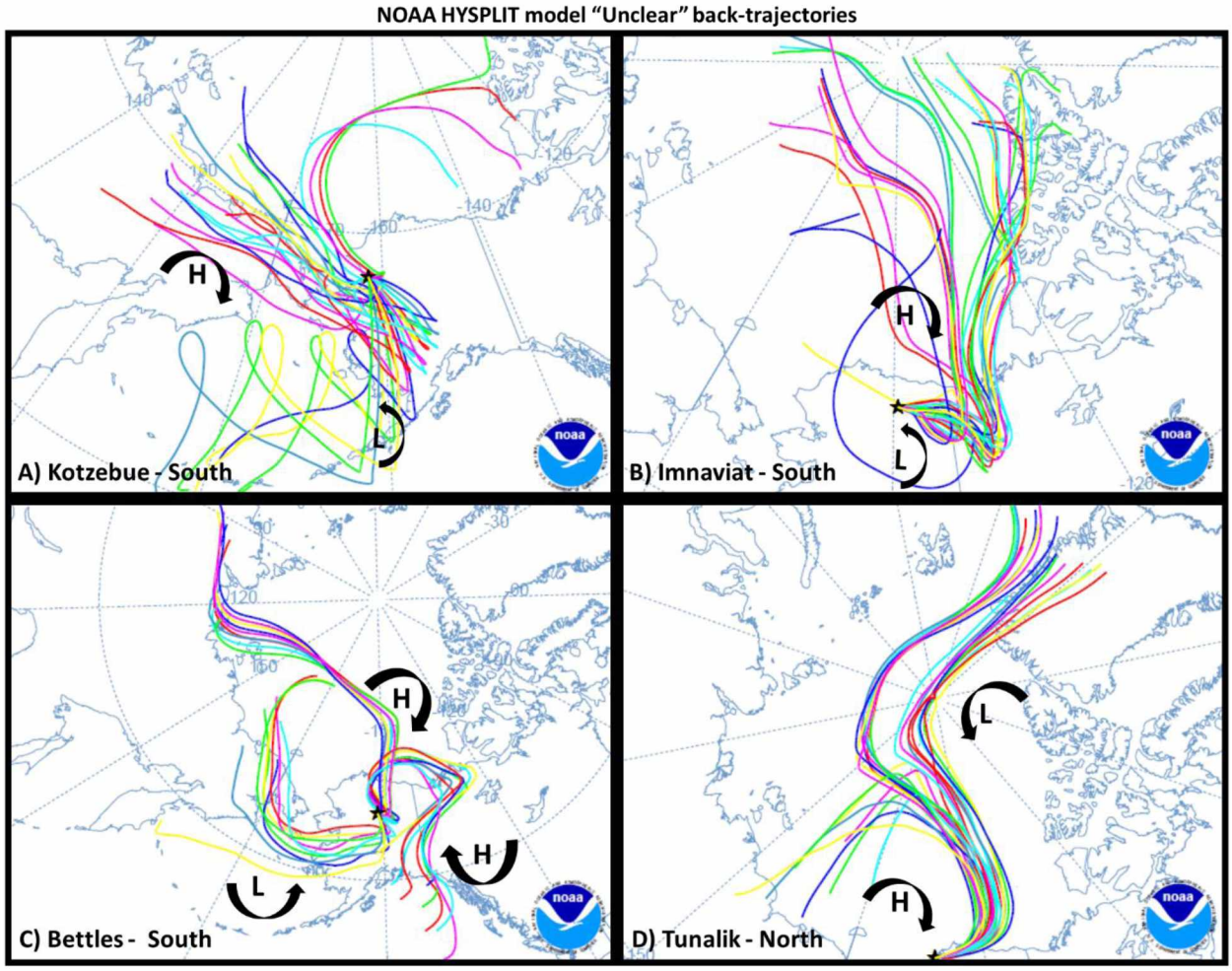

Figure 4.4: Unclear NOAA HYSPLIT model back-trajectory maps for A) Kotzebue, B) Imnavait, C) Bettles, and D) Tunalik. Each map has colored lines that represent 27 different back-trajectory ensembles, all starting at the same location, but calculated by offsetting the meteorological data by a fixed grid factor. The location of low (L) and high (H) pressure centers obtained from NOAA surface analysis weather maps is also provided. Using pressure system information along with the HYSPLIT back-trajectories, the moisture source was determined for unclear storm pathways.

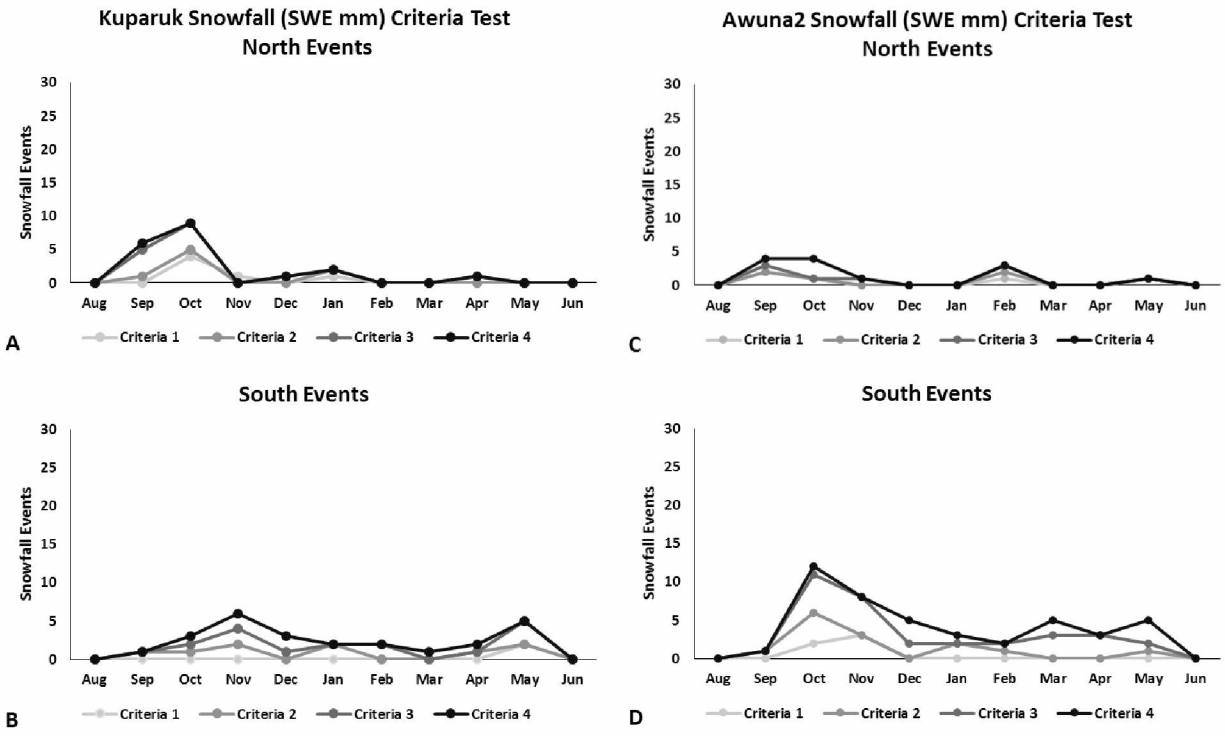

Figure 4.5: The number of snowfall events from 2000 to 2014 based on different SWE (mm) accumulation criteria requirements outlined in Table 4.2. Stations north of the Brooks Range divide in the Alaska Arctic: A) Kuparuk north events, B) Kuparuk south events, C) Awuan2 north events, and D) Awuan2 south events. For comparison purposes, the *y*-scales in Figs. 4.4 and 5 were made the same.

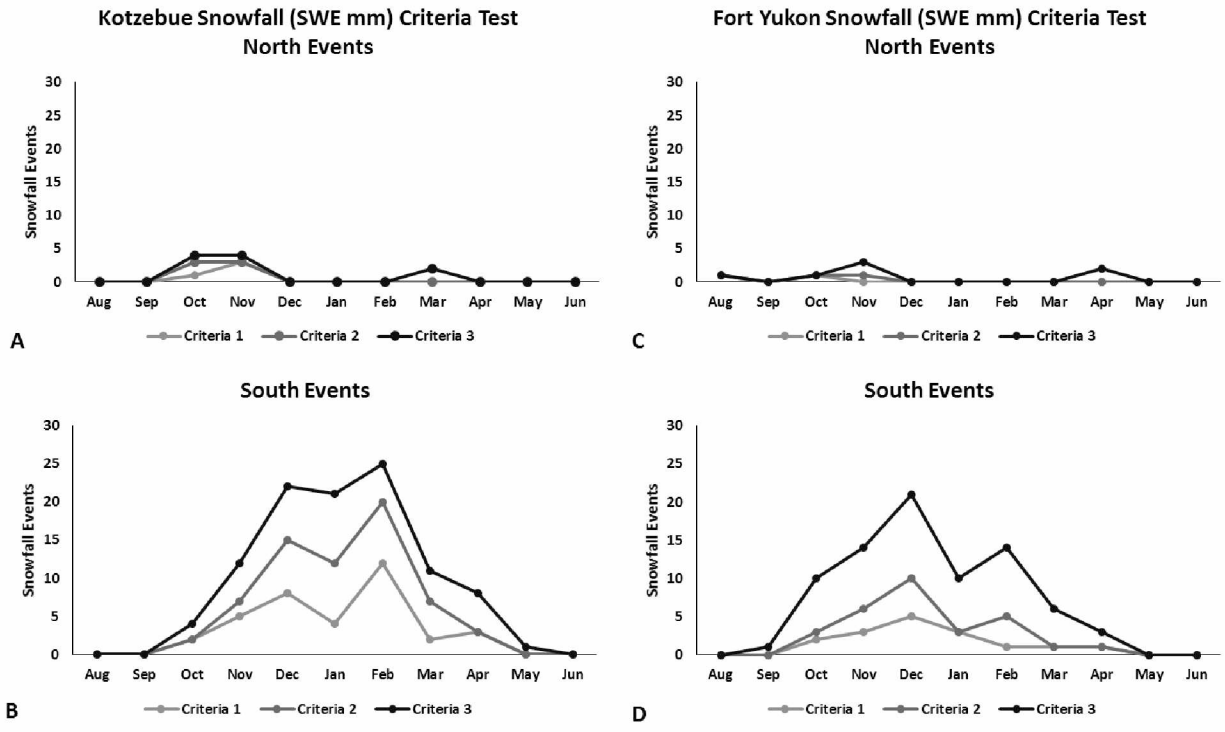

Figure 4.6: Snowfall events from 2000 to 2014 based on different SWE (mm) accumulation criteria requirements outlined in Table 4.2. Stations south of the Brooks Range divide in the Alaska Subarctic: A) Kotzebue north events, B) Kotzebue south events, C) Fort Yukon north events, and D) Fort Yukon south events. For comparison purposes, the *y*-scales in Figs. 4.4 and 4.5 were made the same.

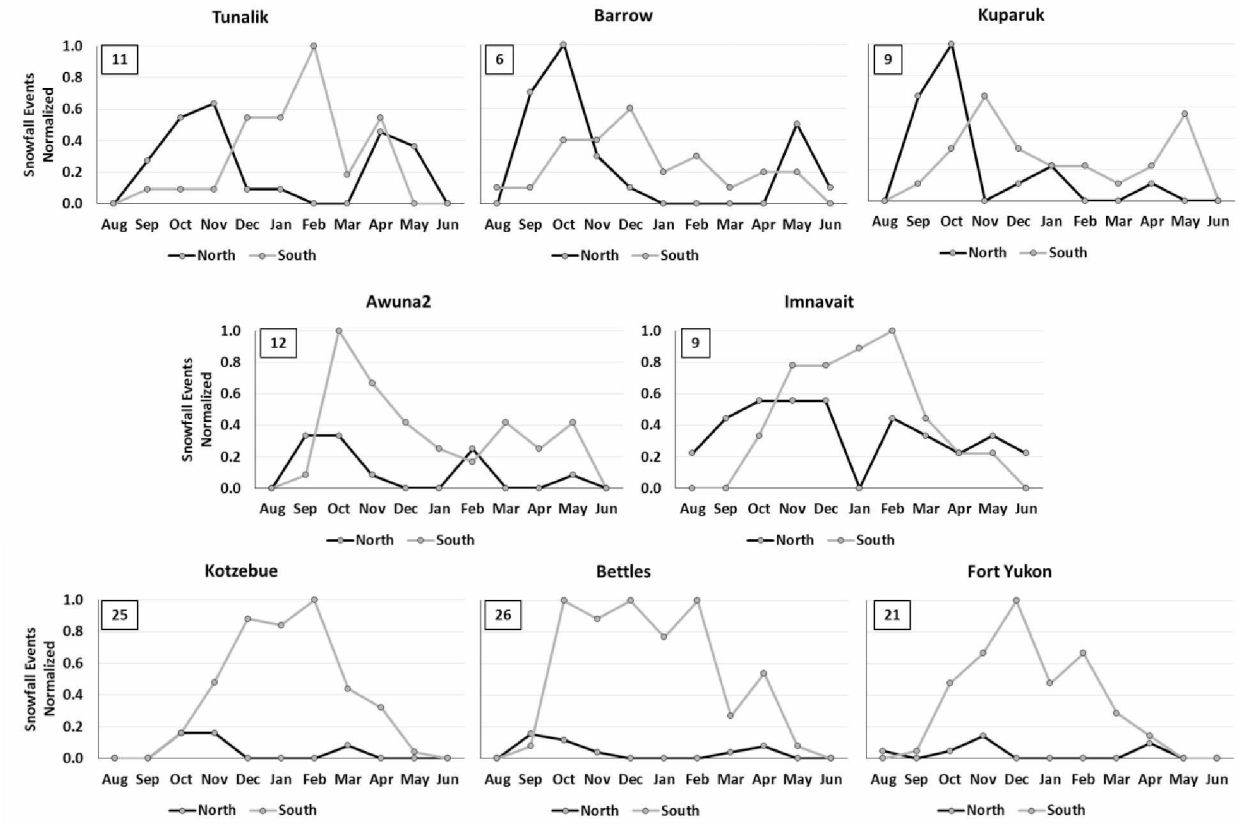

Figure 4.7: Normalized snowfall events from 2000 to 2014 for each of the eight high-latitude meteorological stations. Plots organized roughly in the same spatial distribution as physically in field. Data were normalized by dividing the observed number of events per month by the maximum number observed at the station. This value is shown for each station in the upper left corner of the graph.

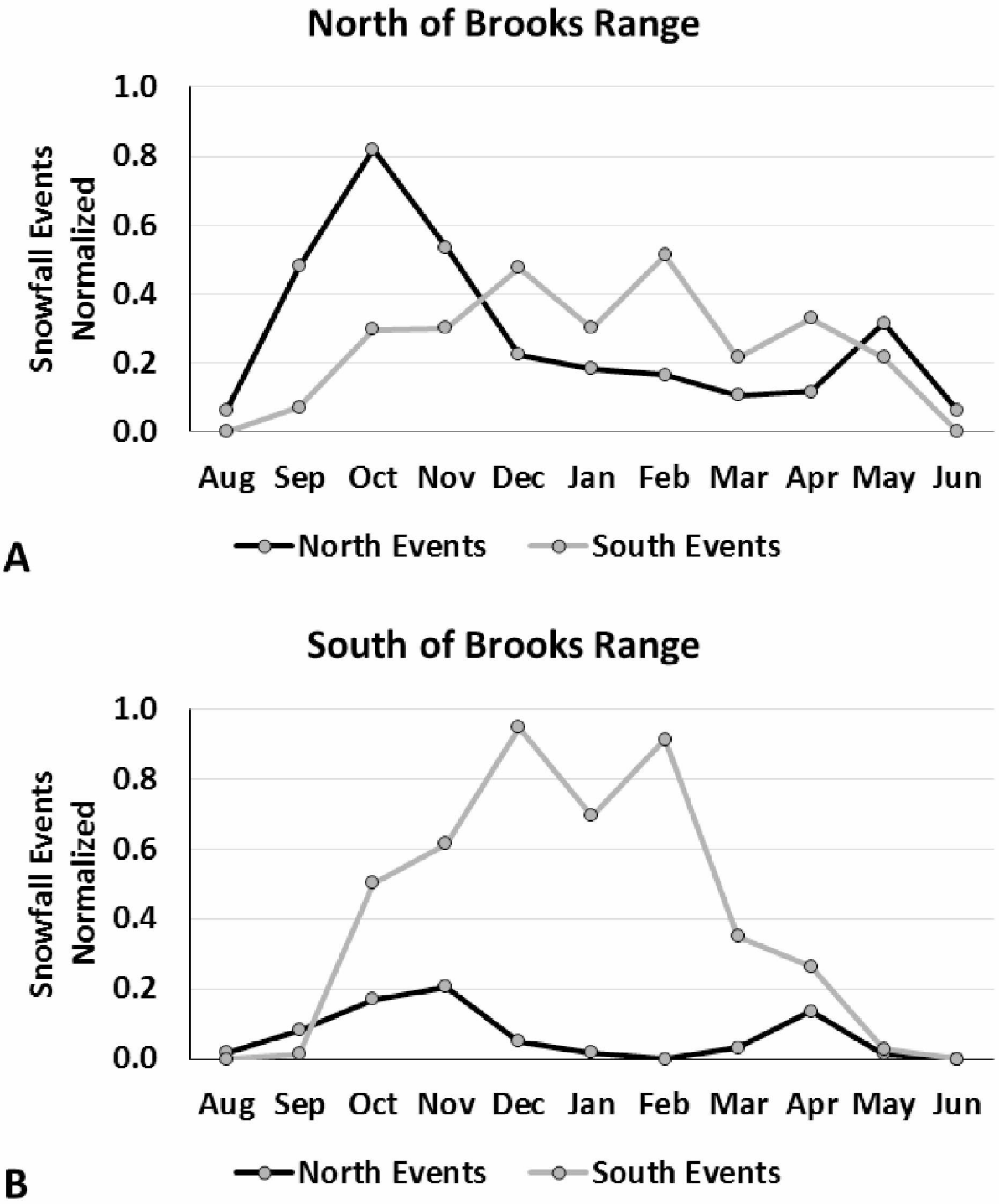

Figure 4.8: Averaged normalized snowfall events from 2000 to 2014 for A) the five meteorological stations located in the Arctic, and B) the three meteorological stations located in the Subarctic.

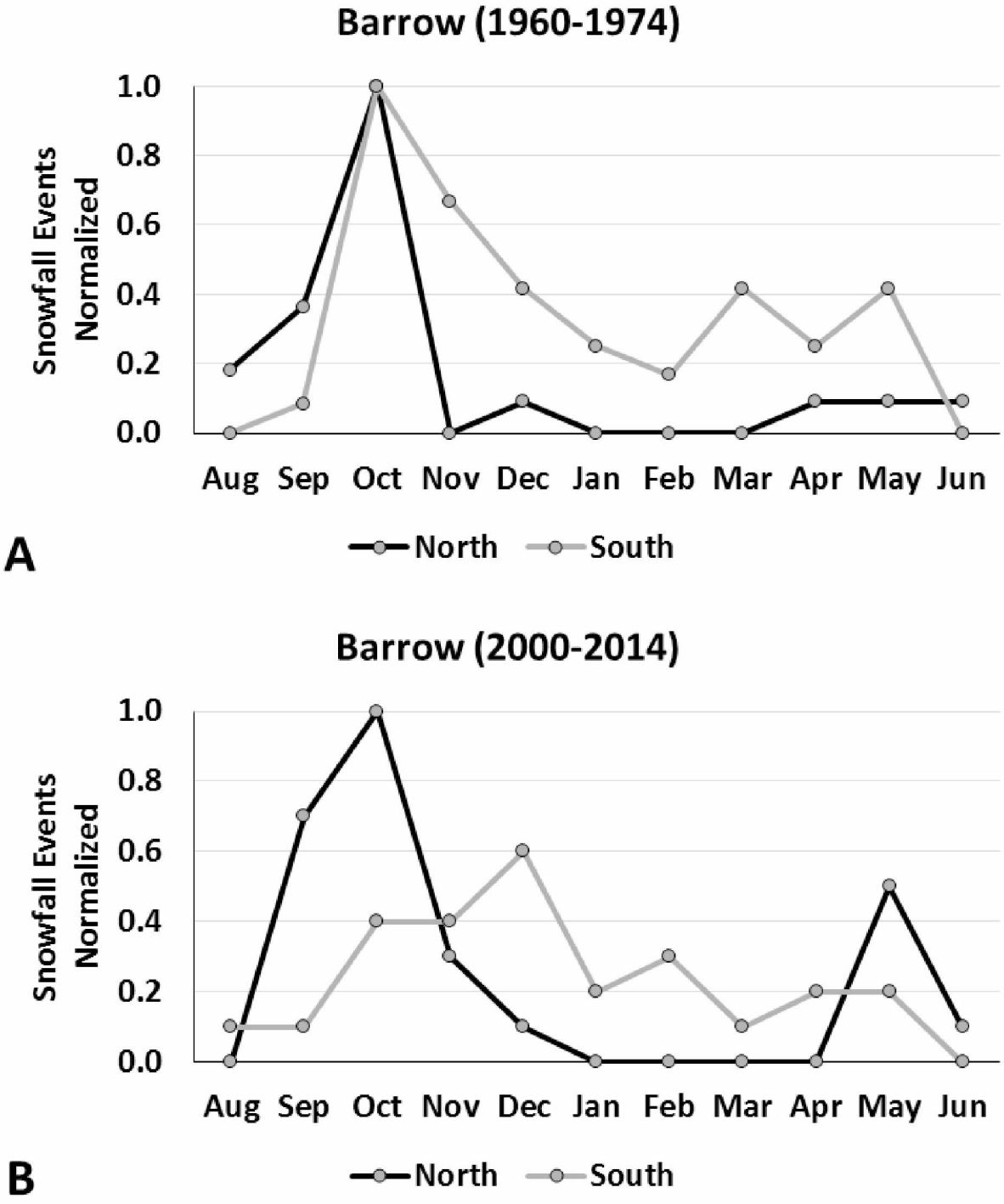

Figure 4.9: Historical comparison of snowfall events from two different 15-year data records recorded at the Barrow meteorological station.

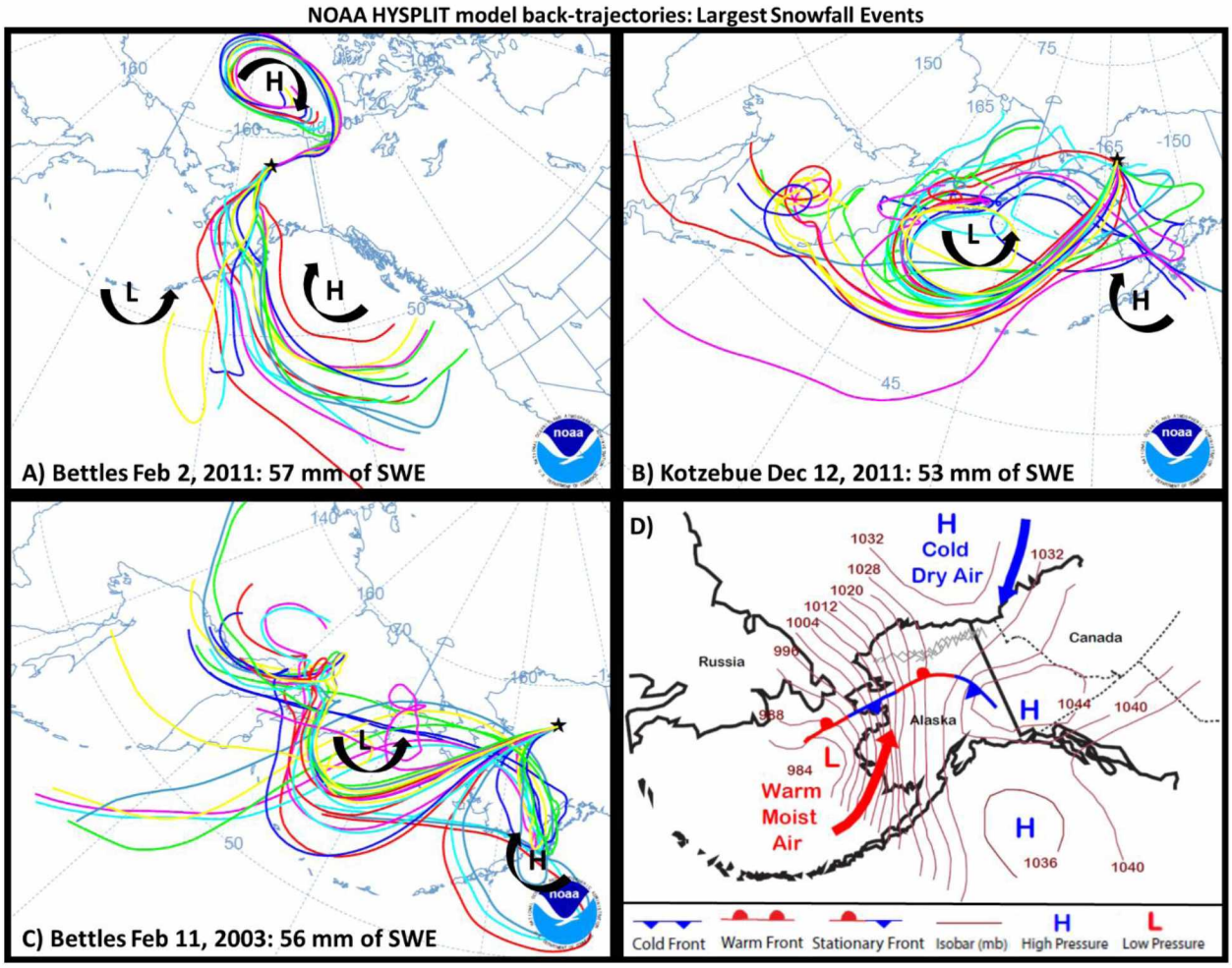

Figure 4.10: NOAA HYSPLIT model backwards trajectory maps for the three largest snowfall events recorded at the eight meteorological stations during the 15-year record (2000–2014). All three examples are of "south" pathways. Each map has colored lines that represent 27 different trajectory ensembles, all starting at the same location, but calculated by offsetting the meteorological data by a fixed grid factor. The location of low (L) and high (H) pressure centers obtained from NOAA surface analysis charts is also provided. The lower right map is an example of a NOAA surface analysis chart.

4.11 Tables

Table 4.1: Treatment 1 through 4 for data unit conversions. For all SD to SWE conversions, ρ_w = 1000 kg/m^3 and ρ_s was based on different temperature ranges if available (Judson & Doesken, 2000; U.S. Department of Commerce, 1996; Super & Holroyd, 1997).

Treatment	Data Downloaded	Air Temperature (T)	Requirements for use as SWE
1	Liquid Precipitation (SWE)	Available	$T < 0^{\circ}C$
2	Liquid Precipitation (SWE)	No Data	$T < 0^{\circ}C$ Air temperatures aquired from neighboring meteorological stations
	Use SWE = SD*(ρ_s / ρ_w) to convert SD to SWE		
3	Snow Depth (SD)	Available	$0^{\circ}C > T > -2^{\circ}C$; ρ_s = 120 kg/m3 $-2^{\circ}C > T > -10^{\circ}C$; ρ_s = 100 kg/m3 $-10^{\circ}C > T$; ρ_s = 80 kg/m3
4	Snow Depth (SD)	No Data	ρ_s = 100 kg/m3

Table 4.2: Snowfall event criteria (mm) requirements for sensitivity analysis. Single and multi-day snowfall accumulations criteria (e.g., Criterion 2; Single-day with at least 7.5 mm of SWE or multi-day (2 or more consecutive days) with at least 4 mm of SWE per day and a total of at least 8 mm).

	ΔSWE (mm)			
	Criterion 1	**Criterion 2**	**Criterion 3**	**Criterion 4**
Single-day event	10	7.5	5	4
Multi-day event	5	4	3	2.5

Table 4.3: Number of snowfall events from 2000 to 2014 at each of the eight meteorological stations, the pathway orientation of the snow-producing storm (direction traveled from), and the average size of the snowfall events. Blank spaces are the result of no snowfall events recorded during a given month during the study duration. Criterion 4 (Table 4.2) was used in the selection of Arctic snowfall events, while Criterion 3 was used for the Subarctic stations.

	Tunalik						Barrow						Kuparuk					
	# of Snowfall Events			Ave Event Size (mm)			# of Snowfall Events			Ave Event Size (mm)			# of Snowfall Events			Ave Event Size (mm)		
	N	S	All	N	S	Ave	N	S	All	N	S	Ave	N	S	All	N	S	Ave
Aug								1	1		9	9						
Sep	3	1	4	5	6	6	7	1	8	8	6	7	6	1	7	7	12	10
Oct	6	1	7	6	8	7	10	4	14	8	11	10	9	3	12	9	6	8
Nov	7	1	8	5	11	8	3	4	7	10	9	10		6	6		10	10
Dec	1	6	7	7	6	6	1	6	7	13	8	11	1	3	4	8	4	6
Jan	1	6	7	13	12	12		2	2		11	11	2	2	4	14	9	11
Feb		11	11		8	8		3	3		8	8		2	2		6	6
Mar		2	2		6	6		1	1		6	6		1	1		4	4
Apr	5	6	11	8	7	7		2	2		10	10	1	2	3	6	6	6
May	4		4	6		6	5	2	7	9	6	8		5	5		10	10
Jun	1		1				1		1	9		9						
Total	28	34	62	7	8	7	27	26	53	10	8	9	19	25	44	9	8	8

	Awuna2						Imnavait					
	# of Snowfall Events			Ave Event Size (mm)			# of Snowfall Events			Ave Event Size (mm)		
	N	S	All	N	S	Ave	N	S	All	N	S	Ave
Aug							2		2	9		9
Sep	4	1	5	11	9	10	4		4	9		9
Oct	4	12	16	9	10	9	5	3	8	9	5	7
Nov	1	8	9	7	11	9	5	7	12	5	5	5
Dec		5	5		6	6	5	7	12	6	7	6
Jan		3	3		7	7		8	8		5	5
Feb	3	2	5	8	8	8	4	9	13	9	7	8
Mar		5	5		6	6	3	4	7	5	12	9
Apr		3	3		7	7	2	2	4	15	5	10
May	1	5	6	17	6	12	3	2	5	5	9	7
Jun							2		2	8		8
Total	13	44	57	10	8	8	35	42	77	8	7	8

	Kotzebue						Bettles						FortYukon					
	# of Snowfall Events			Ave Event Size (mm)			# of Snowfall Events			Ave Event Size (mm)			# of Snowfall Events			Ave Event Size (mm)		
	N	S	All	N	S	Ave	N	S	All	N	S	Ave	N	S	All	N	S	Ave
Aug													1		1	10		10
Sep							4	2	6	11	8	10		1	1		5	5
Oct	4	4	8	9	14	12	3	26	29	8	11	10	1	10	11	15	6	11
Nov	4	12	16	15	12	14	1	23	24	6	18	12	3	14	17	6	7	7
Dec		22	22		14	14		26	26		12	12		21	21		8	8
Jan		21	21		14	14		20	20		15	15		10	10		7	7
Feb		25	25		15	15		26	26		16	16		14	14		7	7
Mar	2	11	13	19	10	14	1	7	8	6	14	10		6	6		6	6
Apr		8	8		12	12	2	14	16	17	9	13	2	3	5	5	14	10
May		1	1		6	6		2	2		21	21						
Jun																		
	0	0	0										0	0	0			
Total	10	104	114	14	12	13	11	146	157	10	14	13	7	79	86	9	8	8

Conclusion

This thesis presents the results of an extensive examination of precipitation inputs into the Alaska Central Arctic. The central hypothesis of this research is that the spatial distribution of solid and liquid precipitation is linearly related to elevation. This hypothesis is accurate for liquid precipitation, which demonstrates a strong linear relationship with topography, and as such, liquid precipitation increases with elevation from the Coastal Plain to the continental divide in the Brooks Range. Solid precipitation acquired from end-of-winter snow water equivalent (SWE) measurements were however inconsistent with this hypothesis, and concluded to be relatively independent of elevation in the Alaska Central Arctic, with roughly an average of 100 mm during the cold season from the Coastal Plain to the Mountains. The lack of linear relationship for solid precipitation greatly differs from the liquid precipitation warm season distribution pattern, which linearly increases from approximately 80 mm near the Arctic Ocean to over 300 mm at the continental divide of the Brooks Range. The solid precipitation dataset included over 1000 end-of-winter snow surveys conducted at roughly 200 locations from 2000 to 2013. The liquid precipitation dataset includes measurements from 31 meteorological stations, with collection durations that range from 2 to 31 years.

The unique datasets of solid and liquid precipitation were combined to evaluate my second hypothesis, which stated that the annual precipitation inputs into the Alaska Central Arctic are dominated by liquid precipitation when potential moisture sources are ice free. The combined datasets illustrated annual precipitation to vary temporally and spatially over the Alaska Central Arctic. At the higher elevations of the Foothills and Mountains, annual precipitation is approximately 70% liquid and 30% solid, with a maximum liquid precipitation contribution of roughly 90% at some individual locations. On the Coastal Plain, the precipitation contribution is almost the opposite. Here solid precipitation represents on average 60% of the annual precipitation budget, with a maximum contribution of 70% at one location. In general, therefore, at the lower foothills, the annual precipitation contribution consists of nearly equal amounts of liquid and solid precipitation, while at higher elevations in the mountains, the annual precipitation contribution is mostly from liquid precipitation. On the coastal plain, the primary annual precipitation contribution is from solid precipitation.

With the snowpack and subsequent runoff being such a significant part of the Alaska Arctic hydrologic cycle each year, it may seem surprising that annual snowfall totals are generally quite low. During the long and cold Arctic winter, there is both limited energy to drive evaporation/sublimation and reduced moisture storage capacity within the cold air masses. Excess of precipitation over evaporation and sublimation results from the inflow of moisture through atmospheric circulation. My final hypothesis was centered on where moisture responsible for snow-producing storms in the Arctic originated, suggesting it was primarily advected through atmospheric circulation. It was discovered that during fall when the Beaufort and Chukchi Seas are open or covered with relatively thin and fractured ice, the ocean is a substantial moisture source for snow-producing storms. We determined that snowfall events derived from the Arctic seas (north events) occur primarily during this time. During mid-winter, however, when the concentration of sea ice off Alaska's northern coast is at a maximum, snow-producing storms are advected from the Gulf of Alaska and the southern Bering Sea, which remain ice-free throughout winter, providing an open source of moisture. Starting after the Spring Equinox, a second smaller episode of northern storms were found to occur, which is thought to be the result of the Arctic Ocean developing more leads and open water as solar radiation quickly increases. Data from this study indicate that the Brooks Range divide affects moisture availability throughout the Alaska Arctic by acting as a moisture passage barrier. In the Alaska Arctic, where localized moisture sources can be ephemeral, both atmospheric circulation and sea ice cover are key components in the accumulation and amount of snow storage.

Implications and Future Work

Precipitation measurements, both solid and liquid, have acquisition challenges, sources of measurement error and ways for improvement. Challenges measuring the accumulation of newly fallen solid precipitation are described in chapter one and include the fact that snow is redistributed between the times of deposition and melt. Sublimation also occurs during this interim, thus reducing the snowpack. To get around these challenges, the accumulation of SWE during the cold season was not examined while sublimation and redistribution were ongoing. Instead, only the SWE that contributes to runoff was measured and evaluated at winter's end. Solid precipitation acquired from end-of-winter SWE measurements was shown to be relatively independent of elevation in the Alaska Central Arctic. Is the lack of a spatial relationship with elevation, however, the same for newly fallen snow? Or does newly fallen snow exhibit an orographic influence? To answer these questions, the spatial distribution of SWE accumulation would need to be measured when it occurs and not at winter's end. Solid precipitation gauges can collect and record wind-blown and redistributed snow as true precipitation, which unfortunately result in erroneous snowfall events or false increases in SWE, making quality SWE accumulation measurements difficult. On the contrary, solid precipitation gauges can undercatch or miss snowfall as a result of wind during an actual snowfall event, furthermore causing erroneous measurements. Results from a World Meteorological Organization (WMO) intercomparison on the NWS 8-inch standard gauge, which was primarily used for the liquid precipitation measurements presented here, indicate that gauge-measured annual precipitation values need to be increased about 10-140% to account for undercatch (Yang et al., 1998). The intercomparison also indicated that the adjustment of undercatch is greater in winter and smaller in summer owing to the increased effect of wind on gauge undercatch of less dense snow. The average catch ratios for snow and rain were reported to be 70 and 90%, respectively (Yang et al., 1998). The catch ratio of snow as a function of wind speed was shown to be 100% when no wind was present, but reduced to 20% collection when gauge height wind speeds reached 9 m/s. Winter-long sublimation must also be evaluated if SWE accumulation is at question. Sublimation rates are partially a function of relative humidity, air temperature and windspeed. Sublimation rates increase with warmer air temperatures and higher windspeeds, along with lower humidity. It is known that these three components of sublimation vary from the Coastal Plain to the Mountains in the Alaska Central Arctic (Kane et al., 2014). During the winter, the Coastal Plain

has higher windspeeds and relative humidity, but lower air temperatures. At higher elevations, windspeed and relative humidity decrease, while air temperatures increase. Determining the magnitude of sublimation rates and its spatial distribution from the Coastal Plain to the Mountains, would benefit the evaluation of winter long SWE accumulation across the Alaska Central Arctic.

Challenges of measuring the accumulation of liquid precipitation are described in chapter two and include undercatch which occurs for all precipitation gauges. All liquid precipitation measurements used in this thesis were acquired from shielded precipitation gauges, which helps minimize undercatch, but does not eliminate it. The current analysis presented here of the spatial distribution of liquid precipitation did not account for undercatch. Undercatch is known to be a factor of windspeed, which varies spatially. With higher windspeeds on the Coastal Plain, is undercatch more problematic in this region? If undercatch is proven to be greater on the Coastal Plain, then the change in liquid precipitation with elevation might not be as high as currently thought.

The datasets of solid and liquid precipitation illustrated annual precipitation to vary temporally and spatially over the Alaska Central Arctic. If SWE accumulation during the cold season was used as the solid precipitation input instead of end-of-winter SWE, would that have an impact on the overall precipitation distribution; and as well the contribution between solid and liquid precipitation? And what would the effects be of using undercatch corrected liquid precipitation values? The use of SWE accumulation and undercatch corrected liquid precipitation would likely increase the overall amount of annual precipitation. The question, however, is would this increase be homogeneously distributed?

In order to obtain good spatial and temporal precipitation data, a network of widespread meteorological stations is required for an informative duration. Consequently, this project used meteorological stations from a collection of different organizations and research projects. Only 7 of the 31 stations used in this investigation, however, still exist as of 2015, the others having been removed recently with the completion of research projects. Gauges and gauge networks in use today were not designed for studying climate, but rather for input data for infrastructure design. The removal of so many stations will significantly limit future evaluation of precipitation in the Alaska Central Arctic. With environmental change currently stimulating much of the

interest in high-latitude hydrologic studies (northern areas are expected to be more strongly impacted by warming than areas of lower latitude), a stable network of meteorological stations is essential. With the reduction of meteorological stations, the present precipitation dataset is still the largest of its kind for the study domain, and will continue to be so for quite some time. The need for the implementation of long-term and spatially distributed meteorological stations can't be emphasized enough. Without such a network, meteorological fluctuations and variations cannot be fully quantified in this changing environment.

Environmental changes, such as changing sea ice extent and ice cover duration, have implications for future precipitation patterns. The current research shows that when the Beaufort and Chukchi Seas are open or partially covered with relatively thin and fractured ice, these water bodies are substantial moisture sources, and snowfall events originating from the north occur primarily during this time. When the concentration of sea ice off Alaska's northern coast is at a maximum, mid-winter snow-producing storms are advected from the south where water bodies remain ice-free throughout winter. Changes in sea ice areal extent and ice cover duration will likely influence synoptic atmospheric activity, thus shifting where the Alaska Arctic snowfall moisture originates and its timing. In this warming environment, a longer ice free duration would expand the period of time the Arctic Ocean is a viable moisture source, which could lead to increases in precipitation and subsequent runoff. Current precipitation patterns for the Alaska Central Arctic are outlined in this thesis, but future patterns cannot presently be predicted. Environmental warming will likely result in changes to these patterns, which highlights the need for the continuation of precipitation observations and a long-term network of meteorological stations.

References

ACIA, 2005: Arctic climate impact assessment: Cambridge University Press, New York, NY

Cavalieri, D., Parkinson, C., and Vinnikov, K. Y., 2003: 30-Year satellite record reveals contrasting Arctic and Antarctic decadal sea ice variability. *Geophysical Research Letters,* 30(18).

Draxler, R. R. and Hess, G., 1997: Description of the HYSPLIT4 modeling system, *NOAA Technical Memorandum ERL ARL-224*, December, 24 pp., [Available from National Technical Information Service, 5285 Port Royal Road, Springfield, VA 22161.].

IPCC, 1996: Climate change 1995: The science of climate change. Contribution of Working Group 1 to the Third Assessment Report of the Intergovernmental Panel on Climate Change, Cambridge University Press, Cambridge, UK, and New York, USA.

IPCC, 2001: Climate change 2001: The scientific basis. Contribution of Working Group 1 to the Third Assessment Report of the Intergovernmental Panel on Climate Change, Cambridge University Press, Cambridge, UK, and New York, USA.

Kane, D. L., Hinzman, L. D., McNamara, J. P., Zhang, Z., and Benson, C. S., 2000: An overview of a nested watershed study in Arctic Alaska. *Nordic Hydrology,* 31(4-5): 245-266.

Kane, D. L., Hinzman, L. D., Gieck, R. E., McNamara, J. P., Youcha, E. K., and Oatley, J. A., 2008: Contrasting extreme runoff events in areas of continuous permafrost, Arctic Alaska. *Hydrology Research,* 39(4): 287-298.

Kane, D. L., Youcha, E. K., Stuefer, S., Myerchin-Tape, G., Lamb, E., Homan, J. W., Gieck, R. E., Schnabel, W., and Toniolo, H., 2014: Hydrology and meteorology of the central Alaskan Arctic: Data collection and analysis, University of Alaska Fairbanks, Water and Environmental Research Center, Report INE/WERC 14.05, Fairbanks, AK.

Maslanik, J. A., Serreze, M. C., and Agnew, T., 1999: On the record reduction in 1998 western Arctic sea-ice cover. *Geophysical Research Letters,* 26(13): 1905-1908.

Serreze, M. C., Bromwich, D. H., Clark, M. P., Etringer, A. J., Zhang, T., and Lammers, R., 2002: Large-scale hydro-climatology of the terrestrial Arctic drainage system. *Journal of Geophysical Research: Atmospheres (1984–2012),* 107(D2): ALT 1-1-ALT 1-28.

Vinnikov, K. Y., Robock, A., Stouffer, R. J., Walsh, J. E., Parkinson, C. L., Cavalieri, D. J., Mitchell, J. F., Garrett, D., and Zakharov, V. F., 1999: Global warming and Northern Hemisphere sea ice extent. *Science,* 286(5446): 1934-1937.

Yang, D., Goodison, B., Benson, C., and Ishida, S., 1998: Adjustment of daily precipitation at 10 climate stations in Alaska: Application of WMO intercomparison results. *Water Resour. Res,* 34(2): 241-256.